Isolation of arabinoxylan consumers in the human gut microbiota using fluorescent glycan labelling

Elaine Xing

Department of Pharmacology & Therapeutics

McGill University, Montreal

April 2023

A thesis submitted to McGill University in partial fulfillment of the requirements of the degree of Master of Science

TABLE OF CONTENTS

ABSTRACT	4
RÉSUMÉ	5
ACKNOWLEDGEMENTS	6
CONTRIBUTION OF AUTHORS	7
1. INTRODUCTION	9
1.1 The human gut microbiota	9
1.2 Importance of the gut microbiota to human health	10
1.2.1 Genetic diversity in the human gut microbiome	10
1.2.2 Physiologic effects of the human gut microbiota	10
1.3 Composition of the gut microbiota	11
1.3.1 Disruption in the gut microbiota composition and host health	12
1.4 Modulating the gut microbiota towards a healthy composition	14
1.4.1 Fecal Microbiota Transplantations (FMTs)	14
1.4.2 Probiotics	15
1.4.3 Postbiotics	16
1.4.4 Prebiotics	17
1.5 Glycan metabolism by the gut microbiota	18
1.6 Commonly studied prebiotics and their health implications	19
1.7 Arabinoxylan	20
1.8 Studying the gut microbiome	24
1.8.1 Functional analysis of the gut microbiota	25
1.8.2 Functional analysis of glycan metabolism by the gut microbiota	27
1.8.3 Metabolic labeling coupled with fluorescence-activated cell sorting and culturomics.	
1.9 Hypothesis & Aims	29
2. METHODS	30
2.1 Human stool sample selection and storage	30
2.2 Synthesis of Arabxylo-Fl and CD-Fl probe	31
2.3 Culturomics protocol	
2.3.1 Metabolic labeling of stool samples with Arabxylo-Fl probe	31
2.3.2 Cell sorting with flow cytometry	32
2.3.3 Isolation of labeled stool bacteria	32

2.3.4 Selection for Firmicutes bacteria from sorted cells	33
2.4 Culture of bacterial isolates	33
2.5 Growth curves	34
2.6 Gram stain	34
2.7 DNA extraction and 16S rRNA sequencing	35
2.7.1 DNA extraction of bacterial isolates	35
2.7.2 DNA extraction of fecal samples	35
2.7.3 16S rRNA amplification and Sanger sequencing of bacterial isolates	36
2.7.4 Nanopore sequencing of bacterial isolates and fecal samples	37
2.8 Polysaccharide utilization loci (PUL) characterization of AX metabolism for	
2.9 Metabolic labeling of bacterial isolates	38
2.10 Susceptibility assessment of <i>Bacteroides</i> sp. CEX23003 to chloramphenicol	39
2.11 Liquid chromatography in tandem with mass spectrometry (LC-MS)	39
2.12 Colony PCR	40
3. RESULTS	42
3.1 Metabolic labeling of human stool samples with the Arabxylo-Fl probe	42
3.2 Isolation of arabinoxylan consumers from YM54 stool using the Arabxylo-F	El probe44
3.3 Identification of bacterial isolates	48
3.5 Labeling of B. ovatus CEX23001 and B. xylanisolvens CEX23002 with Arab	
3.6 Assessing the integrity of the Arabxylo-Fl probe using LC-MS	61
3.7 Optimizing culture conditions to recover more diverse bacteria consumers of	of arabinoxylan 67
3.8 Susceptibility assessment of <i>Bacteroides</i> sp. CEX23003 to chloramphenicol .	72
4. DISCUSSION	76
5. CONCLUSION	84
REFERENCES	86
APPENDIX A: ABBREVIATIONS	95
APPENDIX B: MEDIA + SOLUTION PREPARATION	98

ABSTRACT

The composition of the gut microbiota has important consequences in human health. A loss of biodiversity in gut bacteria, known as dysbiosis, is implicated in disease states including inflammatory bowel disease, obesity, and Clostridioides difficile infection. Balance in the endogenous bacterial composition can be restored using prebiotics, which are molecules such as glycans and polyphenols, capable of supporting specific bacteria. Diet-derived complex glycans are being investigated for their potential as prebiotics since gut bacteria use these carbohydrates as an energy source. The gut microbiome is enriched with genes encoding carbohydrate-active enzymes that are needed to break down complex glycans. Hence, we can shape the gut microbiota using diet. However, glycan metabolism in the gut microbiota is still not completely elucidated. Furthermore, clinical trials and animal studies have focused on only a few glycan structures for their potential as therapeutic prebiotics, such as fructooligosaccharide, despite the vast repertoire of diet-derived glycans that are metabolized by the gut microbiota. Arabinoxylan (AX), the main non-starch polysaccharide in wheat bran, is a prebiotic glycan that can be further investigated. Currently, we are using a workflow that metabolically labels stool samples with fluorescently-labelled glycans, and isolates labeled bacteria using FACS and culturomics. Positive glycan consumption phenotype was validated using growth curves and bacteria species were identified using DNA extraction and 16S rRNA sequencing of the entire 16S gene (V1-V9 region). Beyond optimizing this workflow for the isolation of AX consumers from the human gut microbiota, this work presents the potential of the metabolic labeling workflow to study glycan metabolism of lesser investigated glycans.

RÉSUMÉ

La composition du microbiote intestinale a des conséquences importantes sur la santé humaine. Une perte de biodiversité des bactéries intestinales, connue sous le nom de dysbiose, est impliquée dans plusieurs maladies. L'équilibre de la composition bactérienne endogène peut être restauré en utilisant des prébiotiques, c'est-à-dire des molécules, tels les glycanes ou polyphénols, capables de soutenir certaines bactéries de façon spécifique. En effet, les glycanes complexes dérivés de l'alimentation sont étudiés pour leur potentiel en tant que prébiotiques car ils sont utilisés comme source énergétiques par certaines bactéries intestinales. Le microbiome intestinal est enrichi en gènes codant pour des enzymes actives sur les glucides, nécessaires à la dégradation des glycanes complexes. Cependant, le métabolisme des glycanes dans le microbiote intestinal n'est pas encore complètement élucidé. De plus, les essais cliniques et les études sur les animaux se sont concentrés sur seulement quelques structures de glycanes comme prébiotiques thérapeutiques, telles que les fructo-oligosaccharides, malgré le vaste répertoire de glycanes dérivés de l'alimentation qui sont métabolisés par le microbiote intestinale. L'arabinoxylane (AX), le principal polysaccharide non-amidonique dans le son de blé, est un prébiotique potentiel qui peut être étudié plus en détail. Nous utilisons un protocole qui marque métaboliquement les échantillons de selles avec des glycanes marquées par fluorescence, ensuite les cellules positives ont été isoler par cytométrie de flux et de la culturomique. Le phénotype de consommation de glycanes positif a été validé en utilisant des courbes de croissance, et les espèces bactériennes ont été identifiées en utilisant l'extraction d'ADN et le séquençage de l'ARNr 16S (région V1-V9). Au-delà de l'optimisation de ce protocole pour l'isolation des consommateurs d'AX provenant du microbiote intestinal humain, ce travail démontre le potentiel du marquage métabolique pour étudier le métabolisme de glycanes moins étudiées.

ACKNOWLEDGEMENTS

I would first like to thank my supervisor, Dr. Bastien Castagner, for his guidance over the duration of my degree that helped me grow as a scientist, and for his support in my future endeavors after graduate school. I would also like to thank my advisor, Dr. Ajitha Thanabalasuriar, and my committee members, Dr. Corinne Maurice and Dr. Lisa Münter, for their valuable feedback and guidance into improvements for my project. Next, I would like to thank Dr. Lharbi Dridi for training me on stool labeling, flow cytometry and bacteria culture, and for his kindness and patience when helping me troubleshoot my experiments. I am grateful to my amazing lab members (Rebecca, Reilly, Justin, Felix and Catherine) for all your help and making the lab a welcoming place to be. I'd also like to thank Camille Stegen and Julien Leconte for their assistance with FACS analysers and sorters, and all the members of our collaborator Dr. Corinne Maurice's lab, especially Michael for helping me with nanopore sequencing. I want to express my gratitude to the department of Pharmacology and Therapeutics of McGill University; I couldn't have asked for a better group of researchers to work alongside and learn from. I am eternally grateful to DBZ and Truegrit for being my family in Montreal. Finally, thank you to my friends and family in Toronto for their support in all my endeavours, and to Max and Jeffery, I miss you both.

CONTRIBUTION OF AUTHORS

Elaine: Metabolic labelling of stool samples (PY31 and YM54) and bacterial isolates with

Arabxylo-Fl and CD-Fl. Flow cytometry analysis of Arabxylo-Fl labeled bacteria. Cultivation

and isolation of sorted cells, Preparation of culture media. DNA extraction, PCR amplification of

16S rRNA and purification of extracted DNA from bacterial isolates labeled with Arabxylo-Fl

probe. Growth curves and Gram stains of bacterial isolates. Literature review on known AX

consumers and metabolic mechanisms, and identification of putative PULs from the PULDB.

Preparation of LC-MS samples and analysis of spectra. Susceptibility assessments of bacterial

isolates to chloramphenicol. Experimental design. Writing of this thesis.

Bastien: Experimental design and project supervision

Lharbi: Experimental workflow and optimization: for metabolic labelling of stool and bacterial

isolates, flow cytometry of labeled stool bacteria, isolation and cultivation of bacterial isolates,

16S rRNA sequencing of bacterial isolates by Sanger sequencing (DNA extraction, PCR

amplification and purification of DNA), Gram stains of bacterial isolates. Isolation of

Bacteriodes xylanisolvens CLD22001 from VF74 stool and identification by 16S rRNA

sequencing. Project advising (microbiology).

Corinne Maurice: Project advising (microbiology)

Fernando Altamura: Synthesis, purification and characterization of β-cyclodextrin-Fl and

arabinoxylotetraose-Fl.

Reilly Pidgeon: Experimental workflow for LC-MS analysis of Arabxylo-Fl probe.

7

Michael Shamash: PCR amplification of extracted DNA from bacterial isolates and stool samples for nanopore sequencing, and identification and analysis of sequence reads using Guppy, Emu and rrnDB.

1. INTRODUCTION

1.1 The human gut microbiota

The human microbiota consists of trillions of microorganisms that colonize the human body, specifically on the skin, in nasal passages, gastrointestinal tract, and the urogenital tract¹⁻³. The largest subset of human microflora resides in the gastrointestinal tract, known as the human gut microbiota, and is compartmentalized into the oral cavity, esophagus, stomach, small intestine, and large intestine, which harbours the majority of the gut microbiota^{4,5}. The composition and diversity of microbes found at different sites along the gut (throat, stomach and distal gut) were compared using 16S rRNA sequencing⁴. Notably, the gut sites had similar taxonomic characteristics but also presented site-specific clustering, which can be explained by the different environmental conditions and selective pressures at each site^{1,4}.

Interactions between the human host and microbes occurs along a mucosal surface, the largest of these interfaces found in the colon^{5,6}. While the gut microbiota is comprised of bacteria, archaea, eukaryotes and viruses, most studies focus on gut bacteria as they have evolved to dominate this microbial community in both density and diversity^{1,7}. An estimate of 10¹¹-10¹² bacteria/g of colonic content reside in the colon, and make up 60% of fecal mass^{6,7}. There are at least 1000 different known bacterial species found in the gut, with more than 90% of species-level phylogenetic groups belonging to two phyla: Bacteroidetes and Firmicutes^{1,2,5}. Other phyla present in the gut are Actinobacteria, Proteobacteria and Verrucomicrobia⁷. The Bacteroidetes phyla can be further divided into major genera, such as *Bacteroides* and *Prevotella*⁸. Major genera from the Firmicutes phyla include *Clostridium*, *Blautia*, *Faecalibacterium*, *Roseburium*, *Ruminococcus*, *Streptococcus*, and *Lactobacillus*⁸. The Actinobacteria phylum is represented by the genera *Bifidobacteria*, *Atopobium* and *Collinsella*⁸.

1.2 Importance of the gut microbiota to human health

1.2.1 Genetic diversity in the human gut microbiome

The aggregate of microbial and human cells formulates a human "supra-organism". Notably, the gut microbiome exceeds the number of human genes by ~150-fold and compliments the human genome with its extensive metabolic and biosynthetic capabilities⁹. The vast gene catalog in the human gut microbiome, reported by the Metagenomics of the Human Intestinal Tract (Meta-HIT) consortium and the Human Microbiome Project (HMP), contribute to a better understanding of the genetic factors influencing human health and disease beyond the ~20,000 protein-coding human genes^{1,5,9}.

1.2.2 Physiologic effects of the human gut microbiota

The symbiotic relationship maintained by the gut microbiota and its host is integral to human physiology and health. An important function of the gut microbiota is to provide enzymes to metabolize dietary nutrients that would otherwise be indigestible by enzymes encoded in the human genome^{2,10,11}. This includes the fermentation of dietary polysaccharides, polyphenols, carbohydrates that were not fully digested by proximal digestion machinery, and dietary proteins (host enzymes, mucins, dead intestinal cells)^{10,11}. Short-chain fatty acids (SCFAs) are important fermentation products that act as rich energy sources for host colonocytes, regulate inflammation, and regulate glucose homeostasis; the three most abundant types of SCFAs are acetate, propionate, and butyrate^{2,10-13}. Butyrate and propionate have roles in intestinal gluconeogenesis, either through direct activation of the pathway or by acting as a substrate (propionate)¹⁰. Butyrate is also known to potentially reduce the risk of colorectal cancer by inducing apoptosis in cancer cells^{10,13}. Acetate is a key metabolite for the growth of other gut bacteria, such as pure cultures of *Faecalibacterium prausnitzii*, and has a role in regulation of

central appetite^{10,12}. The host further benefits from vitamins synthesized by the gut microbiota, particularly vitamin K and B vitamins, which are important for bacterial metabolism as well as host physiology^{10,11}. Furthermore, while bile acids (BAs) are produced by the liver and mainly facilitate lipid metabolism, some BAs enter the colon after digestion, rather than being reabsorbed, and interact with the gut microbiota¹⁰. There is a two-way relationship between BAs and the gut microbiota, whereby microbes can convert primary BAs into secondary BAs, but BAs can also shift the gut microbiota composition through selective pressures such as inducing DNA damage^{10,11}.

The human gut microbiota defends the host against pathogens by training the innate gutassociated lymphoid tissue (GALT)^{2,6,10}. Immunosensory cells found in the innate GALT have
pattern recognition receptors (PRRs) that are primed by antigens presented by commensal
bacteria and recognize them as self ⁶. Not only does this help the host discriminate between
commensal and pathogenic bacteria in the gut lumen, primed immune cells migrate to other
mucosal surfaces in the body to influence the systemic immune system^{6,14}. The physical presence
of the gut microflora in the intestine lumen also protect the host from opportunistic pathogens by
competing for attachment sites and nutrients¹⁵. Indeed, the contribution of the gut microbiota has
been demonstrated in germ-free (GF) mice with reduced digestive enzyme activity, deficient
immune cell types and lymphoid structures, impaired epithelial cell turnover and barrier
integrity, and reduced production of the colonic mucus layer ^{6,15}.

1.3 Composition of the gut microbiota

The fetal gut is sterile prior to birth and is colonized by microbes during delivery¹.

Depending on the mode of delivery, the infant gut microbiota will resemble that from the mother's vagina, if vaginally delivered, or will resemble the maternal skin flora, if delivered via

Cesarean section^{1,8,11}. The composition of the infant gut microbiota is shaped in early life and diversifies for the first 2.5-3 years of life due to infant diet (breast milk vs. formula feeds for the early infant, and the introduction of solid foods). While the gut microbiota stabilizes during adulthood, perturbations can occur due to diet habits, antibiotic use, and environmental factors (such as hygiene conditions)^{1,6,8,11,15}. These factors all lead to inter-individual and intraindividual variations in the composition of the gut microbiota¹⁶. Interestingly, it has been shown that diet and drug use contribute more significantly to variability in gut microbiome composition than host genetics¹⁷.

1.3.1 Disruption in the gut microbiota composition and host health

A rich and diverse gut microbiota defines a healthy gut microbiota composition and allows for optimal host intestinal barrier integrity, immune system function and protection against pathogens¹⁶. Given that the gut microbiota composition is different for each individual, like a fingerprint, there is no "core" optimal gut microbiota composition^{16,18}. The inter-individual variation in the gut microbiota composition makes it difficult to define a "healthy" gut microbiota; however, it is known that an imbalance in the microbial community composition, known as dysbiosis, has serious implications on human health¹⁸. Disruptions in the gut microbial community can occur in three manners: a loss of beneficial microorganisms, an expansion of pathogens, or a loss in biodiversity in the gut microflora¹⁹. In addition, dysbiosis is a state in which the gut microorganisms produce harmful effects through altered metabolic activities and changes in their local distribution in the colon²⁰. Factors associated with dysbiosis include environmental factors related to the modern Western lifestyle, namely antibiotic usage and diet^{19,20}. The human gut microbiota is composed of microbes that maintain a symbiotic relationship with the human host as well as asymptomatic opportunistic pathogens²¹. Antibiotics

that disrupt the gut microflora allows for opportunistic pathogens, such as *Clostridioides difficile*, to expand, cause infection and acquire resistance to antibiotics^{20,21}. In particular, antibiotic use can lead to long lasting changes in the gut microbiota composition, even permanent loss of some microorganisms²². Humanized mice fed Western diets high in fat and sugar have been shown to have a decrease in the *Bacteroides* to Firmicutes ratio^{23,24}. Furthermore, high-fat diets can indirectly disrupt the gut microbial community through the antimicrobial activities of bile secreted for lipid digestion^{10,23}. Diets high in salt, non-nutritive artificial sweeteners, dietary emulsifiers, and animal-based proteins (such as red meat) are also associated with dysbiosis in the gut microbiota²⁵. Aside from influencing the composition of the gut microbiota, emulsifiers are associated with an increase in bacterial translocation along the intestinal epithelium and systemic inflammation²⁵. Digestion of animal-based proteins upregulates the activity of some bacterial enzymes, such as azoreductase, resulting in the production of toxic metabolites²⁰. It is important to realize that while dysbiosis can lead to human diseases and disorders, infectious agents can also trigger dysbiosis^{18,26,27}.

Associations have been made between an imbalanced gut microbiota and human disorders, such as intestinal disorders (inflammatory bowel disease, *C. difficile* infection and colorectal cancer) and extra-intestinal disorders (obesity, Type 2 Diabetes, asthma, autism spectrum disorder, Alzheimer's disease, and stress)^{16, 18,28-30}. The bidirectional relationship between the gut and the brain explains the metabolic and neurological disorders that are associated with gut microbiota variations¹⁶. The central nervous system can modulate the composition of the gut indirectly by altering its environment, or directly via the autonomous nervous system^{16,31}. Likewise, bacteria colonizing the gut can produce metabolites that act as signalling molecules to communicate with the brain^{31,32}. Importantly, the links between the

composition of the gut microbiota and many human diseases are not just mere associations³⁰. Indeed, it has been found that there are causal links to specific diseases, such as obesity and Alzheimer's disease (AD), through the use of GF mouse models^{33,34}. The gut microbiome was shown to be a contributing factor to the pathophysiology of obesity; GF mice that were colonized with the gut microbiota of obese mice had a greater increase in total body fat than mice colonized with a 'lean microbiota'³³. Similarly, Aβ precursor protein (APP) transgenic mice, a model of AD pathology, was found to have a reduction in cerebral Aβ pathology when also generated without a gut microbiota (GF)^{34,35}. Cerebral Aβ pathology phenotype was transferrable to GF APP transgenic mice using fecal microbiota transplants (FMTs) from transgenic mice with intestinal microbiota, and colonization from healthy wild-type mice reduced disease phenotypes³⁴.

1.4 Modulating the gut microbiota towards a healthy composition

Given the link between the gut microbiota and diseases, its modulation for therapeutic purposes emerged as an attractive strategy³⁰. Four broad approaches have been used to that end: fecal microbiota transplantation (FMT), live bacteria (probiotics), postbiotics, and prebiotics.

1.4.1 Fecal Microbiota Transplantations (FMTs)

FMTs utilize fecal matter for therapeutic purposes by transplanting the gut microbiota from a healthy donor to a recipient, comparable to an organ transplant³⁶. Follow-up investigations for patients that received FMTs observed changes in the fecal microbiota composition converging towards that of the healthy donor³⁶. Using *in vitro* models of antibiotic-induced dysbiosis in the human colon, FMTs were shown to restore microbial diversity and richness, fermentation activity, and SCFA production to baseline levels³⁷. Currently, therapeutic uses and clinical experiences with FMTs have been mostly applied to patients with recurrent *C*.

difficile infection (CDI)^{37,38}. Individuals colonized with C. difficile can develop an infection from the pathogen due to perturbations to the gut microbiota homeostasis, such as from antibiotic treatment and long-term hospitalization³⁷⁻³⁹. Moreover, C. difficile are spore-forming bacteria that can transmit spores through the fecal-oral route⁴⁰. The standard treatment for patients diagnosed with CDI is antibiotic therapy (vancomycin or fidaxomicin), further damaging the gut microbiota and leaving the patient more susceptible to infection leading to recurrent CDI^{37,38}. The mechanism by which FMTs exert health benefits is likely through restoration of the gut microbiota composition so that it is unfavourable for pathogens like C. difficile to grow³⁸. Other intestinal disorders and metabolic syndromes associated with dysbiosis make FMTs a promising therapeutic; however, there still poses some risks to using FMTs. While donors are screened against family histories of autoimmune, metabolic and malignant diseases, as well as colonization with potential pathogens, unrecognized pathogens and family histories can still be transferred^{30,37,38}. In addition, previous FMT studies have identified side effects that can occur, such as constipation, diarrhea, bloating, fever, and complications due to FMT colonoscopy (mucosal tears and sedation)³⁶⁻³⁸. Particularly, most clinical studies have an up to 6-month follow-up period, the longest being 68 months; it is difficult to predict the risks due to the FMT or delivery procedures^{30,36-38}.

1.4.2 Probiotics

An alternative to FMTs is to use probiotics, defined as live strains of microorganisms that are commensal to the gut microbiota, designated GRAS (generally regarded as safe), and result in a health benefit to the host when engrafted in the gut^{36,41}. Probiotics have similar mechanisms to FMT, including restoring balance in the gut microbiota composition, outcompeting pathogens, and ameliorating the severity of infectious and non-infectious diseases^{36,37,41}. *Lactobacillus* and

Bifidobacterium strains are the traditionally administered probiotics, which have been made easily accessible to the general public by supplementing foods with probiotics, such as dairy products, fruit juices and cereal^{36,37}. An important criteria for probiotic strains is the ability to survive and maintain metabolic activity in the intestinal environment^{36,42}. Yet, most human studies have shown transient engraftment of probiotic strains in the host gut microbiota^{42,43}. Introduction of exogenous bacteria into the gut ecosystem can be viewed as an invasion of the resident microbial community⁴². While probiotics overcome the logistical risks of FMTs, the reduced genetic diversity lowers the chances that probiotic strains successfully adapt to the new colonic environment⁴². Aside from the few generic commensal strains widely administered as probiotics, second generation probiotics in the form of bacterial consortia have more targeted therapeutic potential. For instance, Tanoue et al. isolated 11 bacterial strains, that were found to improved the efficacy of immune checkpoint inhibitors (ICIs) for cancer treatment when administered together⁴⁴. The use of a defined FMT or consortium of bacterial strains can allow for more control over the bacterial composition, introduce nonconventional probiotic strains, and increase the genetic diversity; however, the problem with transient engraftment remains⁴³.

1.4.3 Postbiotics

The health benefits of probiotics depend on bacterial viability and stability in the intestinal environment^{36, 41,42}; however, soluble factors produced by probiotics, called postbiotics, can also provide host health benefits^{45,46}. Some known properties of postbiotics include antioxidant, antimicrobial and immunomodulatory effects^{45,46}. These by-products do not contain live microorganisms, hence reducing the risks associated with administering live bacteria as a therapeutic, such as microbial translocation of the exogenous microbes⁴⁵. Types of metabolic by-products secreted by bacteria include enzymes, cell wall derivatives, organic acids, and

vitamins⁴⁶. Currently, the main findings on postbiotics are based on *Lactobacillus* species, and more research is needed to elucidate the efficacy and safety of postbiotics for clinical use^{45,46}.

1.4.4 Prebiotics

The composition of the endogenous gut microbial community can be modulated using prebiotics. Prebiotics are food ingredients that are resistant to stomach acid and digestive enzymes found in the human gastrointestinal tract, and instead are selectively metabolized by gut microorganisms, leading to host health benefits^{41,47}. Dietary prebiotics can be classified into two categories: carbohydrate-based and non-carbohydrate-based^{47,48}. The more prevalent carbohydrate-based prebiotics include inulin and fructooligosaccharides (FOS), and noncarbohydrate-based prebiotics include polyphenols and polyunsaturated fatty acids⁴⁷⁻⁴⁸. The main fermentation products of carbohydrate-based prebiotics are SCFAs, which can diffuse into the systemic blood circulation to affect multiple systems in the human body⁴⁹. SCFAs have antimicrobial activity, promote colonic epithelium health, and influence metabolic, immunological and neuroendocrine responses^{49,50}. Incorporating a dietary adjustment using prebiotics are not known to induce severe side effects aside from diarrhea, bloating, cramping and flatulence from fermentation of the prebiotic⁴⁹. Nonetheless, considerations regarding nutrition should be included when taking a dietary approach, such as the effect of micronutrients on the gut microbiota composition, as well as the effect of a short-term and long-term diet³⁶. In addition, the inter-individual variability that exists in the gut microbiota composition means that a personalized prebiotic approach is likely required³⁶. Administration of specific prebiotics that induce a specific microbial change in the gut according to the type of dysbiosis a patient presents would allow us to provide a more effective therapeutic^{30,36}.

1.5 Glycan metabolism by the gut microbiota

Glycans are an important food source to stimulate the proliferation of gut bacteria. Two main sources of glycans that are metabolized by gut bacteria are the diet and human-produced glycans in mucus secretions and breast milk^{12,13}. Dietary glycans are carbohydrate polysaccharides and oligosaccharides that are found mostly in fruits, vegetables, cereals, and legumes^{12,51,52}. Human milk oligosaccharides (HMOs) are a form of natural prebiotic glycan found in human breast milk, and are essential for the growth and development of infants and their gut microbiota composition^{12,53}. The mucosal layer lining the colonic epithelium acts as a protective barrier as well as a source of endogenous mucin glycan for members of the gut microbiota residing in the mucosal niche^{12,54}.

To breakdown these complex glycans, gut bacteria have evolved systems allowing for efficient glycan acquisition and breakdown, with these genes encoded in clusters called polysaccharide utilization loci (PUL)^{12,51}. Carbohydrate-active enzymes (CAZymes) are an essential element of glycan utilization systems in the gut microbiota, and is reflected in the plethora of CAZyme-encoding genes enriched in the gut microbiome^{51,55}. Indeed, most gut bacteria dedicate 1-5% of their genome to these genes, whereas there is a limited CAZyme repertoire in the human genome, encoding approximately 17 enzymes⁵¹. CAZymes are classified into families, namely: glycoside hydrolases (GHs), carbohydrate esterases (CEs), and polysaccharide lyases (PLs)^{51,55}. The distribution of metabolic capacities varies between bacteria species, in which species such as bacteria from the *Bacteroides* genus have broad glycandegrading abilities and are known as 'generalists'^{12,51,55}. In comparison, species with narrower glycan-degrading abilities are known as 'specialists'^{12,51}. Bacteria from the Firmicutes phylum are classified as 'specialists' and keystone microorganisms required to degrade particular

carbohydrates⁵¹. In the case that a preferred substrate is unavailable, it is speculated that 'specialists' avoid extinction by evolving into 'generalists' and metabolize more ubiquitously available glycans and host mucin¹².

PULs contain glycan-binding proteins at the cell surface and carbohydrate transporters to facilitate the uptake of glycans across the cell membrane and peptidoglycan layer⁵⁵. Notably, the uptake mechanisms differ between gram-negative and gram-positive bacteria^{12,51,55}. The archetypal PUL for gram-negative bacteria is based on the starch utilization system (Sus) of *Bacteroides thetaiotaomicron*, termed Sus-like systems to accommodate for the metabolism of glycans outside of starch with a similar mechanism as Sus¹². The Sus-like system contains the homologue pair SusC-SusD transporter system, encoding a TonB-dependent transporter (TBDT) adjacent to a surface glycan-binding protein (SGBP), respectively ^{12,55}. Gram-positive bacteria, largely represented by the Firmicutes and Actinobacteria phyla, utilize ATP-binding cassette (ABC) transporters rather than TBDT and have extracellular solute binding proteins (SBPs) at the cell surface that are analogous to SGBP^{12,55}.

1.6 Commonly studied prebiotics and their health implications

The main prebiotic glycan structures recognized in the literature are fructans (inulin and FOS), galactans (galactooligosaccharides (GOS)) and resistant starch^{30,49,56}. Clinical trials have shown that inulin, FOS and GOS improve mineral absorption, particularly of calcium^{57,58}. The increased calcium bioavailability in the colon is associated with the decrease in pH from SCFA production^{57,58}. Administering these prebiotic glycans also increases the proliferation of beneficial *Bacteroides* and *Bifidobacterium* species while reducing the numbers of harmful bacteria such as *Clostridium* species^{40,57,59-61}. While these clinical trials present important breakthroughs to uncover the therapeutic potential of prebiotic glycans, there still lacks a

comprehensive understanding of which specific gut bacteria are selectively stimulated by which prebiotic glycans³⁰. Selective fermentation was demonstrated in clinical studies by comparing changes in the gut microbiota composition before and after exposure to the prebiotic by using colony forming unit (CFU) counts and sequencing^{40,57,61}. Yet this is not sufficient to make conclusions about glycan utilization mechanisms. For instance, are the proliferating gut bacteria primary consumers of the glycan or secondary consumers that were stimulated by fermentation products through a 'cross-feeding effect'?^{47,49,62} It is also possible that proliferating bacteria are taking advantage of available colonic space due to bacterial species that decreased in numbers after glycan exposure⁶³. Identifying the specific glycan consumers will allow a better understanding as to how glycan supplementation can lead to health benefits. Furthermore, there is still a lot of therapeutic potential to be investigated amongst other complex dietary glycans, such as arabinoxylan^{30,64,65}.

1.7 Arabinoxylan



Figure 1: Structure of wheat arabinoxylan. Adapted from Rogowski et al⁶⁶.

Arabinoxylan (AX) is the main non-starch polysaccharide found in cereals, such as wheat, corn, rye, barley, rice and oat⁶⁷. The polysaccharide is made up of a β -1,4-xylose backbone with arabinose branching units⁶⁷. Wheat AX in particular has been shown to be selectively consumed

by gut bacteria, namely *Bacteroides ovatus*, *Eubacterium rectale*, and *Roseburia intestinalis*⁶⁸. Previous animal studies in piglets have also demonstrated that benefits of consuming wheat bran on gut health is largely due to the fiber components, namely AX, rather than the whole fiber⁶⁹. The potential of a dietary glycan to be considered as a prebiotic is influenced by several factors, such as solubility, chain length and the structure of the glycan^{47,70}. Resistant oligosaccharides and polysaccharides like fructans and galactans are the most studied prebiotic glycans due to their chain size, which slows down fermentation and leads to a more gradual degradation along the length of the colon^{47,70}. Non-starch polysaccharides, such as AX, are made up of more complex structures, increasing their fermentability since a spectrum of enzymes is needed for gut bacteria to metabolize the carbohydrate^{65,71}. The complex structure of AX improves gut health as fermentation and metabolites produced by gut bacteria can also benefit distal regions of the colon⁶⁵.

AX supplementation is associated with a reduction in total cholesterol and an increase in bile acid excretion⁷². Multiple mechanisms have been suggested to explain how AX influences cholesterol levels⁷². AX consumption has been shown to shift the gut microbiota composition, and seems to select for microbes that either directly contribute to lowering cholesterol or indirectly through shifting the bile acid pool. AX can directly sequester cholesterol, inhibiting absorption in the intestine and allowing for cholesterol to be excreted⁷²⁻⁷⁵. AX is also suggested to bind to bile acids and increase bile acid excretion^{74,76}. This alteration in the bile acid pool creates an imbalance in sterol numbers, which can be mitigated by producing more primary bile acids from cholesterol in the liver^{76,77}. In addition, AX can diversify the bile acid pool indirectly via a shift in the gut microbiota composition which converts primary bile acids into secondary bile acids through a structural modification⁷⁷. Secondary bile acids subsequently act as signalling

molecules binding to the nuclear receptors FXR (Farnesoid X Receptor) and LXR (Liver X Receptor) to regulate the conversion of cholesterol in the liver to more primary bile acids, thereby reducing the total cholesterol stored^{72,75,78}.

In vitro and animal studies (mice, rats, piglets) that investigated the effect of administering isolated wheat AX on the gut microbial community have consistently seen a significant increase in the abundance of *Bifidobacteria*, specifically *B. animalis lactis* and *B. longum*⁷⁹⁻⁸¹. Other bacterial populations that have been reported to be stimulated by AX are Roseburia spp., Bacteroides/Prevotella spp., Lactobacillus, Akkermansia muciniphila, and Eubacteria^{69,79,80,82}. Compared to *Bifidobacteria*, these populations have less consistent results, in which some studies did not report any changes in abundance other than *Bifidobacteria*. Moreover, Grootaert et al. used an in vitro model of the gut, Simulator of the Human Intestinal Microbial Ecosystem (SHIME), and found a decrease in abundance of *Roseburia* spp. and Bacteroides/Prevotella/Porphyromonas spp. after administration of arabinoxylan oligosaccharide (AXOS)⁸³. The authors' rationale for this discrepancy was that there was glucose present in their gut model, which was absent in other in vitro studies, because glucose can repress the production of arabinoxylan-degrading enzymes in gut bacteria⁸³. Salden *et al*. published the first clinical trial testing AX in overweight and obese patients. They saw an improvement in the health of the gut barrier but no differences in the relative abundance of dominant phyla compared to the placebo group treated with maltodextrin⁶⁵. However, this clinical trial did not control for other factors that can influence the composition of the gut microbiota, like diet and exercise patterns for participants⁶⁵. While a prebiotic effect was observed in participants, namely an increase in the production of SCFAs and anti-inflammatory effects, it is possible that a significant shift in the microbial composition is not present⁶⁵. There is

currently a limited number of studies that have identified isolated consumers of AX from the human gut microbiota that are specifically contributing to a health benefit.

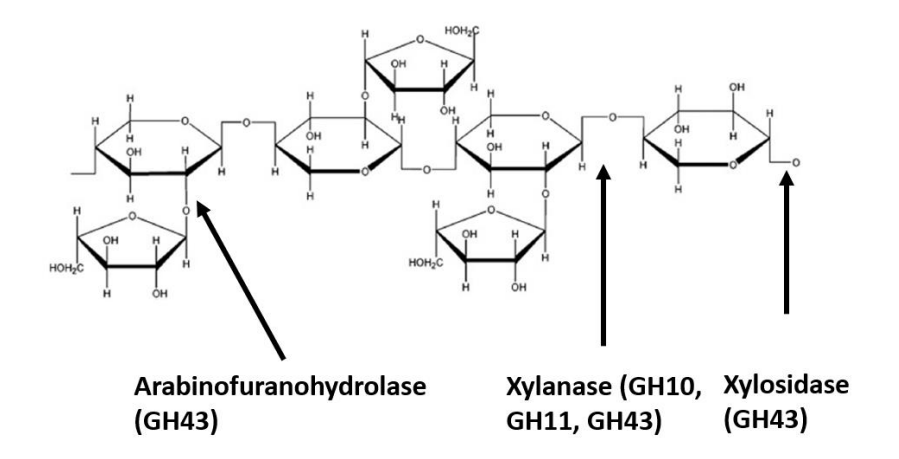


Figure 2. Glycoside hydrolases (GHs) reported to be involved in AX degradation⁸³⁻⁸⁵. Adapted from Schupfer *et al*⁸⁴.

Some GHs that are involved in AX metabolism have been characterized. The common GH families known to hydrolyze AX are GH10, GH11, and GH43 (Figure 2) ⁸⁵⁻⁸⁷. GH10 and 11 are endo-β-1,4-xylanase that cleave the xylan backbone of AX to produce oligosaccharides ⁸⁵. Specifically, GH10 prefers cleaving regions with arabinose branching chains whereas GH11 cleaves unsubstituted regions ^{85,86}. Since AX are known to stimulate *Bifidobacteria*, Saito *et al.* used transcriptomics to investigate the molecular mechanisms that *B. pseudocatenulatum* use to consume AX and AXOS ⁸⁸. Notably, five enzymes from the GH43 family were upregulated ⁸⁸. By using recombinant proteins of the enzymes and subjecting them with AX, it was found that two of the enzymes were arabinofuranohydrolase that cleave arabinose units from O-2 or O-3 substituted xylose residues and the remaining three were xylosidases liberating xylose ⁸⁸. Other families that have been reported to be involved are GH5, GH8 and GH120, but the mechanisms in which these GHs interact with AX are not well characterized ^{88,89}. While glycan consumers can

be isolated using sequencing to identify bacterial strains with GH genes involved in AX metabolism, having the genes to metabolise a glycan is not sufficient for predicting their response to a fiber (Figure 2) ⁹⁰. GH enzymes are classified in the CAZy database based on sequence similarity rather than substrate specificity ⁹¹. In addition, glycan degradation is also dependent on the wider microbial community interactions, such as competition and crossfeeding; glycan consumers need to be isolated based on their functional growth phenotypes ^{62,63,90}.

1.8 Studying the gut microbiome

Metagenomic studies provide a taxonomic profile of the diverse gut microbial community by sequencing DNA extracted from stool samples or colonic biopsies ⁹²⁻⁹⁴. 16S rRNA sequencing is the gold standard used for sequence-based bacterial analysis due to the conserved nature of this gene across bacterial species; however, there are still a number of limitations to sequencing methods ⁹⁵. The 16S rRNA gene can identify bacteria at the taxonomic genus level more than 90% of the time, but difficulties still arise with distinguishing between closely related bacterial species and strains of the same species using 16S rRNA sequencing ⁹⁵. In addition, bacteria with near-identical 16S rRNA gene sequences can still present different phenotypes ⁹⁶. Whole-metagenome shotgun sequencing (WMS) is an alternative method to 16S rRNA sequencing, with the advantage that microbial communities can be identified at the species and strain levels; however, WMS is more costly to perform ⁹⁷.

Metabolic activities of gut bacteria can be inferred from their sequenced genomes but they cannot provide information on the actual activities and biological interactions of these microbes in the gut environment⁹⁸. Furthermore, DNA can be isolated from both live and dead bacteria, making it difficult to infer their metabolic functional roles, such as in relation to a

prebiotic stimulation⁹⁹. DNA-sequencing approaches used to identify gut bacteria are limited to known microorganisms as 16S rRNA sequences are referenced to deposited nucleotide databases^{94,95}. Using solely metagenomics has the risk of losing potentially interesting metabolic information from uncultured species with unknown sequences. In particular, metagenomic methods don't allow for downstream studies on bacterial species as only sequencing data is retrieved and viable microorganisms are not isolated¹⁰⁰.

To study the functional profile of the gut microbiome, metatranscriptomics and metaproteomics can be employed^{92,98}. Metatranscriptomics analyzes the extracted mRNA to provide information on the genes that are expressed by the gut microbial community⁹⁸. Yet, genes can be constitutively expressed, and mRNA abundance does not have a direct predictable relationship to enzyme activity⁹⁸. A solution to this problem is to use metaproteomics with metatranscriptomics⁹⁸. Nonetheless, the disadvantages of sequencing described in the previous section remains and limits the ability of "meta" approaches to uncover metabolic functions of the gut microbiome under specific environmental conditions.

1.8.1 Functional analysis of the gut microbiota

The culturomics approach uses an extensive array of culture conditions to isolate and recover bacterial colonies from stool samples¹⁰¹. Notably, bacterial strains can be directly isolated from a microbiota ecosystem of interest (eg. disease model) and cultivated by comprehensive culture conditions that mimic the physiochemical conditions of the natural gut environment^{100,101}. Furthermore, Lagier *et al.* demonstrated that culturomics identified more microbial biodiversity than was observed using 16S rRNA amplicons¹⁰¹. Metagenomics are still used in tandem with culturomics to sequence and identify the isolated bacterial colonies^{101,102}. However, in comparison to employing metagenomics alone, culturomics also captures the

functional and viable gut microbiota¹⁰¹. New isolated bacterial species are sequenced, their 16S rRNA sequence deposited in the NCBI nucleotide database. In addition, information about the viability of the isolated gut bacteria is gathered, such as the culture conditions and temperatures that are optimal for growth, resistance to common antibiotics, sporulation ability and biochemical characteristics^{100,102}.

Due to the heterogeneity of gene expression and the inability to reliably predict phenotypic characteristics from genomic and metabolic data, it is beneficial to study microbial physiology at the individual cell level⁹⁶. Beyond cultivation-based and sequencing-based methods that expand the known repertoire of commensal gut bacteria, microbial physiologytargeted techniques allow for microbes with specific cellular functions to be isolated⁹⁶. Traditional approaches to study microbial physiology largely relied on destruction of studied cells⁹⁶. Some common techniques include genetically encoded fluorescent reporters and linking the genotype of a cell to a phenotype using deletion mutants⁹⁶. Methods that require prior knowledge of the genetic make-up of a cell result in the destruction of original cell samples due to cell lysis and a different cell is used for subsequent phenotype experiments⁹⁶. Novel approaches, termed next-generation physiology methodologies, isolate microbes based on cellular function and independent of genetic information ⁹⁶. In particular, each next-generation physiology approach is made up of three characteristics: non-destructive phenotype observation, cell sorting based on phenotype, and downstream applications⁹⁶. Individual cells are differentiated from a gut microbiome sample using label-free or label-based approaches, and are observed using Raman microspectroscopy or fluorescence microscopy, respectively⁹⁶. Label-free approaches depend on native cellular properties or chemical compositions of cells⁹⁶. Label-based approaches use chemical reporters, such as functional groups, stable isotopes or fluorophores⁹⁶.

Cells with a phenotype of interest are then separated from the gut microbiome sample using cell sorting based on morphological, optical, fluorescence or Ramen spectral properties⁹⁶. Similar to culturomics, next-generation physiology allows for isolation of viable cells that can be further investigated through whole-genome sequencing, cultivation and biochemistry studies⁹⁶.

1.8.2 Functional analysis of glycan metabolism by the gut microbiota

Label-based next-generation physiology approaches using fluorophores have been useful for assessing selective glycan metabolism. Fluorescently-labeled polysaccharides (FLA-PS) and epifluorescence microscopy were used to detect glycan uptake of marine polysaccharides (laminarin, xylan and chondroitin sulphate) by marine bacteria 103,104. Subsequently, Hehemann et al. fluorescently-labeled yeast α-mannan (YM) and rhamnogalacturonan-II (RGII) and treated the known consumer *Bacteroides thetaiotaomicron*, a gut bacterium, with the fluorescent glycan conjugates $(FGCs)^{105}$. Fluorescence is specific to the presence of labeled glycans where B. thetaiotaomicron grown on unlabeled YM and RGII were non-fluorescent¹⁰⁵. This group also showed the direct connection between fluorescence and a genetic capacity for glycan degradation¹⁰⁵. In comparison to wild-type *B. thetaiotaomicron* incubated with FGCs, mutant strains with YM and RGII PUL deletion had a significantly lower fluorescent signal intensity measured by flow cytometry¹⁰⁵. Klassen et al. also used fluorescently-labeled YM to identify bovine-adapted B. thetaiotaomicron strains from extracted rumen samples 106. Two populations of bovine strains were observed from growth curves, termed medium and high growers, of which the varied growth phenotype was visualized by a difference in fluorescent YM uptake 106. In comparison to a B. thetaiotaomicron control strain, the medium grower had a lower total fluorescence intensity after 60 minutes of glycan incubation and high growers had a higher fluorescence intensity¹⁰⁶.

Label-free approaches using stable isotope probing (SIP) provides a high-throughput method to study substrate uptake⁹⁶. Growth of gut bacteria on selective glycans can be probed for by isotopically labeling carbon sources with ¹³C, such as glucose, that can be incorporated into DNA^{96,107}. Labeled cells are identified using microautoradiography coupled with fluorescent in situ hybridization (MAR-FISH), using fluorescently labeled nucleotide probes to isolate radiolabeled bacteria genetic material 107. MAR-FISH is a destructive method to study microbial physiology, whereas the non-destructive Raman microspectroscopy can also be used to identify bacteria that took up a heavy isotope and allow for downstream analysis of the cells⁹⁶. An important limitation of isotope probing is off-target labeling and incorporation of ¹³C into metabolites, which can then label non-primary bacteria that participate in cross-feeding ^{107,108}. Metabolically labeled bacteria with fluorescent glycans can overcome this issue. Tao et al. cocultured two rumen bacteria, Streptococcus equinus JB1 and Anaerovibrio lipolyticus 5S, that are known to have a cross-feeding relationship and incubated the bacteria with fluorescently labeled glucose 108. S. equinus JB1 consumes glucose and releases lactate and A. lipolyticus 5S consumes lactate; the group showed that fluorescent labeling was specific to the primary glycan consumer¹⁰⁸.

1.8.3 Metabolic labeling coupled with fluorescence-activated cell sorting and culturomics

To study the metabolic functions of the gut microbiota in relation to prebiotic glycans, our research group is using a workflow that uses fluorescently-labeled glycans to isolate glycan consumers from healthy human stool samples (Dridi *et al.*⁹⁰). Labeled gut bacteria were collected from stool samples by fluorescence-activated cell sorting (FACS) and identified by 16S rRNA sequencing. The labeling of bacteria was first demonstrated by measuring an increase in fluorescence after incubating cultured bacterial isolates with synthesized fluorescent glycans,

fluorescein-conjugated β-cyclodextrin (CD-F) and nystose (NYST-F). Furthermore, metabolic labeling of human stool samples with CD-F and NYST-F showed that the increase in fluorescent signal intensity is specific to the presence of a glycan, in which free fluorescein resulted in no signal. Labeling of bacteria by the fluorescent glycan was also largely an energy-dependent process as heat inactivation prior to incubation with the probe and catabolic repression experiments using glucose led to a lower probe uptake. For a bacterium to be labeled, an intact metabolic machinery is necessary, and therefore probe uptake is specific to active and live cells.

This workflow was applied to three unrelated healthy human stool samples using the two fluorescent glycans mentioned above with the addition of galactosyl-mannopentaose (GMP-F). Notably, nine overrepresented exact sequence variants (ESVs) were labeled by a glycan including some that were not previously reported to metabolize. Growth curves were assessed to confirm specific glycan metabolism of the identified bacterial strains inferred from 16S rRNA sequencing. A limitation of this workflow is that not all bacteria that have been labelled are able to consume the glycan. This could be because the binding proteins and transporters are more promiscuous and recognize related but distinct glycans, but GHs are more specific and need a precise structure in order to metabolize the glycan¹⁰⁹. Finally, this workflow was combined with culturomics to cultivate sorted cells from FACS, which allowed direct assessment of the growth phenotype of the bacterial strains that were metabolically labeled from the stool sample.

1.9 Hypothesis & Aims

The metabolic labeling workflow described above has the potential to identify putative glycan consumers from the gut microbiota⁹⁰. However, metabolic labeling by fluorescent glycans even when combined with the presence of PULs consistent with the glycan used are insufficient to conclude glycan metabolism⁹⁰. Therefore, the combination of metabolic labeling, FACS and

culturomics is a promising method to isolate and investigate the functional growth phenotype of bacterial consumers from stool samples. Using this strategy, Dridi *et al.* identified many *Bifidobacterium* and *Bacteroides* species as consumers of FOS, a well studied glycan⁹⁰. In this thesis, I used this method to identify and isolate consumers of the less studied glycan arabinoxylan. I hypothesized that arabinoxylan consumers can be isolated from a gut microbiota sample by combining metabolic labeling and FACS with culturomics. To test this hypothesis, the following aims were carried out:

- 1. Isolate consumers of arabinoxylan from stool samples using a fluorescent glycan probe and identify them using 16S rRNA sequencing.
- 2. Validate the functional growth phenotype of bacterial isolates.
- 3. Optimize the culture conditions to recover more diverse bacterial species that metabolize arabinoxylan, in particular from the Firmicutes phylum.

2. METHODS

2.1 Human stool sample selection and storage

Fresh human stool samples were collected by our collaborator Dr. Corinne Maurice at McGill University, following the McGill Committee on Human Research Protocol (A04-M27-15B), approved by the McGill Faculty of Medicine Institutional Review Board. The screening eligibility of stool donors are as follows: age (18-60 years), body mass index (18.5-30), no diagnosed gastrointestinal disease, no ongoing therapeutic treatment, and no usage of antibiotics 3 months prior to the stool collection. After collecting stool samples, they were immediately placed in the anaerobic chamber, aliquoted and stored at -80°C.

2.2 Synthesis of Arabxylo-Fl and CD-Fl probe

The Arabxylo-Fl and CD-Fl probes were synthesized by Fernando Altamura by conjugating fluorescein to 3³-α-L-arabinofuranosyl-xylotetraose (from Megazyme, Bray, Wicklow, Ireland) and β-cyclodextrin (Sigma-Aldrich Chemical Co., St. Louis, MO, USA), respectively, as reported in Dridi *et al.* 2023⁹⁰.

2.3 Culturomics protocol

2.3.1 Metabolic labeling of stool samples with Arabxylo-Fl probe

Autoclaved phosphate buffered saline (PBS; Gibco, Waltham, MA, USA) (1X), autoclaved Anaerobe Basal Broth medium (ABB; Appendix B), and Minimum Medium (MM; Appendix B) sterile filtered through a 0.2 µM filter were prepared and reduced in the anaerobic chamber overnight the day before the experiment. The following labeling protocol was performed under anaerobic conditions (87% N₂, 10% CO₂, and 3% H₂). On the day of the experiment, an aliquot of a stool sample was taken from -80°C and immediately introduced into the anaerobic chamber to be diluted in MM (1 mL of MM per 0.1g of stool or a 1:10 dilution). A sterile inoculating loop was used to homogenize the stool sample, and then vortexed to break up any remaining large particles. The homogenous suspension was centrifuged at 700 g for 3 minutes to isolate the gut bacteria (supernatant) from the undigested food particles (pellet). The supernatant was further centrifuged at 6500 g for 5 minutes and the pellet was washed with 5 mL of MM. The tube was centrifuged again at 6500 g for 5 minutes and the pellet was resuspended with the appropriate volume of MM (195 µL of MM per 0.1 g stool). For each labeling reaction, 190 μL of bacteria suspension and the appropriate volume of the Arabxylo-Fl probe was transferred to a 1.5 mL Eppendorf tube for a final probe concentration of 2.74 µM. For the control tube without probe, an aliquot of stool solution (equal to the volume of probe) was added. Eppendorf tubes were incubated at 37° C for 1 hour. After the incubation period, the tubes were centrifuged at 6500 g for 5 minutes and the pellet was washed with PBS to remove any residual fluorescent probe and MM. This wash step was repeated once more. The bacterial pellet was resuspended in $500 \, \mu L$ of PBS and kept on ice until the flow cytometer was set up for cell sorting.

2.3.2 Cell sorting with flow cytometry

Cell sorting was performed on a 3-laser, 13 detector FACSAria-III or 4-laser, 18-detector FACSAria Fusion. FITC fluorescence was measured with excitation at 488 nm and emission at 535 nm. A sample of the PBS for diluting the stool sample was used to detect any background fluorescence or particle contamination that will be accounted for when gating for the bacteria population. A sample of non-labeled stool bacteria (negative control) was used to determine basal fluorescence, in which Fluorescein isothiocyanate (FITC; 530/30 bandpass filter) vs. Phycoerythrin (PE; 710/50 bandpass filter) gating was performed to set the area for bacteria labeled by the fluorescent probe. The labeled samples were diluted in PBS by 1/25 or 1/50, depending on the optimal resolution to set up the gating for FACS, for a total volume of 500 μL. Labeled samples were sorted for 5 or 10 minutes, collecting ~50,000 - 100,000 events per sample and immediately transferred to an anaerobic chamber.

2.3.3 Isolation of labeled stool bacteria

The sorted cells were resuspended in 5 mL of ABB supplemented with 0.1% AX (see Appendix B for AX preparation) (ABB-AX) and incubated at 37°C for 48 h. After incubation, 100 μL aliquots of ABB-AX was passaged into 5 mL of MM supplemented with 0.1% AX (MM-AX) and incubated at 37°C for 48 h. Positive cultures in MM-AX were diluted by 10⁵-10⁶ times (to ensure individual colonies can be isolated), 100-μL aliquots were spread on enriched

MM supplemented with 0.1% AX (MMe-AX; Appendix B) and enriched MM (MMe; Appendix B) plates (control plates), and incubated for 4-5 days at 37°C. Individual clones growing on MMe-AX plates were then isolated on MMe-AX plates to confirm their growth on AX.

2.3.4 Selection for Firmicutes bacteria from sorted cells

Each FACS tube with sorted cells were diluted in 300 μL of Brain Heart Infusion (BHI; BD, Franklin Lakes, NJ, USA) and incubated at 37 °C for 0 h, 1 h or overnight. The cultures from each tube were distributed across an array of selective media supplemented with 0.1% AX in order to isolate Firmicutes bacteria from the stool sample. The sorted cells that were incubated in BHI for 0 h were directly passed into selective media after dilution in BHI. Isolation of labeled stool bacteria were as described previously (Section 2.3.3). The following liquid medium conditions were assessed: BHI + 10 μg/mL chloramphenicol (BioBasic, Markham, ON, Canada), modified Mannitol Salt Agar (mMSA), supplemented BHI (sBHI), and supplemented Cooked Meat Broth (sCMB) (see Appendix B for preparation of selective media). Only sorted cells exposed to BHI + chloramphenicol were not first diluted in BHI as this condition was tested before the addition of the dilution step to the protocol.

2.4 Culture of bacterial isolates

Isolated bacteria were cultured in the anaerobic chamber on ABB and glycerol stocks were stored at -80 °C. The following bacterial isolates were used: *Bacteroides ovatus* CEX23001 (isolated from YM54 stool and identified by 16S rRNA sequencing, this work), *Bacteroides ovatus* 3_8_47FAA (from BEI Resources, Manassas, VA, USA), *Bacteroides xylanisolvens* CEX23002 (isolated from YM54 stool and identified by 16S rRNA sequencing), *Bacteroides xylanisolvens* CLD22001 (isolated from VF74 stool and identified by 16S rRNA sequencing⁹⁰), *Bacteroides* sp. CEX23003 (isolated from YM54 stool and identified by 16S rRNA sequencing,

this work), and *Bifidobacterium adolescentis* DSM 20083 (from DSMZ, Braunschweig, Germany).

2.5 Growth curves

Bacteria isolates were cultured in ABB at 37°C overnight or until there was visible growth (turbidity of the culture) under anaerobic conditions (87% N₂, 10% CO₂, and 3% H₂). The overnight cultures were diluted at 1/25 in ABB/BHI (a rich medium acting as a positive control condition), MM, and MM supplemented with 0.1% of carbohydrate (glucose and AX) for a total volume of 250 μL. Some bacterial isolates were also grown in ABBc (custom ABB; Appendix) and ABBc supplemented with a carbohydrate source (glucose and AX). All media were prereduced overnight. The growth was assessed in a 96-well plate with technical triplicates for each condition and biological triplicates for each growth curve experiment (n = 3). Optical density (OD) was measured in a plate reader at 600nm (EPOCH 2, Biotek, Winooski, VT, USA) or 620nm (MultiSkan FC, Thermo Fisher Scientific Inc., Waltham, MA, USA) under anaerobic conditions and 37°C, and was recorded every 5 min for 48-72 h. OD measurements for some clones were taken manually at various timepoints (Figure 6 and 7). Growth curves were generated in GraphPad Prism 9.

2.6 Gram stain

To confirm the purity of isolated colonies from sorted cells, Gram stains were performed. 250 µL of overnight culture of the bacterial isolate was centrifuged for 5 min at 12,000 rpm, and the pellet was resuspended in 100 µL of PBS. 10 µL of bacterial suspension was transferred to a microscope slide. The bacterial suspension was fixed by passing the slide through a flame and spreading the inoculum with an inoculating loop. The fixation step was completed by washing the slide with ethanol for 30 seconds and passing through a flame a second time. Gram stain was

performed using the BD BBL Gram Stain Kit. The gram-stained microscope slides were visualized using a Leica DM1000 microscope (Leica Microsystems, Wetzlar, Hesse, Germany) with oil immersion at 100X objective.

2.7 DNA extraction and 16S rRNA sequencing

2.7.1 DNA extraction of bacterial isolates

To prepare bacterial cultures for DNA extraction, bacterial isolates were cultured overnight by picking a few colonies from an agar plate and resuspending the bacteria in liquid BHI. On the day of the experiment, 1 mL of bacteria culture was centrifuged for 5 min at 12,000 rpm, after which the pellet was resuspended in lysis buffer following the protocol in the BioBasic One-4-All Genomic DNA MiniPrep Kit. DNA extraction of the bacterial isolates was performed following the protocol and materials in the kit for gram-positive bacteria, as this will ensure extraction of DNA from bacterial isolates with unknown identity. The Thermo Scientific NanoDrop 2000c spectrophotometer was used to measure the concentration and purity of extracted genomic DNA.

2.7.2 DNA extraction of fecal samples

To identify the diversity in the fecal sample (YM54) used for culturomics, DNA was extracted from the sample and identified using 16S rRNA sequencing using nanopore technology. An aliquot of frozen fecal sample was taken from -80 °C and thawed at room temperature for 5 min. Using an inoculating loop, a maximum of 200 mg stool was added to 750 µL of lysis solution from the ZymoBIOMICS DNA Miniprep Kit (Zymo Research, Irvine, CA, USA). The Biospec Mini-BeadBeater-16 (BioSpec Products, Bartlesville, OK, USA) was used to homogenize the tube. DNA extraction was performed using the protocol and materials provided in the ZymoBIOMICS DNA Miniprep Kit.

2.7.3 16S rRNA amplification and Sanger sequencing of bacterial isolates

Polymerase chain reaction (PCR) was used to amplify the V1-V9 region of the rRNA gene. The PCR reaction mix for bacterial isolates was prepared with a master mix composed of extracted genomic DNA (10-100 ng), 10 µL of 10X ThermoPol Reaction Buffer (New England Biolabs, Ipswich, MA, USA), 2 μL of dNTP Mix (FroggaBio, Concord, ON, Canada), 2 μL each of forward (F) and reverse (R) primers (10 µM each) from Invitrogen, 0.5 µL of Taq DNA Polymerase (FroggaBio), and nuclease-free water (Invitrogen, Carlsbad, CA, USA) to bring the total volume to 100 µL. 3 regions of the 16S gene was amplified for each bacterial isolate: V1-V9 region, V1-V5 region, and V3-V9 region. This was to ensure that enough genomic DNA from the 16S rRNA gene was amplified to identify the bacterial isolates at the taxonomic classification level of species. The specific sequences of the primers used were as follows: 27F (AGAGTTTGATCMTGGCTCAG), 357F (CCTACGGGAGGCAGCAG), 926R (CCGTCAATTCMTTTRAGT), and 1492R (TACGGYTACCTTGTTAYGACTT). Amplification was carried out with the following PCR cycles: 1 cycle at 94 °C for 3 min; 35 cycles at 94 °C for 30 sec, 55 °C for 20 sec, and 72 °C for 45 sec; 1 cycle at 72 °C for 5 min; and PCR products were held at 4 °C.

10 μL of gel-loading dye (Appendix B) was added to each PCR product and the total volume of product was loaded into the wells of a 1% agarose gel (150 mL) with 10 μL of ethidium bromide dye (FroggaBio) to verify amplification for each 16S gene region. QuickLoad Purple 1kb ladder (New England BioLabs) was used as a reference for the size of PCR products, with the following expected lengths: ~1.5 kb (V1-V9), ~900 bp (V1-V5), and ~1.2 kb (V3-V9). The BioRad Molecular Imager Gel Doc XR system (Bio-Rad Laboratories, Hercules, CA, USA) and Fisher Biotech Electrophoresis Systems UV transilluminator (Thermo Fisher Scientific) was

used to visualize the bands on the gel corresponding to genomic DNA and extracted from the gel. The BioBasic EZ-10 Spin Column DNA Gel Extraction Kit was used to purify the PCR product from the gel and a Thermo Scientific NanoDrop 2000c spectrophotometer was used to measure the concentration and purity of PCR product.

PCR products were sent to Génome Québec to perform Sanger sequencing. The forward and reverse primer complement sequence were trimmed by Génome Québec to exclude sequence reads with a Phred quality score below 10. The sequences were further manually trimmed to exclude long chains of N found at the beginning and end of the sequences with ambiguity from the chromatogram. Any bases that were identified by an N within the sequence were replaced with the appropriate nucleotide observed in the chromatogram. The forward and reverse complement sequences for each gene region were combined, and a full 16S rRNA sequence was assembled by aligning the sequences from each region, excluding overlapping segments of the sequence. The full 16S rRNA sequence, and ultimately the corresponding bacterial isolate, was identified using BLASTn by searching for related strains deposited in the National Center for Biotechnology Information (NCBI) database.

2.7.4 Nanopore sequencing of bacterial isolates and fecal samples

The full 16S rRNA gene (V1-V9 region) from extracted DNA (bacterial isolates or fecal samples) was amplified with the KAPA2G Robust HotStart ReadyMix (Sigma-Aldrich Chemical Co.), and 27F and 1492R ONT-tailed primers (TTTCTGTTGGTGCTGATATTGC-AGRGTTYGATYMTGGCTCAG and ACTTGCCTGTCGCTCTATCTTC-CGGYTACCTTGTTACGACTT respectively). Nanopore sequencing using the MinION flow cell (Oxford Nanopore Technologies, Oxford, UK) allows 24 samples to be sequenced at once. To differentiate each amplicon, a barcode PCR master mix was prepared and cycled using the

PCR Barcoding Kit from Oxford Nanopore Technologies (ONT). Amplicons were purified using AMPure XP beads and quantified with the Qubit dsDNA HS Kit (Invitrogen). Samples were sequenced according to the MinION flow cell loading protocol by ONT. Sequencing data was acquired in real-time using the MinKNOW software. This data is in fact a measure of the electric current produced when DNA passes through a nanopore; the base calling program Guppy was used to convert the raw voltage signals to A/T/C/G. The full 16S rRNA sequence was identified using the tool Emu with the default NCBI combined with rrnDB (ribosomal RNA operons database). All preparation steps for nanopore sequencing, excluding DNA extraction, were performed by Michael Shamash from the Maurice lab.

2.8 Polysaccharide utilization loci (PUL) characterization of AX metabolism for bacterial isolates

The related strains for the bacterial isolate were searched for in the PUL database (PULDB) from the Carbohydrate-Active enZYme database (cazy.org). The resulting putative PULs were compared to reported PULs in the literature with AX degradation activity.

2.9 Metabolic labeling of bacterial isolates

Bacterial isolates were cultured overnight in ABB under anaerobic conditions. All media were pre-reduced before usage. On the day of the experiment, $100~\mu L$ of culture was added to 5 mL of liquid MM-AX or MMe-AX and grown until the exponential growth phase. 1 mL of culture was centrifuged for 5 min at 9500 rpm, the supernatant was discarded, and the pellet was washed with 1 mL of MM. The wash step was repeated another time and the sample was centrifuged for another 5 min at 9500 rpm. The pellet was resuspended in 190 μL of MM or MMe and the appropriate volume of the fluorescently labelled glycan probe. Two concentrations of Arabxylo-Fl probe were tested (2.74 and 5.49 μM) and one concentration for CD-Fl probe was

tested (8.71 μ M). For the control tube without probe, an aliquot of MM/MMe (equal to the volume of probe) was added. Eppendorf tubes were incubated at 37°C for 1 hour. After the incubation period, the tubes were centrifuged at 9500 rpm for 5 minutes and the pellet was washed with PBS to remove any residual fluorescent probe and MM/MMe. This wash step was repeated once more. The bacterial pellet was resuspended in 500 μ L of PBS and protected from the light until the flow cytometer was set up. Flow cytometry analysis was performed on a 5-laser LSR Fortessa 20-parameter analyzer and FlowJo Software was used for data analysis.

A heat shock experiment was performed by preparing the bacterial pellet as described above. Before adding the glycan probes, the tubes were incubated at 65 °C for 10 min and cooled at room temperature for 5 min.

2.10 Susceptibility assessment of *Bacteroides* sp. CEX23003 to chloramphenicol

The susceptibility of isolated *Bacteroides* sp. CEX23003 (from section 2.3.4) to chloramphenicol was assessed, with and without the presence of AX (Figure 17). 100 μ L of overnight culture was passaged into 3 mL of BHI or BHI + 0.1% AX (BHI-AX), both BHI conditions supplemented with chloramphenicol (10, 20, 30, 40, 50 μ g/mL) and incubated at 37 °C for 24 h. 100 μ L of culture from each BHI and BHI-AX tube was passaged into fresh BHI and incubated at 37 °C for 24 – 48 h. OD measurements were taken using a plate reader at 600nm (EPOCH 2, Biotek) before and after each incubation period.

2.11 Liquid chromatography in tandem with mass spectrometry (LC-MS)

To assess the integrity of the Arabxylo-Fl probe, 25-30 μ L of the probe was diluted in water or MM, with a total volume of 80 μ L. The mixture was centrifuged for 5 min at 2000 g and the supernatant was transferred into autosampler vial inserts. Control vials with only water or only

MM were also prepared. In addition, a vial containing probe diluted in MM after exposure to a *B. ovatus* CEX23001 (from section 2.3.3) was prepared. On the day before the experiment, a bacterial culture was started and grown until exponential phase. Following the metabolic labeling protocol for bacterial isolates, the bacteria were isolated after centrifugation and washes using MM, after which the pellet was resuspended in 60 μL of MM and incubated with 20 μL of Arabxylo-Fl probe for 1 hour at 37 °C. After incubation, the tube was centrifuged at 9500 rpm for 5 minutes and the supernatant was kept for liquid chromatography-mass spectrometry (LC-MS) analysis. The samples were analyzed using reverse-phase analytical LC-MS and analytical high-performance liquid chromatography (HPLC), in which constituents of the samples were determined by comparing spectra at 254 nm.

2.12 Colony PCR

Isolated colonies from sorted cells (refer to sections 2.3.3 and 2.3.4) were rapidly screened with colony PCR. Group-specific primers for *Bacteroides fragilis* (Eurofins Genomics, Louisville, KY, USA) were used to amplify regions of the 16S rRNA gene predominantly conserved at the genus level. The specific sequences of the primers used were as follows: f-Bfra-F (ATAGCCTTTCGAAAGRAAGAT) and f-Bfra-R (CCAGTATCAACTGCAATTTTA).

Amplification was carried out with the following PCR cycles: 1 cycle at 94 °C for 5 min; 35 cycles at 94 °C for 30 sec, 55 °C for 30 sec, and 72 °C for 30 sec; 1 cycle at 72 °C for 5 min; and PCR products were held at 4 °C. PCR reactions were prepared with the master mix described in section 2.7.3, excluding genomic DNA. Colonies were picked from agar plates using an inoculating loop and resuspended in 300-500 μL of nuclease-free water (Invitrogen). 2 μL of resuspended colony was added into the PCR reaction mix. Clones A9 and A12 (also annotated as *Bacteroides* sp. CEX23003) were screened using extracted DNA rather than colonies (section

3.7). Amplification for the 16S rRNA gene region was verified by running each PCR product in a gel (refer to section 2.7.3), with expected product lengths of ~500 bp.

3. RESULTS

3.1 Metabolic labeling of human stool samples with the Arabxylo-Fl probe

Figure 3: Structure of arabinoxylotetraose. This oligosaccharide was conjugated to fluorescein (Arabxylo-Fl) and used as a probe to study the metabolism of AX.

Prior to isolating and investigating arabinoxylan consumers from human stool samples, metabolic labeling using the Arabxylo-Fl probe were carried out to re-validate the workflow demonstrated by Dridi *et al.*90 and the ability of the probe to label stool samples. Frozen stool samples were taken from -80 °C and immediately placed in anaerobic conditions for further manipulations. Bacteria isolated from PY31 stool after repeated centrifugation and washing with MM were incubated with 2.74 μ M Arabxylo-Fl probe for 1 hour at 37 °C. A negative control sample (unlabeled bacteria) was used to exclude background and autofluorescence signals from the sample (Figure 4.1). No labeling was detected for the PY31 stool (Figure 4.1B). Higher concentrations of the fluorescent probe (4.38 and 5.49 μ M) did not result in an increase in fluorescence (Figure 4.1C and D, respectively).

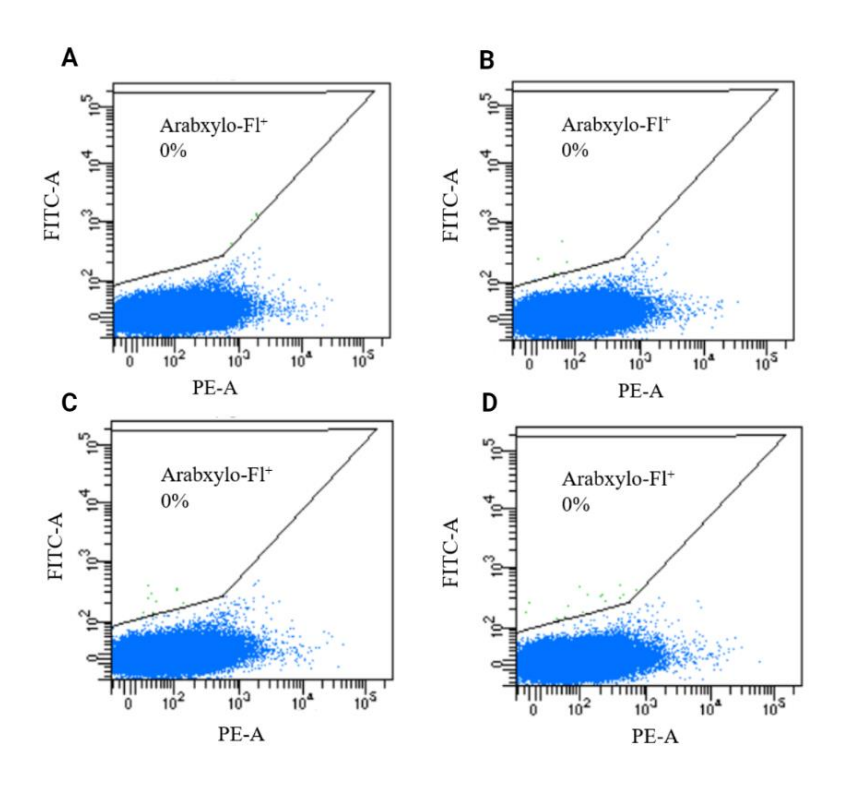


Figure 4.1. Flow cytometry analysis of PY31 stool labeled with Arabxylo-Fl. Unlabeled bacteria were used to adjust the gating to account for background particles in PBS and adjust the side scatter (SSC) to exclude doublets. Arabxylo-Fl⁺ cells (bacteria labeled by fluorescein-conjugated arabinoxylan) were gated on a FITC (530/30 bandpass filter) vs. PE (710/50 bandpass filter) scatterplot to exclude autofluorescence signals from the sample. A) Negative control (unlabeled bacteria). Bacteria labeled with B) 2.74 μM, C) 4.38μ M, and D) 5.49μ M Arabxylo-Fl probe.

Metabolic labeling of stool samples using Arabxylo-Fl probe (2.74 μ M) was repeated with a stool sample from another donor (YM54). Flow cytometry analysis revealed an increase in fluorescence in labeled bacteria samples (Figure 4.2B) and no labeling in the negative control sample (Figure 4.2A), indicating successful glycan uptake by gut bacteria isolated from YM54 stool.

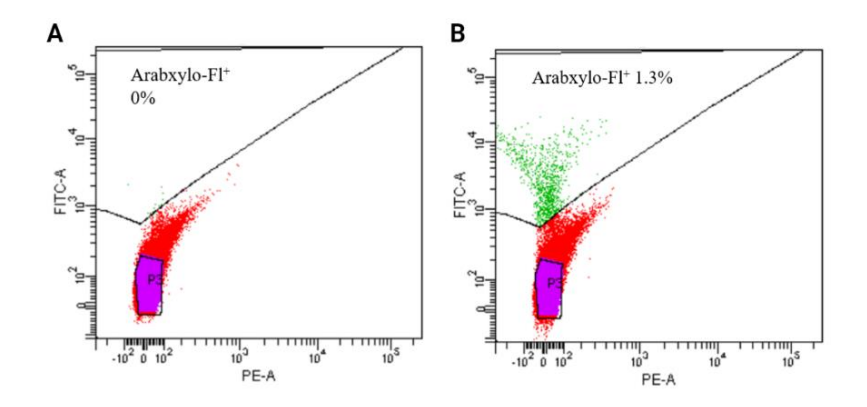


Figure 4.2. Flow cytometry analysis of YM54 stool labeled with Arabxylo-Fl. Unlabeled bacteria were used to adjust the gating to account for background particles in PBS and adjust the side scatter (SSC) to exclude doublets. Arabxylo-Fl $^+$ cells (bacteria labeled by fluorescein-conjugated arabinoxylan) were gated on a FITC (530/30 bandpass filter) vs. PE (710/50 bandpass filter) scatterplot to exclude autofluorescence signals from the sample. A) Negative control (unlabeled bacteria). B) Bacteria labeled with 2.74 μ M Arabxylo-Fl probe.

3.2 Isolation of arabinoxylan consumers from YM54 stool using the Arabxylo-Fl probe

Using the YM54 stool sample, arabinoxylan consumers were isolated following the protocol previously described by Dridi *et al.*⁹⁰ that combines metabolic labeling with cell sorting and culturomics (Figure 5A). Isolated fecal bacteria from YM54 stool were incubated with Arabxylo-Fl for 1 hour and positively labeled bacteria were sorted for 5 min with FACS. Four technical replicate samples of the labeled fecal bacteria were sorted, each for 5 min, collecting approximately 29k sorted cells per technical replicate or ~120k sorted cells in total. The sorted cells were immediately reintroduced in an anaerobic chamber, resuspended in reduced Anaerobe Basal Broth (ABB) supplemented with 0.1% AX and incubated at 37 °C for 48 hours. After

incubation, 100 µL of cultured bacteria was passaged into 5 mL of reduced Minimum Medium (MM) supplemented with 0.1% AX (or a 1/50 dilution) and incubated for another 48 hours. Once positive growth on MM with AX was observed, characterized by an increased turbidity in the culture, the culture was spread on ABB agar plates to collect clones after 72 hours of incubation (Sort 1 from Figure 5A). 25 bacterial clones were isolated and their growth phenotype on MM with 0.1% AX was validated through growth curves.

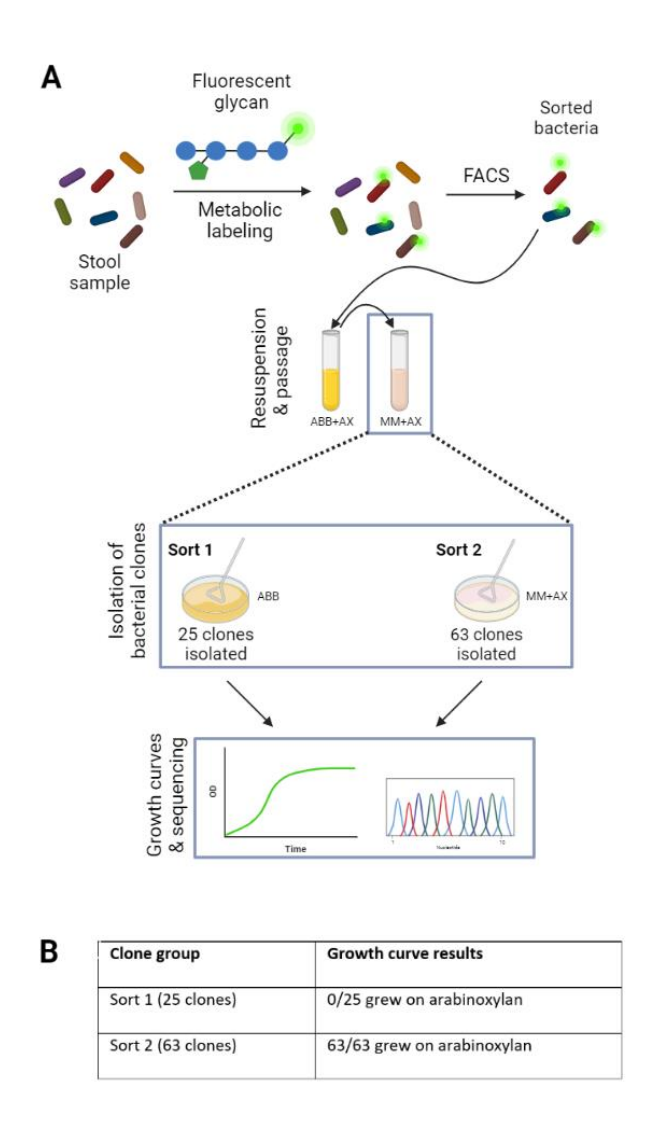


Figure 5. Metabolic labeling coupled with fluorescence-activated cell sorting (FACS) and culturomics. A) Outline of the workflow. Bacteria from Sort 1 were isolated on Anaerobe Basal Broth

(ABB) plates. Minimum Medium supplemented with arabinoxylan (MM+AX) plates for Sort 2 were enriched with beef and yeast extract (Appendix B Media preparation) B) Growth curve validation results for isolated arabinoxylan consumers.

Of the 25 isolated clones from Sort 1, none showed growth on MM + 0.1% AX. The growth curve for clone C2 is a representative growth curve for all isolated clones, in which all isolates had a similar growth phenotype (Figure 6A). There was an increase in OD in Brain Heart Infusion (BHI) and MM supplemented with 0.1% glucose, which demonstrates the successful inoculation with clone C2 in BHI and that the bacterium is capable of metabolizing simple sugars like glucose. The growth curve for the MM supplemented with AX as a sole carbohydrate treatment condition is indistinguishable from MM alone (Figure 6A). To determine if the lack of growth on AX as the sole source of carbohydrate is because the bacterial isolate is not a consumer or due to unfavourable conditions a nutrient depleted medium (MM), ABBc (custom ABB) supplemented with 0.1% glycan (glucose or AX) was tested (Figure 6B). ABBc is a more nutrient-rich medium than MM but still lacks a source of carbohydrate. Growth in ABB, ABBc alone and ABBc supplemented with a glycan were similar and a clear growth on AX was inconclusive.

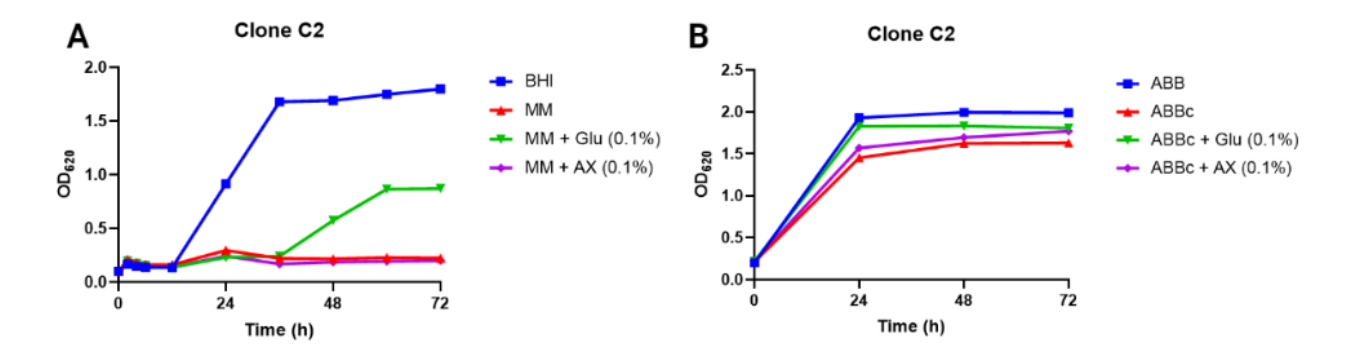


Figure 6. Growth curves for bacteria labeled by fluorescein-conjugated arabinoxylan collected from Sort 1, isolated on Anaerobe Basal Broth (ABB) plates; the growth curve for clone C2 is a

representative isolate for the 25 isolated clones. A) Growth in Minimum Medium (MM) supplemented with glucose (Glu) or arabinoxylan (AX). B) Growth in custom Anaerobe Basal Broth (ABBc; see Appendix B Media preparation) supplemented with glycans. Positive controls were grown in Brain Heart Infusion (BHI) and ABB.

A second sort with YM54 stool (Sort 2, Figure 5A) had four technical replicate samples of Arabxylo-Fl labeled fecal bacteria sorted for 5 and 10 min, with two samples for each sort time, collecting approximately 8k (5 min) and 11k (10 min) sorted cells. A longer sort time was chosen to increase the chance that AX consumers were collected. The same protocol as Sort 1 was carried out: enrich sorted cells in ABB + 0.1% AX and transfer the culture into MM + 0.1% AX in a 1/50 dilution after 48 hours of incubation at 37 °C. In contrast to Sort 1, bacteria from Sort 2 that grew in liquid MM + 0.1% AX were further enriched by passing the culture on enriched MM (MMe) supplemented with AX and MMe agar plates (rather than ABB), incubated for 4-5 days at 37 °C. MM plates were enriched to increase the chance of bacterial clones forming visible colonies on the nutrient-poor medium and enriched MM plates acted as a control. Colonies that formed on MMe-AX plates grew faster and larger than MMe alone, suggesting a positive growth effect from AX supplementation. 63 bacterial clones were isolated in total (Figure 5B). Growth curves were then measured for all clones to determine if they can grow on AX as a sole carbohydrate source. All 63 clones demonstrated growth in MM supplemented with 0.1% AX and no growth on MM alone, suggesting that they are consumers. The growth curve for clone B22 is a representative growth curve for all isolated clones, in which all isolates had a similar growth phenotype (Figure 7). Clone B22 grew in ABB and MM supplemented with a glycan and an additive effect was observed when MM was supplemented with glucose or AX in

comparison to MM alone (Figure 7). The growth curves confirmed that isolated clones could grow on AX. Before identifying all 63 clones, a subset of clones was sequenced first to gauge the diversity and likelihood of clonality in the isolated bacteria.

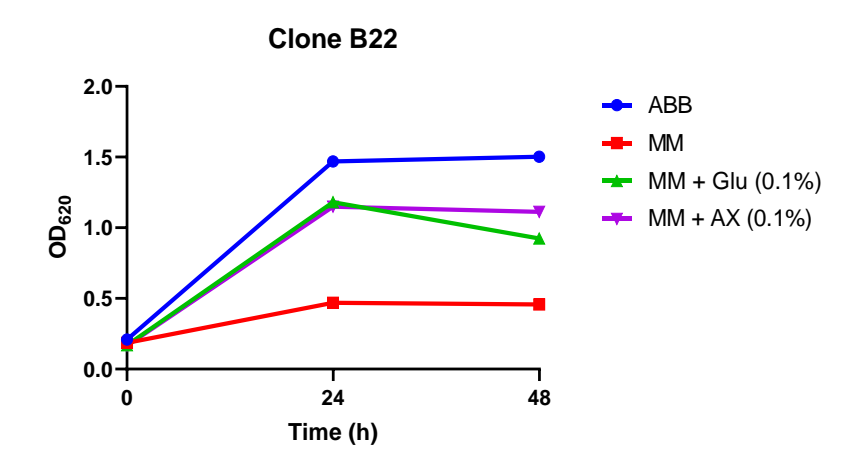


Figure 7. Growth curve for bacteria labeled by fluorescein-conjugated arabinoxylan collected from Sort 2, isolated on Minimum Medium plates supplemented with arabinoxylan, beef and yeast extract. The growth curve for clone B22 is a representative isolate for the 63 isolated clones (N = 1). Positive controls were grown in Anaerobe Basal Broth (ABB). MM: Minimum Medium; Glu: Glucose; AX: Arabinoxylan.

3.3 Identification of bacterial isolates

Of the 63 clones isolated from Sort 2 (Figure 5), 7 clones were identified by nanopore sequencing (Table 1). DNA was extracted from the clones before PCR amplification of the entire 16S rRNA gene (V1-V9 region). Nanopore sequencing data of the amplified 16 rRNA gene was processed using the base calling program Guppy and annotated using the tool Emu with the default NCBI combined with rrnDB database. The sequencing data identified the isolates and the relative abundance of bacterial species present in each extracted DNA sample (which

corresponds to one isolated clone), in which pure isolates were characterized by a 100% relative abundance value. All 7 clones were identified as either a pure *Bacteroides* strain or a mix with the dominant strain as *Bacteroides* (clone A8 and B7) (Table 1). Since all the sequenced bacterial isolates were identified as *Bacteroides* species, there is a high chance of clonality among the rest of the bacterial isolates. Hence, rather than sequencing the remaining bacterial isolates, two of the 5 sequenced pure isolates were chosen for further investigation: B22 (annotated as CEX23001) and C6 (annotated as CEX23002). The contamination in A8 is likely to be a nonconsumer as we have previously observed non-consumers labeled by fluorescent glycans⁹⁰, so we did not investigate the clone further. Since all the pure isolates seemed to belong to 2 Bacteroides species, we picked one of each and validated the identification by Sanger sequencing, confirming that CEX23001 is a B. ovatus strain and CEX23002 is a B. xylanisolvens strain (Table 1). Extracted DNA was amplified using three PCR reactions (V1-V9 region, V1-V5 region, and V3-V9 region) to increase the chances of obtaining enough genomic DNA to sequence the isolates at the taxonomic classification level of species (Figure 8). The aligned sequences were identified using BLASTn and referencing the nucleotide data deposited in the NCBI database, in which the three most related strains to each isolate were listed in Table 1 using the Total Score criteria in BLASTn that measures the total alignment score for the subject sequence (from the bacterial isolates) and reference sequence in the database.

Table 1: 16S rRNA sequencing to identify bacterial isolates (Sort 2; bacteria labeled by fluorescein-conjugated arabinoxylan and isolated on Minimum Medium plates supplemented with arabinoxylan, beef and yeast extract)

Clone ID	Bacterial Species (relative	Sanger sequencing results, list of	
	abundance) from Nanopore	closely related strains according to	
	sequencing	NCBI (Percent Identity)	

A8	Bacteroides ovatus (58.7%), Eisenbergiella massiliensis (23.6%), Eisenbergiella tayi (17.6%)		
A10	Bacteroides ovatus (100%)		
В7	Bacteroides uniformis (78%), Bacteroides ovatus (22%)		
B22	Bacteroides ovatus (100%)	Bacteroides ovatus:	
(CEX23001)		• 3725 D1 iv (99.78%)	
		• BFG-224 (99.78%)	
		• FDAARGOS_733 (99.78%)	
B38	Bacteroides ovatus (100%)		
C6	Bacteroides xylanisolvens (~100%)	Bacteroides xylanisolvens	
(CEX23002)	-	• KR001_HAM_0012	
		(99.64%)	
		• funn3 (99.57%)	
		• BFG-566 (99.57%)	
C10	Bacteroides ovatus (100%)		

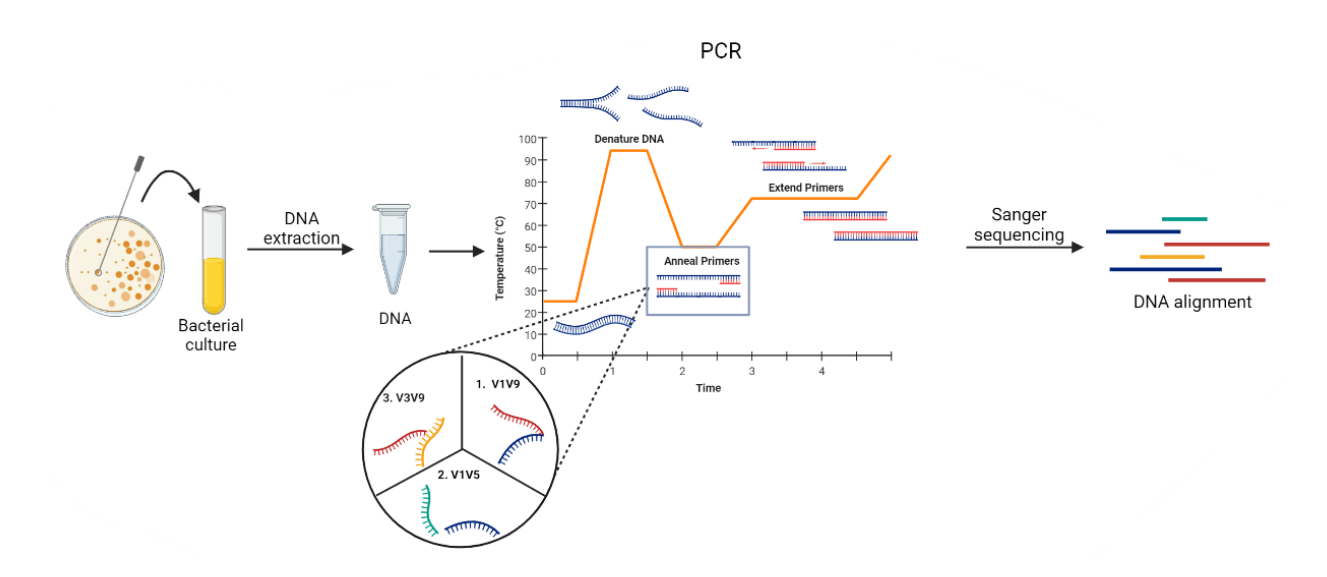


Figure 8. 16S rRNA amplification and Sanger sequencing outline. 3 Polymerase Chain Reactions (PCR) were performed. Three regions of the 16S rRNA gene was amplified: V1-V9, V1-V5, and V3-V9.

Degenerate primers are used for PCR amplification and Sanger sequencing, in which the primer sequence contains several possible base combinations at some positions, resulting in more

than one unique sequence combination for the primer¹¹⁰. These primers are useful for identifying bacterial isolates with unknown taxonomic identification; however, degeneracy can also result in amplification of unrelated and unspecific sequences¹¹⁰. To ensure that Sanger sequencing data (Table 1) was specific, group-specific primers for *Bacteroides fragilis* was used to amplify DNA extracted from *B. ovatus* CEX23001 and *B. xylanisolvens* CEX23002. The amplified region of the 16S rRNA gene is predominantly conserved for the *Bacteroides* genus, with an expected product length of ~500 base pairs (bp). Amplification from the PCR reactions was visualized by running an agarose gel; the bands corresponding to a gene length of ~500 bp indicate successful amplification (Figure 9). From the PCR screen, *B. ovatus* CEX23001 and *B. xylanisolvens* CEX23002 were verified to be *Bacteroides* species.

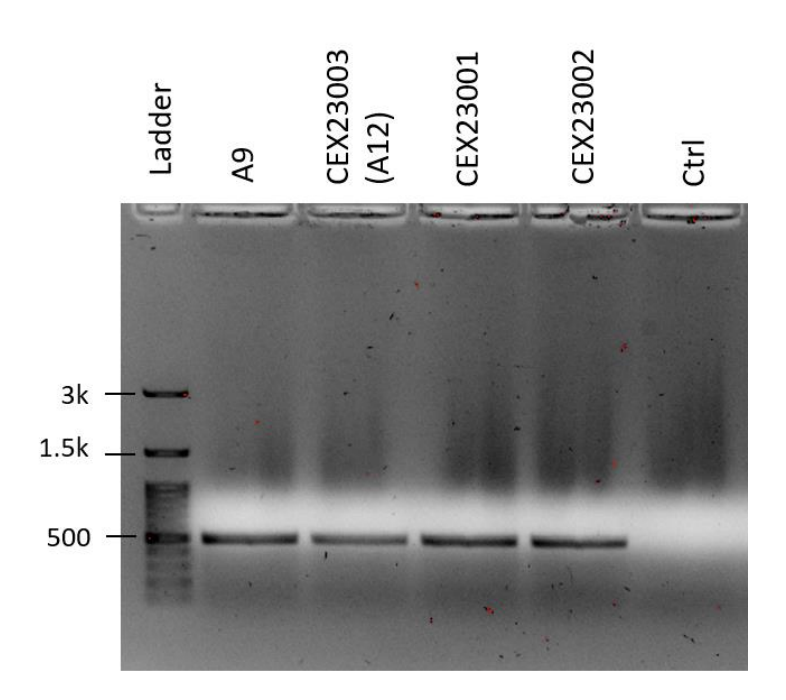


Figure 9. PCR screen of isolated bacterial clones using the group-specific primers for *Bacteroides* fragilis (expected product length of ~500 bp). Strains CEX23001 and CEX23002 were enriched in liquid Anaerobe Basal Broth + 0.1% arabinoxylan (AX) and Minimum Medium (MM) + 0.1% AX, and

isolated from agar MM + 0.1% AX. Clones A9 and A12 (*Bacteroides* sp. CEX23003) were isolated from Arabxylo-Fl⁺ cells (bacteria labeled by fluorescein-conjugated arabinoxylan) treated with Brain Heart Infusion + 10 μ g/mL chloramphenicol supplemented with 0.1% AX and isolated from agar MM + 0.1% AX (see section 3.6). The control (ctrl) is primer diluted in water.

Furthermore, Gram stains for the two isolates were performed and confirmed them as gram-negative bacilli, corresponding to the morphology of *Bacteroides* and matching the sequencing results (Figure 10).

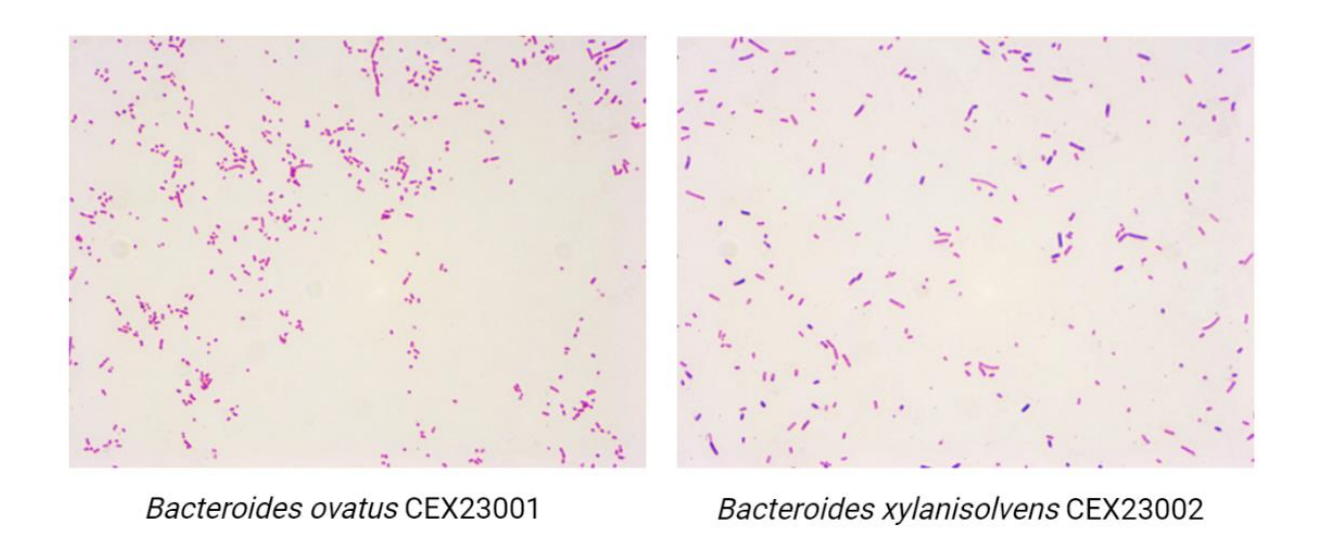


Figure 10. Gram stain imaging of isolated Bacteroides strains.

The growth curves for B. ovatus CEX23001 and B. xylanisolvens CEX23002 with independent triplicate experiments are presented in Figure 11A and B, respectively, which shows that the N=1 result in Figure 7 is reproducible. There was a significant difference in growth between MM supplemented with glycans and MM alone by comparing the mean growth curves

and standard error of mean bars. Growth curves with strains of the same species that we had access to (*B. ovatus* 3_8_47FAA from BEI Resources and *B. xylanisolvens* CLD22001 isolated from VF74 stool) were performed as positive controls (Figure 11C and D, respectively). Similar growth patterns were observed with bacterial isolates, showing that they too were consumers.

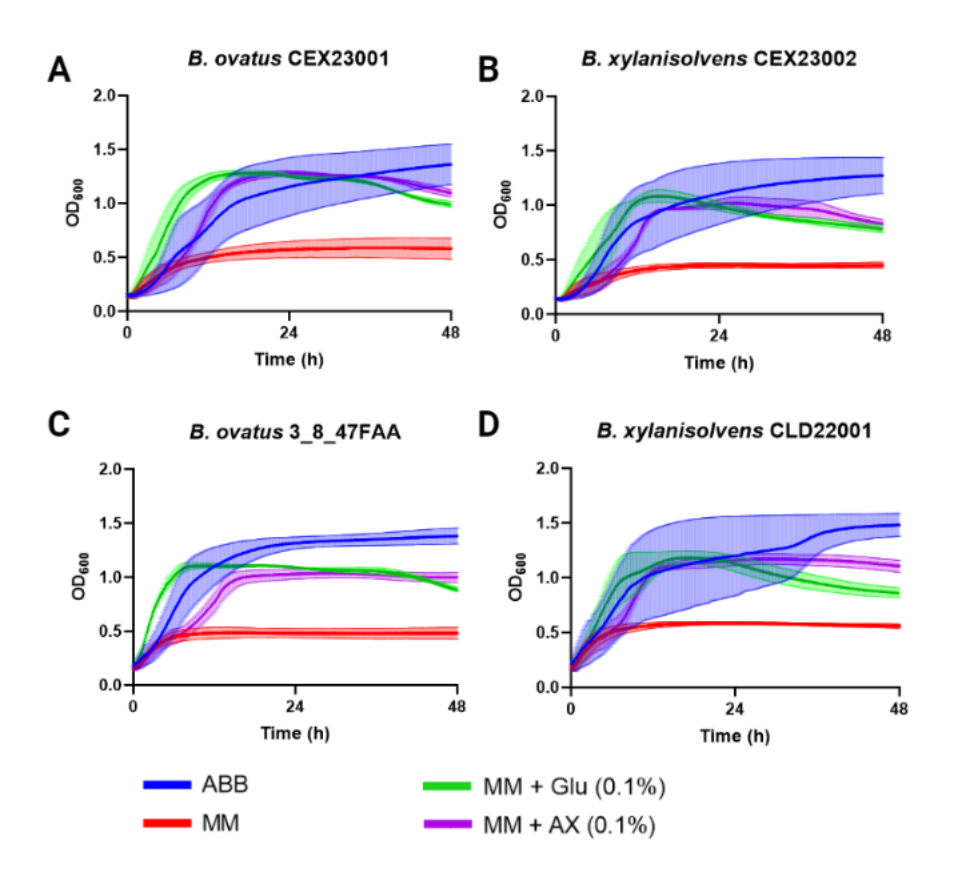


Figure 11. Growth curves for isolated bacteria from Sort 2 (bacteria labeled by fluorescein-conjugated arabinoxylan and isolated on Minimum Medium plates supplemented with arabinoxylan, beef and yeast extract). Growth curves of *B. ovatus* CEX23001 (A) and *B. xylanisolvens* CEX23002 (B), and 2 other strains of *B. ovatus and B. xylanisolvens* as positive controls; *B. ovatus* 3_8_47FAA (C) and *B. xylanisolvens* CLD22001(D). Curves from three independent experiments are shown as mean ± SEM (n = 3). ABB: Anaerobe Basal Broth; MM: Minimum Medium; Glu: Glucose; AX: Arabinoxylan.

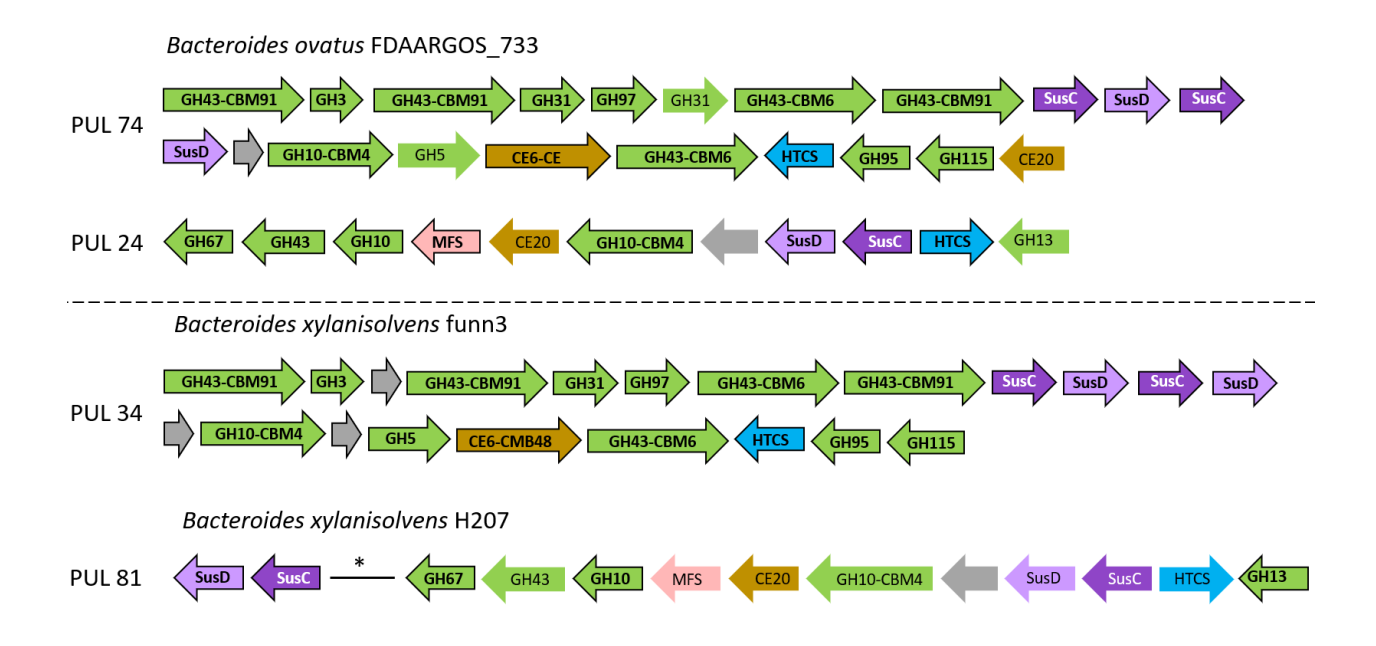
3.4 Putative genes involved in arabinoxylan metabolism in Bacteroides species

Both *Bacteroides ovatus* and *Bacteroides xylanisolvens* are reported consumers of arabinoxylan and the xylan degrading Polysaccharide Utilization Loci (PULs) for *B. ovatus* ATCC 8483 and *B. xylanisolvens* XB1A have been characterized^{66,111} Both species activate two distinct PULs and encode GH families that are known to be involved in AX metabolism, namely GH10 and GH43⁸⁵⁻⁸⁷. In particular, the characterized PULs for strain ATCC 8483 were activated by wheat arabinoxylan and are termed PUL-XylL (large xylan) and PUL-XylS (small xylan)⁶⁶. As their names indicate, PUL-XylL drives the metabolism of more complex forms of hemicellulose and PUL-XylS prioritizes simple linear xylans, but both PULs are upregulated by wheat AX⁶⁶. The characterized PULs for strain XB1A, PUL 43 and PUL 70, were activated by oat-spelt xylan (OSX), yet had a similar gene expression to *B. ovatus* ATCC 8483⁶⁶. Similar to how wheat AX activates both PUL-XylL and PUL-XylS, PUL 43 and PUL 70 were shown to be functionally linked, where interference with PUL 43 expression also repressed PUL 70 expression¹¹¹. In accordance to the Sus-like archetypal PUL for gram-negative *Bacteroides* bacteria, the SusC-SusD transporter system is involved in the uptake of AX^{12,66,111}.

After reviewing the PULs reported in the literature, patterns consistent with AX degradation activity in putative PULs for the bacterial isolates were characterized by comparing the gene clusters with reported PULs for *B. ovatus* ATCC 8483 and *B. xylanisolvens* XB1A (Figure 12). The PULDB (PUL database) found on Cazy.org contains deposited PULs experimentally characterized in the literature. From this database, common GH families involved in AX metabolism (eg. GH43) were used to filter the PULs in the database and narrow down on specific PULs related to AX degradation. Among this narrowed down list of PULs, PULs for the closest related strains of *B. ovatus* CEX23001 and *B. xylanisolvens* CEX23002 (Table 1) were

selected for further investigation; specifically, *B. ovatus* FDAARGOS_733, *B. xylanisolvens* funn3, and *B. xylanisolvens* H207. *B. ovatus* FDAARGOS_733 and *B. xylanisolvens* funn3 were listed in Table 1 as the one of the top 3 closest related strains to the corresponding bacterial isolate, based on the Total Score criteria on BLASTn. *B. xylanisolvens* H207 is not listed in Table 1 but was also chosen as it was the next closest related strain (7th highest Total Score, Percent identity of 99.57%) to *B. xylanisolvens* CEX23002 with a PUL consistent with reported PULs with AX degradation activity. PUL 74 and 24 from *B. ovatus* FDAARGOS_733 parallels PUL-XylL and PUL-XylS expressed in *B. ovatus* ATCC 8483, respectively. PUL 34 from *B. xylanisolvens* funn3 and PUL 81 from *B. xylanisolvens* H207 parallels PUL 43 and PUL 70 expressed in *B. xylanisolvens* XB1A.

Taken altogether, the bacterial strains with published genomes that are the closest matches to the 16S sequence of *B. ovatus* CEX23001 and *B. xylanisolvens* CEX23002 have PULs that complement AX degradation mechanisms reported in the literature, and further validates successful isolation of AX consumers using metabolic labeling, FACS and culture enrichment.



Arrows outlined in black represent conserved genes referenced to strain ATCC 8483 for *B. ovatus*FDAARGOS_733 or strain XB1A for *B. xylanisolvens* strain funn3 and H207. For *B. xylanisolvens*H207, the sequence spanning MFS to HTCS is represented by an unassigned region in *B. xylanisolvens*XB1A¹¹¹; the genomic region assigned by an asterisk contains unassigned genes. CE: Carbohydrate

Figure 12. Polysaccharide Utilization Loci (PUL) sequences adapted from the CAZy PUL Database.

Esterase; CBM: Carbohydrate-Binding Modules; GH: Glycoside Hydrolase; HTCS: Hybrid Two

Component System; MFS: Major Facilitator Superfamily; Sus: Starch utilization system.

3.5 Labeling of *B. ovatus* CEX23001 and *B. xylanisolvens* CEX23002 with Arabxylo-Fl and CD-Fl

The two AX consuming strains were isolated from Arabxylo-Fl⁺ cells from a sorting using the YM54 stool sample. Thus, we decided to validate the AX probe uptake phenotype observed in a mixed microbial community using the cultured isolates *B. ovatus* CEX23001 and *B. xylanisolvens* CEX23002. A culture of each bacterial isolate was grown in MM supplemented with 0.1% AX until the bacteria reached the exponential phase of growth. The enriched bacteria

were incubated with the Arabxylo-Fl probe for 1 hour, washed and analyzed using flow cytometry. Two concentrations of Arabxylo-Fl probe were administered, 2.74 and 5.49 µM. Enriched bacteria were also incubated with and unrelated fluorescent cyclodextrin (CD-Fl) probe (8.71 µM) for 1 hour as a positive control sample. CD-Fl has been shown to proficiently label stool bacteria and bacterial isolates⁹⁰. The isolates were grown in a medium enriched with AX in order to induce the expression of CAZymes involved in AX uptake metabolism^{112,113}. Stool samples do not require induction prior to labeling because food matter present in the stool should upregulate the necessary enzymes for carbohydrate transport. In addition, we wanted to assess isolates during the exponential phase because bacteria are most readily growing on nutrients during this phase, as enzyme synthesis was already induced during the lag phase of growth 114. Unexpectedly, both B. ovatus CEX23001 and B. xylanisolvens CEX23002 had poor labeling with the Arabxylo-Fl probe (Figure 13.1), in seeming contradiction with the stool labeling that lead to their isolation. Yet, CD-Fl successfully labeled both isolates, indicative that the metabolic labeling protocol itself is not the problem. While B. ovatus CEX23001 had minimal labeling at 0.016% and 0.32% (Figure 13.1A), these results were not reproducible (Figure 13.2 and 13.3), and therefore it is difficult to conclude whether the fluorescence signal corresponds to Arabxylo-Fl uptake.

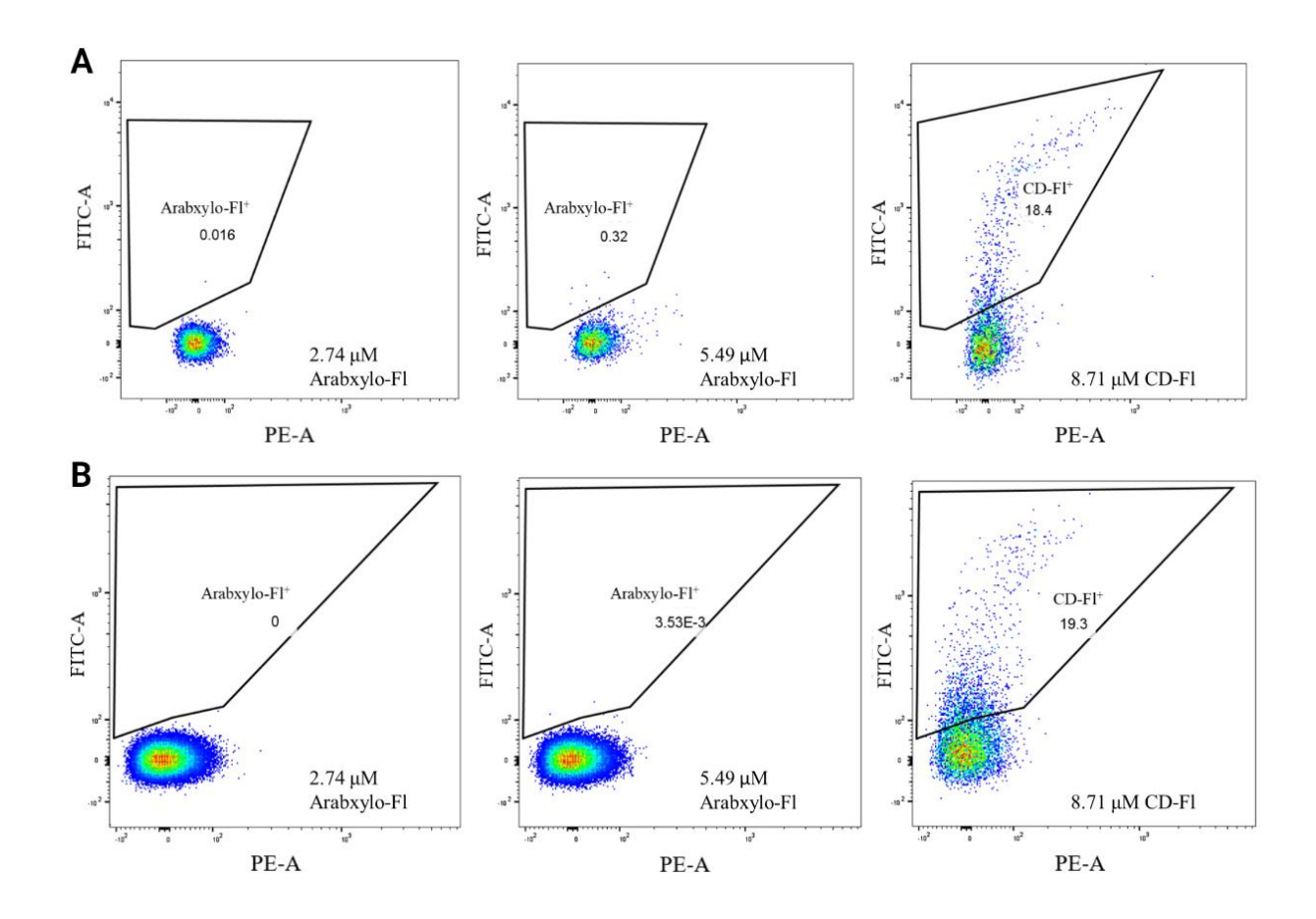


Figure 13.1. Metabolic labeling of bacterial isolates using Arabxylo-Fl (fluorescein-conjugated arabinoxylan) and CD-Fl (fluorescein-conjugated cyclodextrin) represented by flow cytometry scatterplots. A) *B. ovatus* CEX23001 B) *B. xylanisolvens* CEX23002. Concentration of fluorescein-conjugated probe used is displayed in the bottom right corner of each scatterplot.

Initial metabolic labeling experiments with the bacterial isolates were assessed after 18 hours of enrichment in MM + 0.1% AX, which based on the growth curves arrives at the cusp of the exponential and stationary phase of growth (Figure 11A and B). To investigate whether the bacteria are unable to take up the glycan probe due to unfavourable growth conditions, such as build-up of waste products and toxic metabolites that is representative of the stationary phase¹¹², cultures from earlier time points in the exponential phase were labeled and assessed (Figure

13.2). *B. ovatus* CEX23001 was cultured in MM supplemented with 0.1% AX and grown for 8.5 and 14 hours, representative of early and mid-exponential phase, before being incubated with Arabxylo-Fl or CD-Fl (at 2.74 and 8.71 µM respectively) for 1 hour. No fluorescent signal was observed for all conditions.

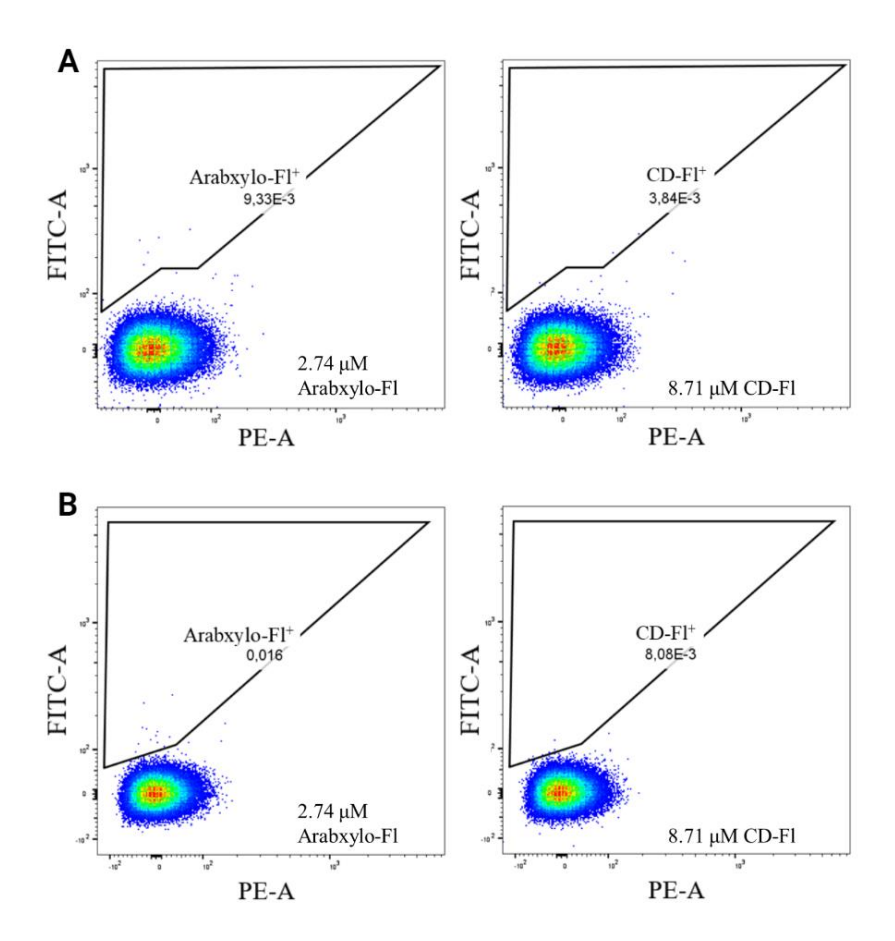


Figure 13.2. Metabolic labeling of *B. ovatus* CEX23001 with Arabxylo-Fl (fluorescein-conjugated arabinoxylan) and CD-Fl (fluorescein-conjugated cyclodextrin) using cultures grown to A) early exponential phase (8.5 hours) or B) mid-exponential phase (14 hours). Concentration of fluorescein-conjugated probe used is displayed in the bottom right corner of each scatterplot.

While visible growth was observed for all overnight cultures in MM + 0.1% AX, perhaps the medium requires more nutrients to induce upregulation of AX metabolism genes to a level resulting in a significant fluorescent signal after metabolic labeling with the Arabxylo-Fl. *B. ovatus* CEX23001 was grown in enriched MM + 0.1% AX for 18 hours before being incubated with Arabxylo-Fl (2.74 and 5.49 μM) and CD-Fl (8.71 μM) for 1 hour. In addition, heat shock inactivation was performed for all conditions, which involved incubating the culture at 65 °C for 10 min prior to exposure to the probes. *B. ovatus* CEX23001 was not labeled by Arabxylo-Fl for the normal or heat-shock condition, and for neither concentration of glycan probe (Figure 13.3). The isolate was labeled by CD-Fl (28.9%) and heat-shock decreased the fluorescent signal to 0.019%, confirming that the observed fluorescence is due to active transport of the CD-Fl probe (Figure 13.3).

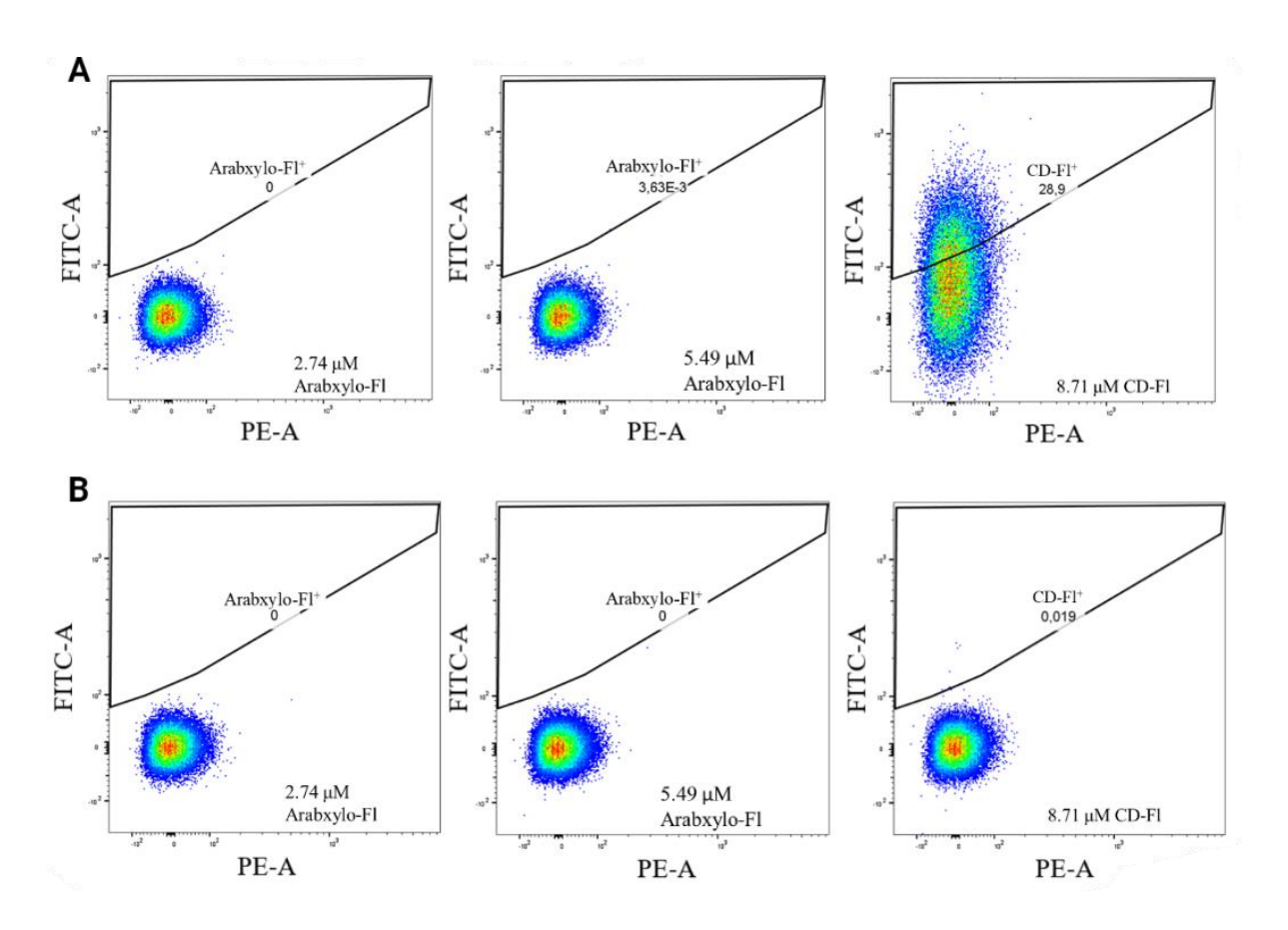


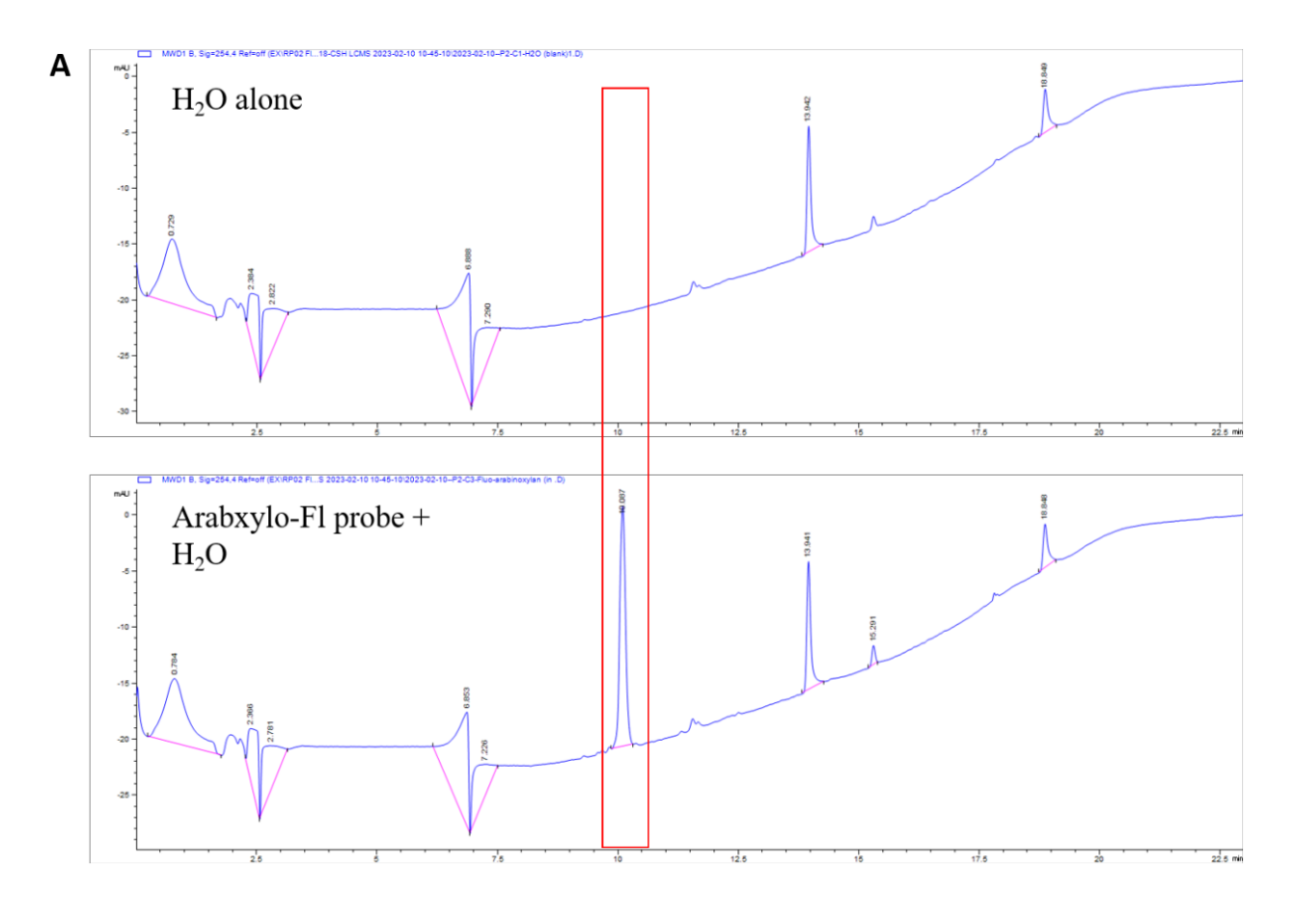
Figure 13.3. Metabolic labeling of *B. ovatus* CEX23001 with Arabxylo-Fl (fluorescein-conjugated arabinoxylan) and CD-Fl (fluorescein-conjugated cyclodextrin). A) without heat inactivation. B) with heat inactivation. Concentration of fluorescein-conjugated probe used is displayed in the bottom right corner of each scatterplot.

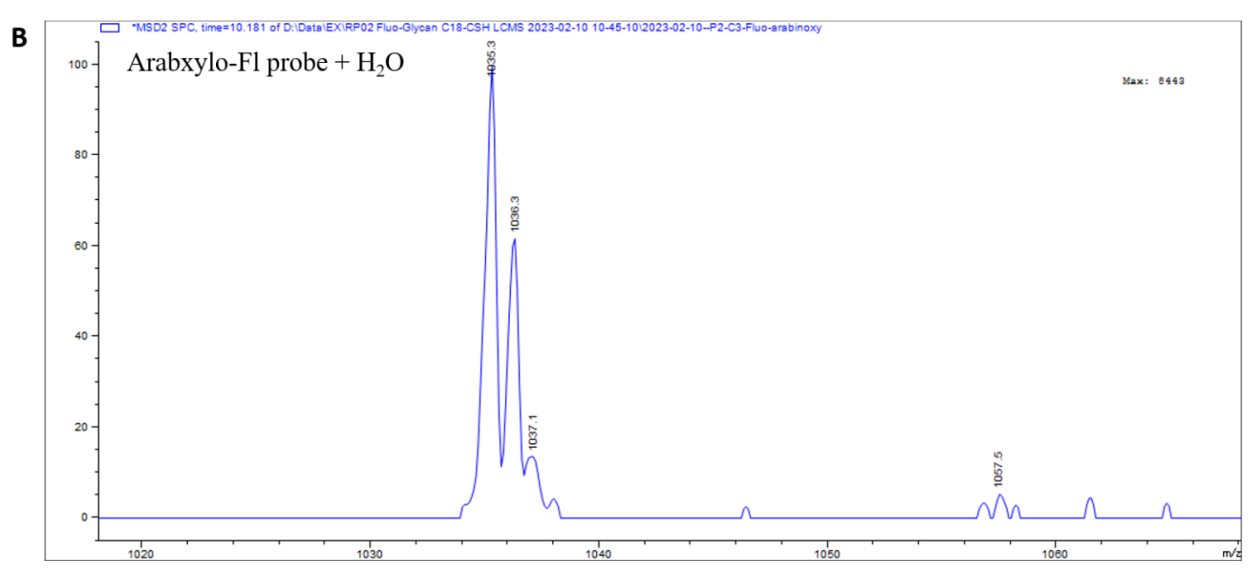
The results demonstrate that metabolic labeling of bacterial isolates with Arabxylo-Fl differs from stool samples. This difference is not affected by the following factors: concentration of the probe, the stage of exponential phase that bacterial isolates are grown to, and the richness of the overnight culture medium. Experiments using CD-Fl to label bacterial isolates and heat inactivation show that our metabolic labeling protocol is effective.

3.6 Assessing the integrity of the Arabxylo-Fl probe using LC-MS

To determine why bacterial isolates were not labeled by Arabxylo-Fl, three perspectives can be considered: optimization of the metabolic labeling protocol, absence of a bacteria that takes up the glycan probe, and a faulty probe. Sections 3.3-3.5 validated the efficacy of the current metabolic labeling protocol to successfully label bacterial isolates with a fluorescent glycan probe, and the bacterial isolates *B. ovatus* CEX23001 and *B. xylanisolvens* CEX23002 were shown to grow on AX. Hence, we decided to evaluate the integrity of the Arabxylo-Fl probe itself, in particular to determine whether the fluorescein molecule was still conjugated to arabinoxylotetraose. During metabolic labeling experiments, the Arabxylo-Fl probe is exposed to MM and bacteria culture. The influence of metabolic labeling conditions on the structure of Arabxylo-Fl probe was assessed using HPLC and LC-MS. Arabxylo-Fl maintained its fluorescein conjugation when diluted in water (Figure 14.1A and B) and MM (Figure 14.1C and

D). Next, a normal metabolic labeling protocol was carried out, preparing a culture for *B. ovatus* CEX23001 until the exponential growth phase and incubating the bacteria in Arabxylo-Fl for 1 hour. Instead of using flow cytometry to analyze uptake of the glycan probe, the probe + culture sample was centrifuged and the pellet was discarded. Taking the supernatant after bacterial incubation, the composition of the supernatant was assessed using HPLC and LC-MS (Figure 14.2). In comparison to Arabxylo-Fl diluted in MM, the HPLC spectrum for the supernatant showed a disappearance of Arabxylo-Fl at (retention time) RT = ~10 min (seen in Figure 14.2A) and appearance of a peak corresponding to free fluorescein at RT = ~ 12 min (Figure 14.2B, 14.3). These results suggest that the lack of fluorescein-conjugated glycan uptake by Arabxylo-Fl+ isolates was due to the fluorophore being cleaved off the glycan, thus no fluorescent signal was detected from bacterial isolates. It is possible that this metabolism takes place within the bacteria and that the free dye is effluxed out of the cell. In any case, this result explains the lack of labeling even if the isolates are clear consumers of AX.





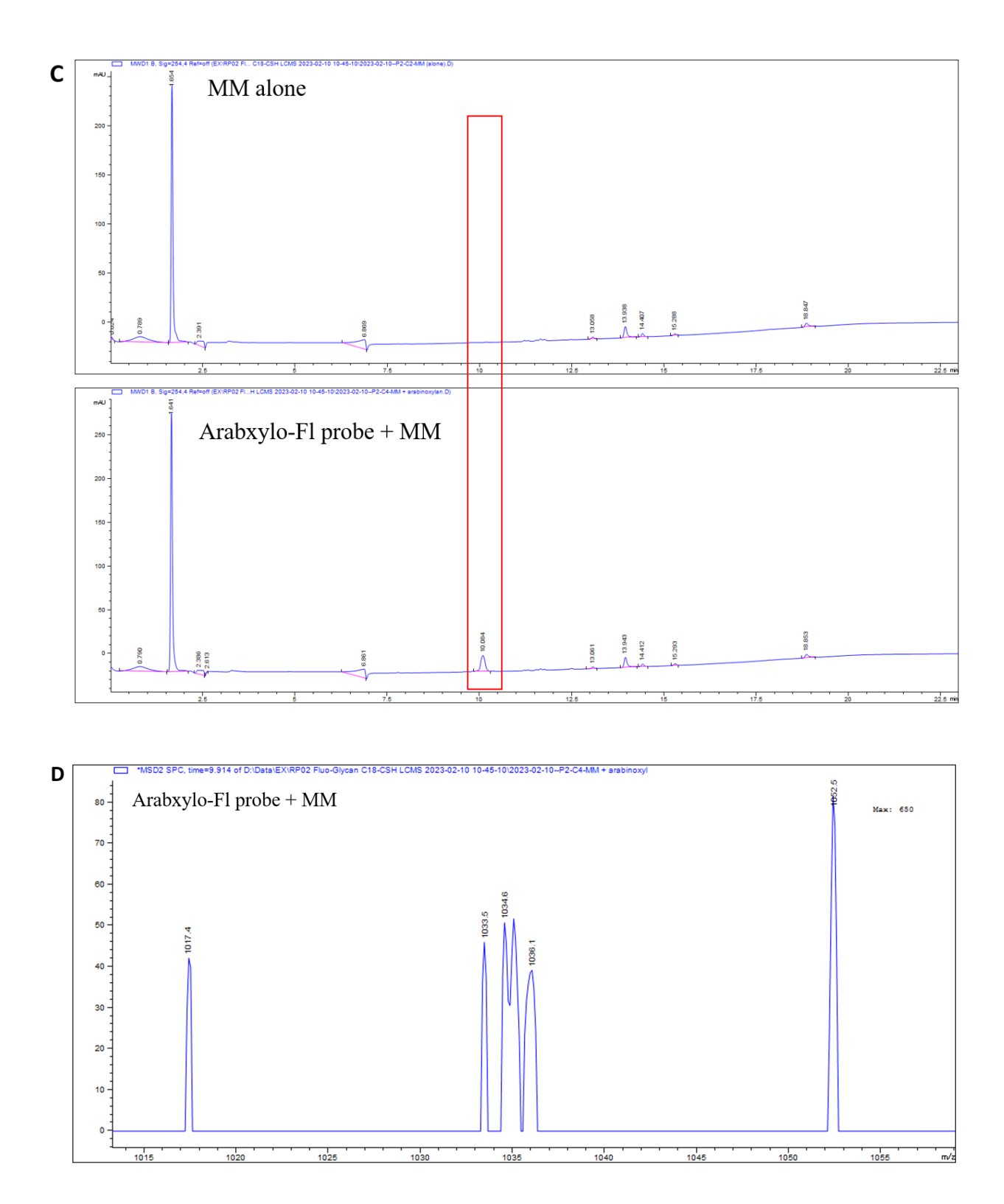


Figure 14.1. Spectra from Arabxylo-Fl (fluorescein-conjugated arabinoxylan) diluted in water and Minimum Medium (MM). A) High-performance liquid chromatography (HPLC) spectra of water alone

compared to Arabxylo-Fl and water, with the difference in the chromatogram spectra outlined in red. B) Liquid chromatography-mass spectrometry (LC-MS) spectrum of Arabxylo-Fl and water $[m/z \ (M-H)^- C_{46}H_{52}O_{27}$ calculated 1036.27, found 1035.3 from MSD2], retention time ~10 min. C) HPLC spectra of MM alone compared to Arabxylo-Fl and MM, with the difference in the chromatogram spectra outlined in red. D) LC-MS spectrum of Arabxylo-Fl and MM $[m/z \ (M-H)^- C_{46}H_{52}O_{27} \ calculated 1036.27, found 1034.6 from MSD2].$

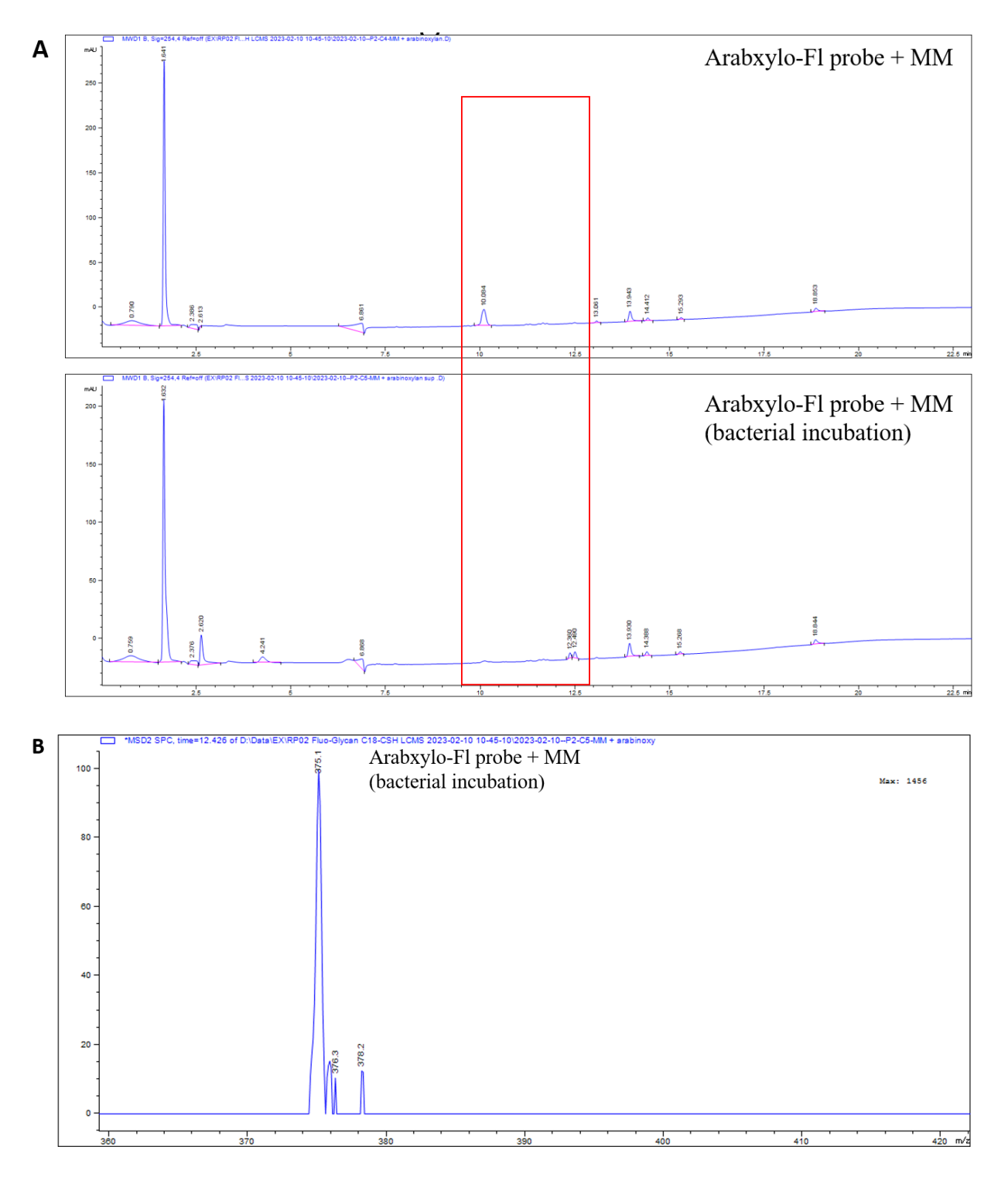


Figure 14.2. Spectra for the supernatant of Arabxylo-Fl (fluorescein-conjugated arabinoxylan) exposed to bacterial isolates resuspended in Minimum Medium (MM). A) High-performance liquid chromatography (HPLC) spectra of Arabxylo-Fl diluted in MM compared to supernatant, with the

difference in the chromatogram spectra outlined in red. B) Liquid chromatography-mass spectrometry (LC-MS) spectrum of supernatant [m/z (M-H) $^{-}$ C₂₁H₁₂O₇ calculated 376, found 375.1 from MSD2], retention time = ~12.

Figure 14.3. Structure of fluorescein molecule. $C_{21}H_{12}O_{7}$, exact mass = 376.06 g/mol.

3.7 Optimizing culture conditions to recover more diverse bacteria consumers of arabinoxylan

After confirming that our metabolic labeling workflow isolated arabinoxylan consumers, we proceeded to optimize the culturomics conditions to recover more diverse bacterial species that metabolize AX. In particular, our current workflow led to the isolation of mostly *Bacteroides* species ⁹⁰. This could be because the culture conditions resulted in a bias for these species. Moreover, research studies on the health impacts of dietary fiber primarily focus on *Bacteroides* species ¹¹⁵. Thus, we are interested in isolating AX consumers from the less-studied Firmicutes phylum. Lau *et al.* showed that extensive culturomics with a variety of specific growth media allows the isolation of a comprehensive portion of the gut microbiota, including less abundant bacteria that are difficult to be detected by sequencing ¹¹⁶. This research group tested stool samples on 33 media conditions and annotated the level of recovery of different

bacterial strains from each condition, which can be used to infer which media conditions are selective for Firmicutes¹¹⁶. We therefore selected Mannitol Salt Agar (MSA) and supplemented BHI (sBHI; termed BHI6 by Lau *et al.*) that showed a bias for Firmicutes for our next experiments.

To select against *Bacteroides*, antibiotic treatment was also performed on sorted Arabxylo-Fl⁺ cells. After comparing minimal inhibitory concentration (MIC) ranges for common antibiotics, clindamycin, chloramphenicol and lincomycin were concluded to be potential antibiotics to use. All three antibiotics have non-overlapping concentrations in their MIC ranges for *Bacteroides* and Firmicutes, allowing us to inhibit *Bacteroides* while selecting for Firmicutes (Table 2). Chloramphenicol was chosen due to availability of the antibiotic.

Table 2: Potential antibiotics to select for Firmicutes. MIC: Minimal Inhibitory Concentration

Bacteria	Antibiotic (MIC range in μg/mL)		
	Clindamycin	Chloramphenicol	Lincomycin
Bacteroides	0.006-8 ¹¹⁷⁻¹¹⁹	$0.5 - 16^{117 - 119}$	$0.125 - 6.25^{117,118}$
Firmicutes	0.1-256	0.5-500 (Clostridium)	2-1024
	(Clostridium) ¹¹⁹	119,120	(Lactobacillus) ¹²¹
	0.1-64		
	(Lactobacillus) 119		
	0.1-256		
	(Peptococcus) 119		

Following the metabolic labeling protocol for stool samples, Arabxylo-Fl⁺ cells were isolated from YM54 stool (3 technical replicate samples sorted for 5 min each, reaching approximately 25k sorted cells/sample) and immediately resuspended in MSA, sBHI or BHI + 10 µg/mL chloramphenicol (selective media were supplemented with 0.1% AX) and incubated at 37 °C. No visible growth was observed for all three conditions; however, after transferring an aliquot into ABB, there was a culture from sorted cells exposed to chloramphenicol, suggesting

that at this concentration of chloramphenicol, the antibiotic is bacteriostatic. In regard to MSA and sBHI, both media contain bactericidal agents, namely sodium chloride (NaCl) and propionic acid, respectively 122-124. Lau *et al* used 7.5% NaCl in MSA and 1% propionic acid in sBHI; the concentrations were lowered to 5% and 0.5%, respectively, to reduce the harsh nature of the selective media. Indeed, gram-positive bacteria are more resistant than gram-negative bacteria to these bactericidal agents; however, sorted bacteria are more vulnerable and my cultures demonstrate that no bacteria are viable in MSA and sBHI.

Labeled bacteria exposed to BHI + chloramphenicol and cultivated in ABB were isolated on MMe agar plates supplemented with AX (12 isolated clones). Prior to validating the phenotype with growth curves, DNA extracted from 2 of the 12 isolated clones, annotated clone A9 and A12 were amplified using group-specific primers for *Bacteroides fragilis* (Figure 9). Genomic DNA from both clones were amplified by the *Bacteroides* genus conserved primer. The gel had bands that were similar to *B. ovatus* CEX23001 and *B. xylanisolvens* CEX23002, suggesting these new isolated clones are *Bacteroides*. This was confirmed from Sanger sequencing of clone A9 and A12 (annotated *Bacteroides* sp. CEX23003); however, not enough genomic DNA was sequenced to identify the clones at the species level.

A second sort with YM54 stool was carried out, with 3 technical replicate samples sorted 5 min each (reaching approximately 30k sorted cells/sample) and were incubated in BHI at 37 °C. Aside from trying to recover more diverse bacterial species from the Firmicutes phyla, we also wanted to isolate bacteria with different rates of growth. Each sorted technical replicate sample was resuspended in BHI for one of the following amounts of time: 0 hours, 1 hour, and 24 hours or overnight. After the allotted incubation time, the cultures were distributed into media selective for Firmicutes species (each supplemented with 0.1% AX): MSA, sBHI, and

supplemented Cooked Meat Broth (sCMB)¹¹⁴ (Figure 15). MSA and sBHI for this new sort were adjusted with a lower concentration of NaCl and propionic acid, respectively. Visible bacterial growth was observed for tubes incubated in BHI for 1 hour and overnight; however, only BHI cultures transferred to sCMB resulted in a culture. MSA and sBHI cultures had no growth as passage and incubation in ABB for up to 72 hours did not yield a culture.

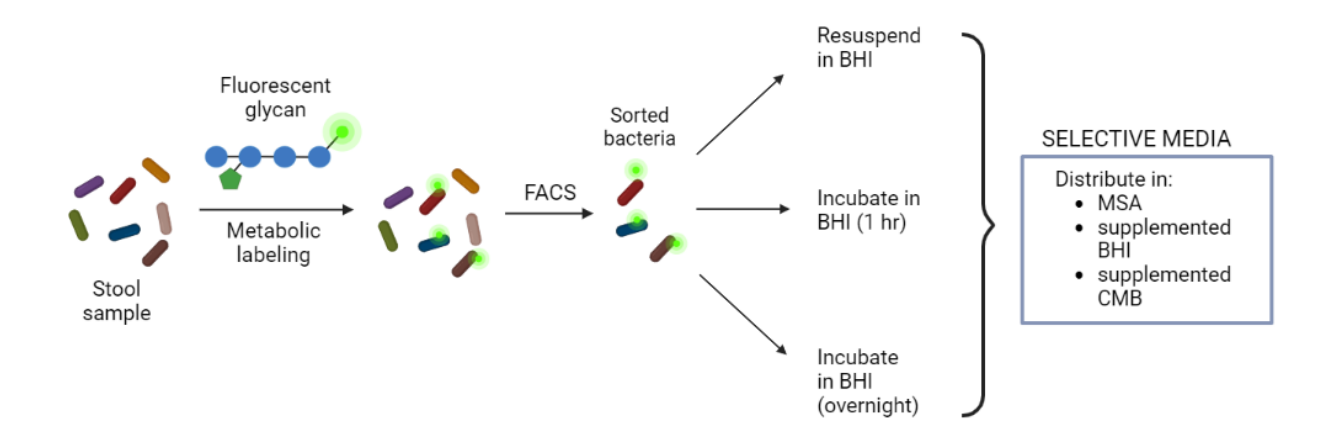
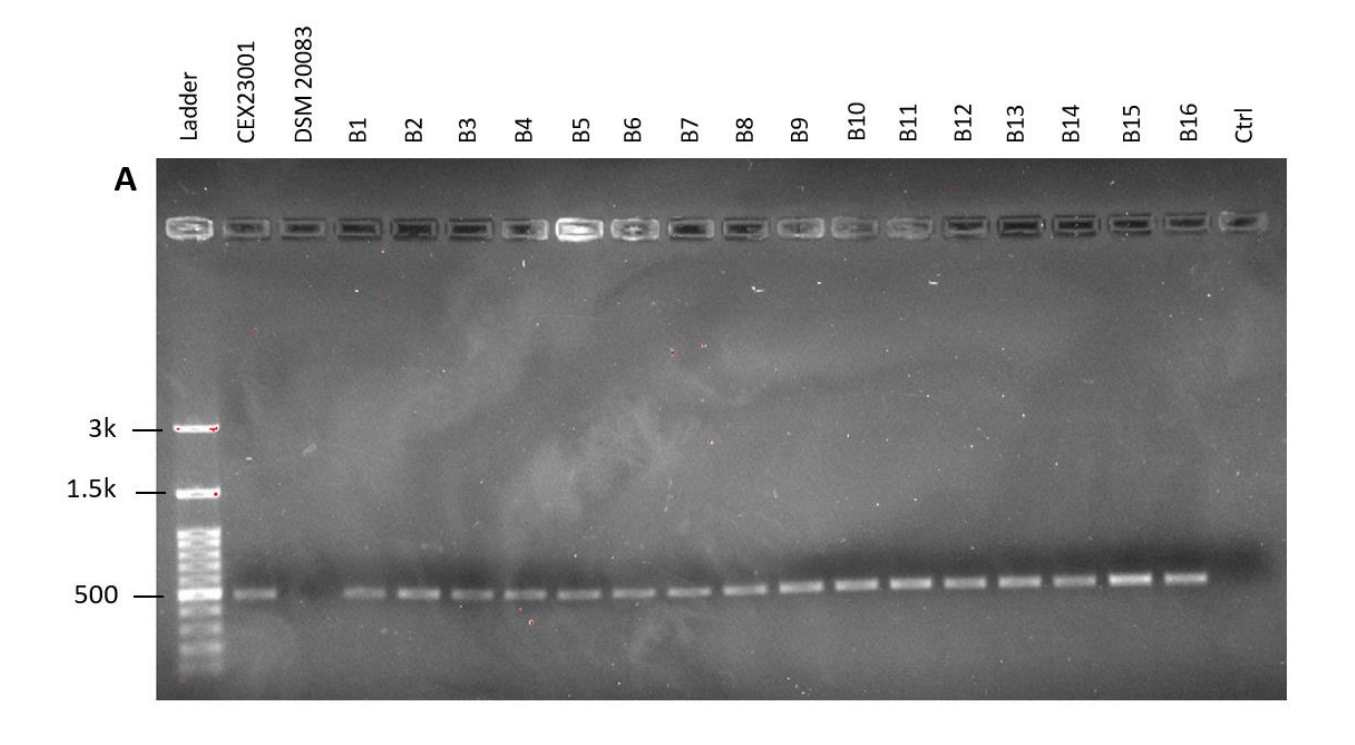
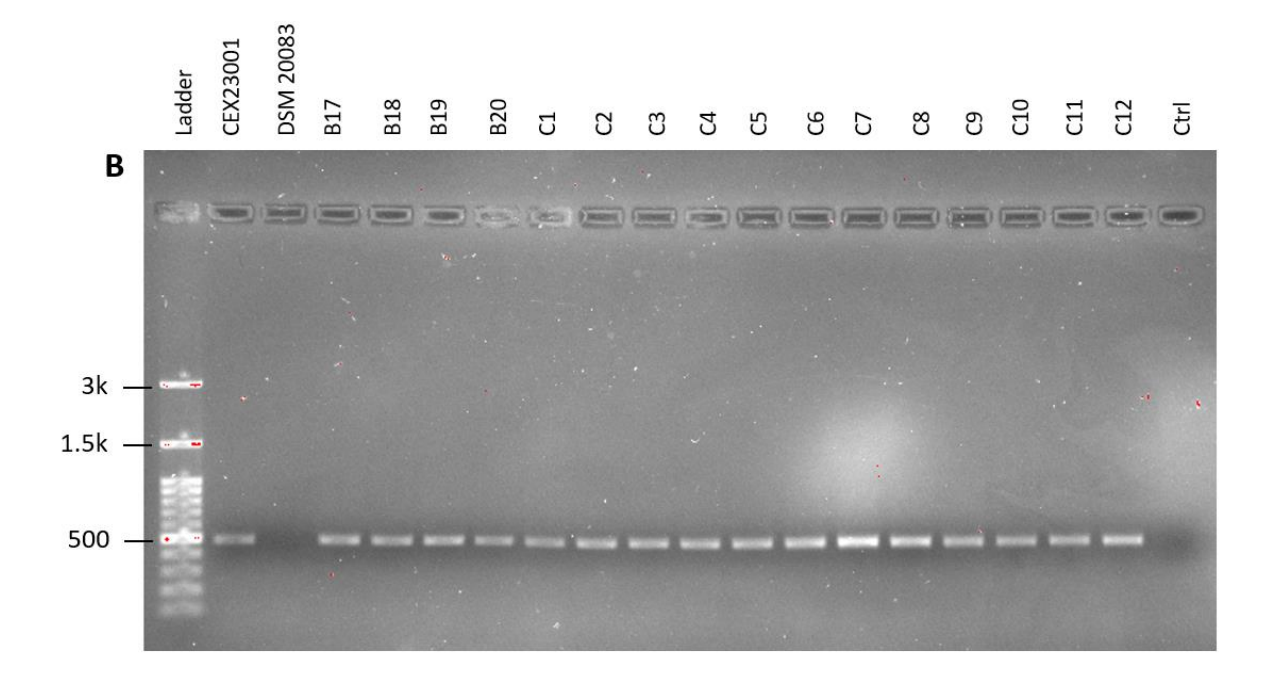


Figure 15. Metabolic labeling coupled with Fluorescence-activated Cell Soring (FACS) and extensive culturomics conditions targeting Firmicutes using selective media and fast vs. slow growing bacteria (incubation in Brain Heart Infusion (BHI) for different amounts of time). MSA: Mannitol Salt Agar; CMB: Cooked Meat Broth.

sCMB culture was further transferred into MM + 0.1% AX (liquid and agar) to isolate clones. 40 clones were isolated (annotated as clone B1-20 and C1-20) and screened using a colony PCR with group-specific primers for *Bacteroides fragilis*, to ensure they were not *Bacteroides*. Controls for the colony PCR included *B. ovatus* CEX23001 (positive control), *Bifidobacterium adolescentis* DSM 20083 and water (negative controls). The resulting gel presented bands for all isolated clones and an absence of a band for *B. adolescentis* DSM 20083

and water, thus demonstrating that sCMB media was unsuccessful at selecting for Firmicutes (Figure 16).





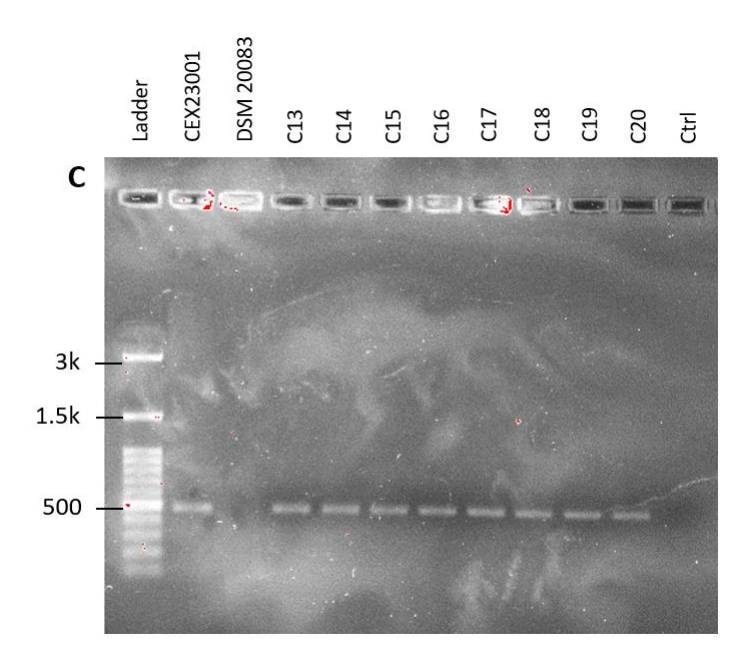


Figure 16. Colony Polymerase Chain Reaction (PCR) of bacterial isolates cultured in supplemented Cooked Meat Broth + 0.1% arabinoxylan (AX) and isolated from Minimum Medium + 0.1% AX.

A) Clones B1-16 B) Clones B17-20 and C1-12 C) Clones C13-20. *B. ovatus* CEX23001, *B. adolescentis* DSM 20083, and water (ctrl) were control samples. The bacterial isolates were amplified using group-specific primers for *Bacteroides fragilis* with expected product lengths of ~500 bp.

3.8 Susceptibility assessment of *Bacteroides* sp. CEX23003 to chloramphenicol

The concentration of chloramphenicol chosen was in accordance to reported MIC ranges for *Bacteroides* and Firmicutes; yet, viable *Bacteroides* species were still selected from FACS sorted cells. Possible explanations for this result that the isolated bacteria are resistant to chloramphenicol or the concentration applied to sorted cells was too low as MIC ranges for *Bacteroides* are reported to range up to 16 µg/mL. Susceptibility tests for *Bacteroides* sp. CEX23003 were evaluated (Figure 17).

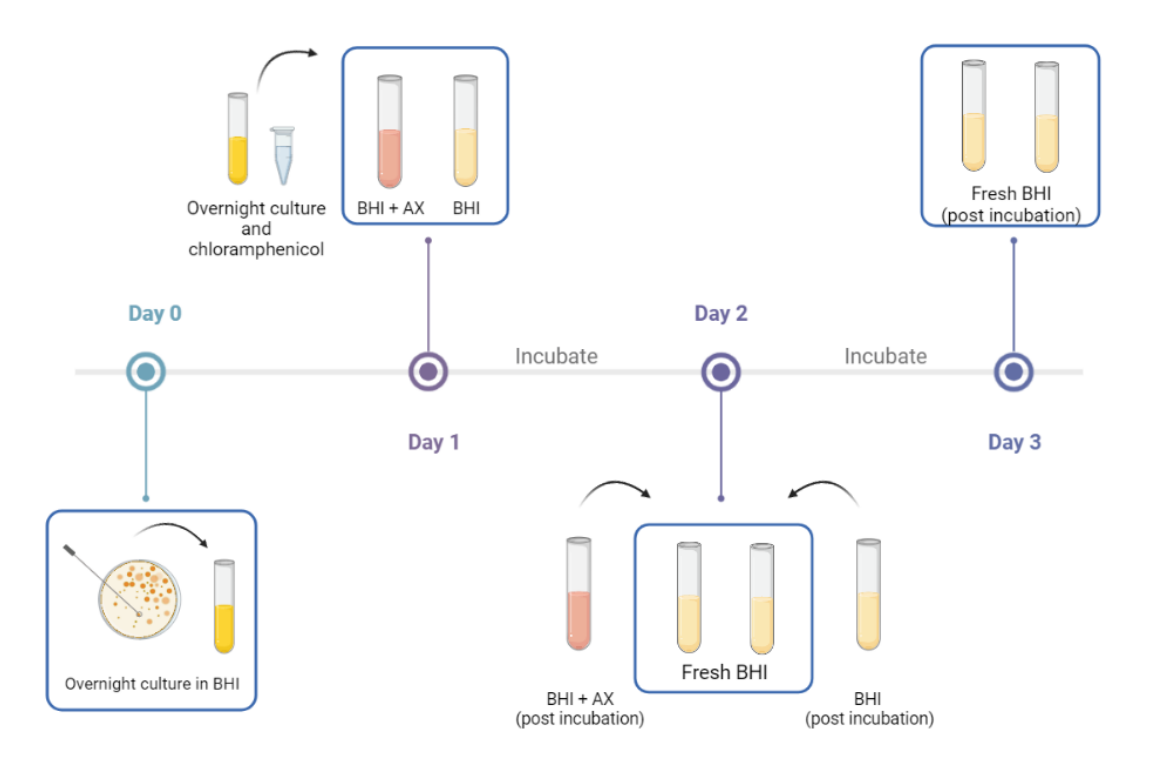


Figure 17. Outline of susceptibility assessment for *Bacteroides* **sp. CEX23003.** The optical density (measured at 600 nm) of cultures and negative controls (media without bacteria inoculum) were measured before and after each incubation period. BHI: Brain Heart Infusion; AX: Arabinoxylan.

An aliquot of overnight culture of *Bacteroides* sp. CEX23003 was transferred into BHI + 0.1% AX or BHI alone, both supplemented with different concentrations of chloramphenicol. The samples were incubated at 37 °C for 24 hours before being transferred and incubated in fresh BHI for another 24 hours. Supplementation of treatment tubes with AX mimics the conditions Arabxylo-Fl⁺ cells were exposed to. No visible growth was observed in initial tubes with chloramphenicol but growth was observed after passage and incubation of cultures in fresh BHI for all treatment tubes exposed to 10 and 20 µg/mL, and some growth in the samples exposed to both 30 µg/mL and AX (Figure 18). The results suggest that the concentration of chloramphenicol used for culturomics was insufficient to select out *Bacteroides* species.

Concentrations for chloramphenicol were chosen based on MIC ranges, but it is important to note that MIC measures the minimal concentration inhibiting visible growth or a bacterial suspension in an overnight culture 125 . Clear bacterial suspensions do not always signify lack of viable bacteria in the culture, as evident from our results demonstrating that chloramphenicol is bacteriostatic at $10 \,\mu\text{g/mL}$. In comparison, the minimal bactericidal concentration (MBC) is the concentration in which an antibiotic kills the bacteria 125 . Interestingly, growth was observed in the samples with AX at $30 \,\mu\text{g/mL}$ but not in BHI alone. This could suggest that the glycan has some protective benefits against the bactericidal activity of the antibiotic at $30 \,\mu\text{g/mL}$. However, the sample size is too small to reliably determine if this is a significant difference.

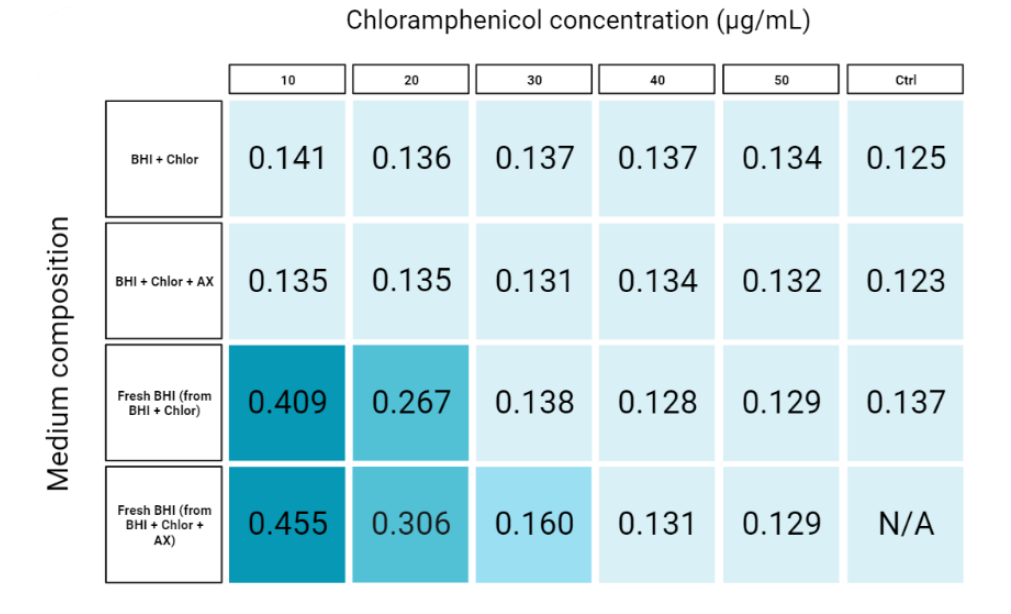


Figure 18. Susceptibility assessment of *Bacteroides* sp. CEX23003 to chloramphenicol (chlor) in the presence or absence of arabinoxylan (AX) represented by optical density values (measured at 600 nm). Values presented were measured after incubation. Negative controls (ctrl) are medium conditions

alone without bacteria inoculation. The control for Brain Heart Infusion (BHI) was measured once, hence the space filled with N/A instead. N=1.

4. DISCUSSION

This thesis investigated the use of human gut microbiota metabolic labeling using fluorescein-conjugated arabinoxylan coupled to FACS and culturomics to isolate putative arabinoxylan consuming bacteria. The functional growth phenotype of labeled bacteria was verified through growth curves in defined media and cross-checking the predicted PULs of bacterial isolates to genes reported to be involved in AX metabolism.

Previous work by Dridi et al. showed successful isolation of FOS and GMP consumers from stool samples by cultivating sorted cells on rich agar media like BHI, ABB or TSA supplemented with 5% sheep blood 90. Surprisingly, the application of this isolation method to Arabxylo-Fl⁺ cells, specifically isolating labeled bacteria on ABB, yielded no AX consumers after isolated clones were assessed using growth curves (Figure 6A). This result was unexpected because sorted cells grew in liquid MM supplemented with 0.1% AX as a sole carbon source, as the medium had a turbid suspension after incubation, indicating the presence of AX consumers among the labeled bacteria. Growth curves for bacterial isolates used the same conditions, inoculating isolates in MM + 0.1% AX, but the phenotype observed for the mixed bacterial community differed from the growth phenotype of bacterial isolates. We investigated whether bacterial isolates required more nutrients to make it favourable for the bacterial isolates to metabolize AX in MM, a medium that only has the minimum nutrients for anaerobic bacteria to survive. Dridi et al. showed that uptake of fluorescently-labeled glycan probes is an energydependent process, hence in a nutrient poor environment, it can become unfavourable to upregulate and synthesize enzymes to metabolize glycans if viability is a priority over growth 90,126. However, even after using a richer carbohydrate-free medium, ABBc, to substitute for MM, there was no significant difference observed between bacteria grown in ABBc alone

and ABBc supplemented with glycans (Figure 6B). These results suggest either that ABBc is too rich in nutrients, therefore leading to high bacterial growth regardless of the presence of a glycan. A potential explanation is that the bacterial isolates are not able to metabolize AX, which is possible as the metabolic labeling workflow has been previously shown to label nonconsumers as well⁹⁰. Dridi e al. speculated that bacterial strains that were labeled but unable to metabolize the glycan activated PULs for a structurally related substrate, as surface proteins and transporters can have promiscuous binding specificity but GHs are more specific 90,109,127. Alternatively, maybe fluorescent glycans bound to proteins upstream of quorum-sensing pathways rather than upregulating glycan degradation enzymes, as observed with fucose utilization in pathogenic bacteria^{90,128}. Another possible explanation is the mixed cultures of cells were growing on MM supplemented with AX using cross-feeding, but that no single isolates could derive energy from AX alone⁶³. Regardless, while sorted bacteria are enriched using AX containing media, there can still be non-consumers present in the background, surviving on nutrients from MM. Both consumers and non-consumers in the liquid culture will form colonies on a rich agar medium. However, it is not possible to differentiate them on the plate. Indeed, here a selective MM + AX agar media turned out to be important to separate glycan consumers from non-consumers in liquid culture and allow for isolation of only AX consumers (Figure 7).

The isolated clones that were clear consumers were identified by nanopore and Sanger sequencing of the 16S rRNA gene (Table 1) as being two *Bacteroides* species, namely *B. ovatus* CEX23001 and *B. xylanisolvens* CEX23002. *Bacteroides* species have been reported as arabinoxylan consumers in the literature; specifically, *B. ovatus* ATCC 8483 and *B. xylanisolvens* XB1A have characterized PULs with AX degradation activity. Furthermore, we looked at the published genomes of strains closest to our two isolates in terms of 16S to

determine if they had genes consistent with AX metabolism (Figure 12). Indeed, PULs consistent with that activity could be found in the published genomes of the closest strains of *B. ovatus* CEX23001 and *B. xylanisolvens* CEX23002.

The final validation experiment involved metabolically labeling the bacterial isolates with the Arabxylo-Fl probe. Interestingly, the bacterial isolates were poorly labeled by Arabxylo-Fl but had a much higher percentage of cells labeled by CD-Fl, a probe used previously 90 (Figure 13.1A: 0.016% Arabxylo-Fl⁺ vs. 18.4% CD-Fl⁺; Figure 13.1B: 0% Arabxylo-Fl⁺ vs. 19.3% CD-Fl⁺). Heat inactivation experiments reduced the percentage of cells labeled by CD-Fl (Figure 13.3), suggesting that the fluorescent labeling was indeed due to specific uptake of the glycan probe and that the poor labeling with Arabxylo-Fl in bacterial isolates is independent of the metabolic labeling protocol itself. This was surprising since validation experiments with growth curves clearly support the conclusion that the clones are AX consumers. However previous work by Dridi et al. showed that Bacteroides isolates were not labeled as much as other bacterial species even when they are clear consumers of the glycan. For instance, labeling was low for Bacteroides uniformis CLD22005 incubated with NYST-Fl but there was still some fluorescent labeling⁹⁰. Additionally, Hehemann *et al.* observed heterogeneity when labeling pure cultures of B. thetaiotaomicron, in which some cells had high fluorescence yet others did not get labeled 105. The research group attributed this heterogeneity to differences in probe uptake efficiency in a bacteria population. It is possible that a similar phenomenon is occurring for isolates incubated with Arabxylo-Fl.

The next step was to assess if the root of the problem was due to the integrity of the Arabxylo-Fl probe itself, such as testing if the fluorescein molecule was still properly conjugated to the arabinoxylotetraose molecule in the probe. The integrity of the probe was investigated by

diluting Arabxylo-Fl in water or MM, in which the composition of the mixture was analyzed using HPLC and LC-MS (Figure 14.1). From the mass spectra, a peak corresponding to an Arabxylo-Fl probe was observed. B. ovatus CEX23001 culture was also resuspended in MM and incubated with the Arabxylo-Fl probe for 1 hour, after which the supernatant from the culture yielded a different HPLC spectrum than probe in water or MM (Figure 14.2). The spectra showed a disappearance of a peak corresponding to the intact probe and the appearance of a peak matching the mass of a free fluorescein molecule (Figure 14.3). Rather than the Arabxylo-Fl probe having a defective conjugation, the probe was actually degraded by the bacteria, leaving the free fluorescein molecule in the medium rather than taken up by the bacteria. Alternatively, the fluorescent conjugate might be taken up and cleaved within the periplasm and the free fluorescein released back into the media. This would prevent the accumulation of the fluorescein in the bacterial periplasm, which is necessary for labeling ^{105,106}. Thus, the difference in fluorescent labeling could be attributed to an insufficient probe concentration and low accumulation of dye in cells, or the extensive and rapid AX probe metabolism resulting in efflux of fluorescein in our two *Bacteroides* consumers.

It would be useful to know whether the Arabxylo-Fl probe was being cleaved by the bacteria using surface structures or if the probe was cleaved inside the cell and the fluorescein products effluxed afterwards. To distinguish between these two possible mechanisms, a large increase in probe concentration could be administered to increase dye accumulation in bacterial isolates, followed by fixation methods to preserve the surface ultrastructure of bacterial isolates, such as through the use of paraformaldehyde (PFA). Fixation would prevent any cleaved fluorescein from being transported out of the cell¹²⁹. Flow cytometry analysis would detect a fluorescent

signal after fixation if the probe is transported into the bacteria before cleavage, or a lack of a signal if surface enzymes cleave the probe without uptake of the glycan probe.

The first putative AX consumers isolated in this thesis using the metabolic labeling workflow were all Bacteroides species. Not only is this consistent with known Bacteroides species that consume AX^{66,111}, but it is also consistent with the known glycan metabolism potential of the Bacteroidetes phylum. Indeed, dietary fiber degradation by bacteria from the Bacteroidetes phylum has been widely studied¹¹⁵. Bacteroidetes are proficient glycan consumers evident from the large number of CAZymes encoded in their genomes compared to other phyla¹³⁰. Culturomics medium conditions were optimized in an attempt to isolate a more diverse array of AX consumers, in particular selecting for bacteria from the Firmicutes phylum. Three selective media were chosen based on the extensive medium compositions Lau et al. screened: MSA, supplemented BHI, and supplemented CMB¹¹⁶. The selective media were chosen based on data compiled by Lau et al. presenting the specific media that different bacteria families prefer, in which MSA, sBHI and sCMB were shown to be preferred by Firmicutes¹¹⁶. In addition, the components of the three media are known and can be modified if necessary, allowing more control for optimization of culturomics. Sorted cells from a stool sample were diluted in BHI before being resuspended in selective media supplemented with AX. This differs from B. ovatus CEX23001 and B. xylanisolvens CEX23002, both of which were resuspended in ABB with AX after FACS. In particular, the new sorted cells were incubated in BHI for 3 different amounts of time to allow for selection of bacteria with different rates of growth: 0 hours (immediately resuspended in selective media after dilution with BHI), 1 hour or 24 hours. However, only sorted cells incubated in sCMB resulted in a culture (for all BHI incubation times). In addition, the medium was unable to select for Firmicutes as bacterial isolates were all *Bacteroides* species

(Figure 16). An explanation for the unsuccessful selection of Firmicutes after metabolic labeling may be the harsh agents in MSA and sBHI, namely NaCl and propionic acid, respectively.

Bacteria that are sorted through FACS are in a vulnerable state due to the exposure of these anaerobic bacteria to oxygen. While gram-positive Firmicutes are generally more resistant to these harsh agents than gram-negative bacteria, the results demonstrate that no sorted bacteria are viable in MSA and sBHI¹²²⁻¹²⁴. sCMB on the other hand is a nutrient rich medium with ingredients that are favoured by Firmicutes and *Bacteroides*, yet only *Bacteroides* species were recovered after culturomics. Perhaps there were no Firmicutes among the Arabxylo-Fl⁺ cells or the stool sample itself had low bacteria diversity. The relative abundance of bacteria present in the stool sample was characterized using nanopore sequencing of the 16S rRNA gene (Figure 19). Sequencing data shows that there are indeed Firmicutes present in the stool sample; however, it is unclear whether this diversity is present in the viable cell population as DNA can be extracted from both live and dead bacteria⁹⁹.

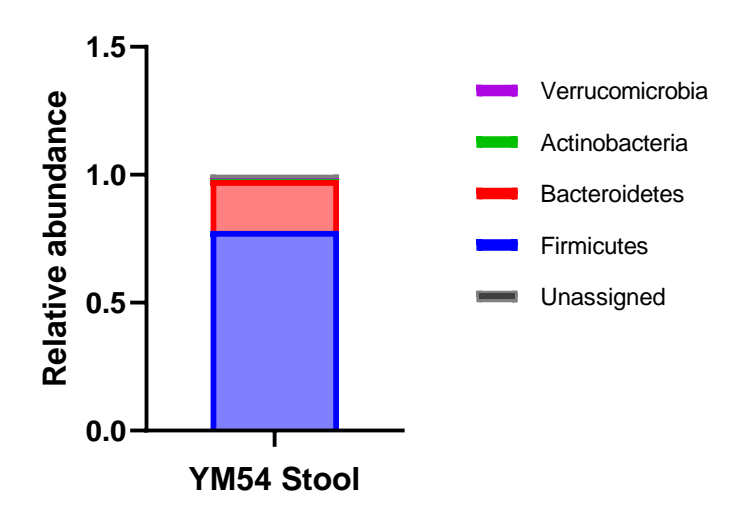


Figure 19. Relative abundance of phyla in a donor stool sample.

A final selective medium condition consisted of BHI supplemented with chloramphenicol (10 µg/mL) in order to select against *Bacteroides* and *Bifidobacteria*, two types of bacteria that have been largely isolated from the metabolic labeling workflow⁹⁰. Sorted bacteria were resuspended in BHI + chloramphenicol supplemented with AX before being isolated on solid MM supplemented with AX. While the antibiotic concentration was chosen based on MIC ranges targeting against Bacteroides and Bifidobacteria, the bacterial isolates were still Bacteroides species (Figure 9). A susceptibility test of the bacterial isolate Bacteroides sp. CEX23003 against 5 concentrations of chloramphenicol (Figure 17) showed that the antibiotic was bacteriostatic where bacteria were able to grow after antibiotic exposure even at a concentration above 10 µg/mL (Figure 18). Specifically, the bacteria grew in 10 and 20 µg/mL of antibiotic without AX, and there was some growth up to 30 µg/mL when antibiotic was supplemented with AX (Figure 18). The results demonstrated that in the absence of AX, the antibiotic was bactericidal at a lower concentration (20 µg/mL) than in the presence of AX (bactericidal above 30 µg/mL), suggesting that the bacteria were protected from chloramphenicol due to the presence of the glycan^{131,132}. Similarly, Cabral et al. showed that fiber supplementation was protective against antibiotics when B. thetaiotaomicron had an increase in tolerance to amoxicillin in the presence of a polysaccharide¹³¹. The isolates seem to have better growth after exposure to chloramphenicol in the presence of AX; however, this experiment would need to be replicated to determine the significance of the growth difference. BHI is an undefined medium that can also have glycans, leading to protection against chloramphenicol ¹³³.

The work of this thesis has demonstrated the usefulness of metabolic labeling coupled with FACS and culturomics to isolate AX consumers from human stool samples. The use of stool samples as a proxy for the gut microbiota is beneficial due to the non-invasive nature of the

collection method in comparison to endoscopies and biopsies¹³⁴. However, the distribution of the microbes in the intestine cannot be inferred from stool samples, in particular whether the bacteria naturally colonize the gut lumen or the mucosal lining, and if the natural niche environment is more proximal or distal along the intestine¹³⁵. Despite these limitations, fecal samples are a convenient source of gut microflora, and the bacterial viability and microbial composition can be preserved by freezing samples at -80 °C^{134,135}. Using stool samples, AX consumers were isolated and the AX metabolism phenotype of bacterial isolates was verified using growth curves. Further investigation is still needed to have a better understanding of the molecular mechanisms involved with glycan probe uptake, such as in the case of bacterial isolates cleaving fluorescein from the probe. Moreover, culturomics needs further optimization to allow for isolation of bacteria from the Firmicutes phylum and investigate arabinoxylan metabolism in new consumers. In this thesis, Firmicutes were selected from Arabxylo-Fl⁺ cells after FACS. Another method would be to enrich for Firmicutes before labeling with the fluorescent glycan probe, which would avoid exposing already vulnerable sorted bacteria to harsh selective media.

5. CONCLUSION

Prebiotic glycans are an attractive therapeutic for gut health as they directly modulate the composition of the endogenous gut microbiota of an individual. Yet, current research on glycan metabolism in the gut microbiota and the functional implications of metabolites is insufficient and incomplete. In particular, a better understanding as to how glycan supplementation can lead to health benefits and which bacteria contribute to this is needed.

The application of metabolic labeling with fluorescently-labeled glycans with FACS and culturomics can isolate specific glycan consumers from the human gut microbiota. The work presented in this thesis focused on isolation of gut bacteria capable of metabolizing arabinoxylan; however, this workflow is not confined to investigating this glycan and can be expanded to isolate gut bacteria that consume other understudied complex glycans, such as pectins, xylans, and galactomannans. In addition, AX consumers were isolated from one healthy human stool sample (YM54) from one sorting session. Future investigations can increase the reliability and scope of AX consumers isolated by increasing the number of sort sessions per stool sample (n = 3 or 4). Given the inter-individual variability that exists in the gut microbiota composition, the results are also restricted to the bacterial community of one individual n = 3 or 4. By testing this workflow on different stool samples, there is an increased chance of isolating different glycan consumers.

It is also important to note that a limitation of the metabolic labeling workflow is its bias towards selecting for primary glycan consumers. Dridi *et al.* showed that fluorescein-conjugated glycans synthesized from monosaccharides (glucose-Fl) and disaccharides (maltose-Fl) were poorly labeled in comparison to oligosaccharides (CD-Fl)⁹⁰. One explanation for this is that the large fluorescein tag interferes with recognition of the glycan by glycan-binding motifs or

transport of the glycan across the cell membrane. The workflow excludes isolation of secondary glycan consumers that depend on metabolites produced through the cross-feeding effect^{62,63}. Gut bacteria are members of a community in the *in vivo* intestinal environment, but our workflow is unable to isolate glycan consumers involved in cross-feeding behaviour and interactions with other bacteria.

The work from this thesis demonstrated that the metabolic labeling workflow can efficiently progress from sorted glycan⁺ cells to isolated putative glycan consumers; however, further optimization is needed to isolate more diverse glycan consumers. While healthy human stool samples were investigated in this thesis, we can expand our protocol to isolate glycan consumers from a relevant patient population and feed the bacterial isolates back into animal disease models to assess whether the isolate is responsible for health benefits. Previous work by Routy et al. on ICIs for cancer immunotherapy showed the benefit of Akkermansia muciniphila for efficacious cancer treatment. Oral supplementation of A. muciniphila restored efficacy to treatment in germ-free mice that received FMTs from cancer patients not responding to ICI cancer immunotherapy¹³⁶. A. muciniphila is an example of a bacterial isolate that can be targeted by camu camu (a prebiotic polyphenol) for proliferation to lead to a health benefit¹³⁷. While Routy et al. demonstrated the benefit of a probiotic strain stimulated by a polyphenol¹³⁶, our metabolic labeling workflow can guide the recognition of beneficial probiotics, which can ultimately be targeted through prebiotic glycan supplementation or symbiotic combinations. Future in vivo work will help distinguish between glycans proliferating beneficial bacteria strains from glycans stimulating detrimental effects, such as proliferation of pathogenic bacteria like C. difficile. Isolation of glycan consumers using our metabolic labeling workflow could contribute to downstream applications of bacterial isolates in a clinically relevant context.

REFERENCES

- 1. Ursell, L. K., Metcalf, J. L., Parfrey, L.W., & Knight, R. Defining the human microbiome. *Nutr Rev* **70**, 38-44, doi: 10.1111/j.1753-4887.2012.00493.x (2012).
- 2. Wang, B., Yao, M., Lv, L., Ling, Z., &Li, L. The Human Microbiota in Health and Disease. *Engineering* **3**, 71-82, doi: 10.1016/J.ENG.2017.01.008 (2017).
- 3. Friedrich, M. J. Genomes of Microbes Inhabiting the Body Offer Clues to Human Health and Disease. *JAMA* **309**, 1447-1449, doi:10.1001/jama.2013.2824 (2013).
- 4. Marchesi, J. R. Prokaryotic and Eukaryotic Diversity of the Human Gut. *Adv Appl Microbiol* **72**, doi: 10.1016/S0065-2164(10)72002-5 (2010).
- 5. Turnbaugh, P., *et al.* The Human Microbiome Project. *Nature* **449**, 804–810, doi: 10.1038/nature06244 (2007).
- 6. O'Hara, A. M. & Shanahan, F. The gut flora as a forgotten organ. EMBO Rep 7 (2006).
- 7. Ley, R. E., Peterson, D. A., & Gordon, J. I. Ecological and evolutionary forces shaping microbial diversity in the human intestine. *Cell* **124**, 837-848, doi:10.1016/j.cell.2006.02.017 (2006).
- 8. Harmsen, H.J.M. & de Goffau, M.C. The Human Gut Microbiota. *Adv Exp Med Biol Advances in Experimental Medicine and Biology* **902**, doi: 10.1007/978-3-319-31248-4_7 (2016)
- 9. Koppel, N. & Balskus, E. P. Exploring and Understanding the Biochemical Diversity of the Human Microbiota. *Cell Chem Biol* **23**, 18-30, doi: 10.1016/j.chembiol.2015.12.008 (2016).
- 10. Rowland, I., *et al.* Gut microbiota functions: metabolism of nutrients and other food components. *Eur J Nutr* **57**, 1–24, doi: 10.1007/s00394-017-1445-8 (2018).
- 11. Jandhyala, S. M. *et al.* Role of the normal gut microbiota. *World J Gastroenterol* **21**, 8787-8803, doi: 10.3748/wjg.v21.i29.8787 (2015).
- 12. Koropatkin, N. N., Cameron, E. A., & Martens, E. C. How glycan metabolism shapes the human gut microbiota. *Nat Rev Microbiol* **10**, 323-335, doi:10.1038/nrmicro2746 (2012).
- 13. El Kaoutari, A., Armougom, F., Gordon, J. I., Raoult, D., & Henrissat, B. The abundance and variety of carbohydrate-activated enzymes in the human gut microbiota. *Nat Rev Microbiol* **11**, 497-504, doi: 10.1038/nrmicro3050 (2013).
- 14. Tlaskalova-Hogenova, H., *et al.* Development of immunological capacity under germfree and conventional conditions. *Ann N Y Acad Sci* **409**, 90-113, doi: 10.1111/j.1749-6632.1983.tb26862.x (1983).
- 15. Thursby, E. & Juge, N. Introduction to the human gut microbiota. *Biochem J* **474**, 1823-1936, doi: 10.1042/BCJ20160510 (2017).
- 16. Rinninella, E., *et al.* What is the Healthy Gut Microbiota Composition? A Changing Ecosystem across Age, Environment, Diet, and Diseases. *Microorganisms* **7**, 14, doi: 10.3390/microorganisms7010014 (2019).
- 17. Rothschild, D., *et al.* Environment dominates over host genetics in shaping human gut microbiota. *Nature* **555**, 210–215 (2018).
- 18. Schippa, S. & Conte, M. P. Dysbiotic Events in Gut Microbiota: Impact on Human Health. *Nutrients* **6**, 5786-5805, doi: 10.3390/nu6125786 (2014).

- 19. Walker, W. A. Dysbiosis: The Microbiota in Gastrointestinal Pathophysiology. 227-232, doi: 10.1016/B978-0-12-804024-9.00025-2 (2017).
- 20. Hawrelak, J. A. & Myers, S. P. The causes of intestinal dysbiosis: a review. *Altern Med Rev* **9**, 180-197 (2004).
- 21. Lamberte, L. E. & van Schaik, W. Antibiotic resistance in the commensal human gut microbiota. *Curr Opin Microbiol* **68**, 102150, doi: 10.1016/j.mib.2022.102150 (2022).
- 22. Petersen, C. & Round, J. L. Defining dysbiosis and its influence on host immunity and disease. *Cell Microbiol* **16**, 1024-1033, doi: 10.1111/cmi.12308 (2014).
- 23. Chan, Y. K., Estaki, M., & Gibson, D. L. Clinical consequences of diet-induced dysbiosis. *Ann Nutr Metab* **63**, 28-40, doi: 10.1159/000354902 (2013).
- 24. Turnbaugh, P. J., *et al.* The effect of diet on the human gut microbiome: a metagenomic analysis in humanized gnotobiotic mice. *Sci Transl Med* **1**, 6-14, doi: 10.1126/scitranslmed.3000322 (2009).
- 25. Rinninella, E., *et al.* Food Components and Dietary Habits: Keys for a Healthy Gut Microbiota Composition. *Nutrients* **11**, 2393, doi: 10.3390/nu11102393 (2019).
- 26. Craven, M., *et al.* Inflammation drives dysbiosis and bacterial invasion in murine models of ileal Crohn's Disease. *PLoS One* **7**, e41594, doi: 10.1371/journal.pone.0041594 (2012).
- 27. Buttó, L. F. & Haller, D. Dysbiosis in intestinal inflammation: Cause or consequence. *Int J Med Microbiol* **306**, 302-309, doi: 10.1016/j.ijmm.2016.02.010 (2016).
- 28. Patterson, E., *et al.* Gut microbiota, the pharmabiotics they produce and host health. *PNS* **73**, 477-489, doi: 10.1017/S0029665114001426 (2014).
- 29. Isolauri, E. Development of a healthy gut microbiota in early life. *J Paediatr Child Health* **48**, 1-6, doi:10.1111/j.1440-1754.2012.02489.x (2012).
- 30. Altamura, F., Maurice, C. F., & Castagner, B. Drugging the gut microbiota: toward rational modulation of bacterial composition in the gut. *Curr Opin Chem Biol* **56**,10-15, doi: 10.1016/j.cbpa.2019.09.005 (2020).
- 31. Mayer, E. A., Tillisch, K., & Gupta, A. Gut/brain axis and the microbiota. *J Clin Investig* **125**, 926-938, doi: 10.1172/JCI76304 (2015).
- 32. Carding, S., Verbeke, K., Vipond, D. T., Corfe, B. M. & Owen, L. J. Dysbiosis of the gut microbiota in disease. *Microb Ecol Health Dis* **26**, 26191, doi: 10.3402/mehd.v26.26191 (2015).
- 33. Turnbaugh, P. J., *et al.* An obesity-associated gut microbiome with increased capacity for energy harvest. *Nature* **444**, 1027-1031, doi: 10.1038/nature05414 (2006).
- 34. Harach, T., *et al.* Reduction of Abeta amyloid pathology in APPPS1 transgenic mice in the absence of gut microbiota. *Sci Rep* **7**, 41802, doi: 10.1038/srep41802 (2017).
- 35. Sasaguri, H., *et al.* APP mouse models for Alzheimer's disease preclinical studies. *EMBO J* **36**, 2473-2487, doi: 10.15252/embj.201797397 (2017).
- 36. Gagliardi, A., *et al.* Rebuilding the Gut Microbiota Ecosystem. *IJERPH* **15**, 1679, doi: 10.3390/ijerph15081679 (2018).
- 37. Zhang, Y., Fleur, A. S., & Feng, H. The development of live biotherapeutics against *Clostridium difficile* infection towards reconstituting gut microbiota. *Gut Microbes* **14**, e2052698, doi: 10.1080/19490976.2022.2052698 (2022).

- 38. Gupta, S., Allen-Vercoe, E., & Petrof, E. O. Fecal microbiota transplantation: in perspective. *Therap Adv Gastroenterol* **9**, 229-239, doi: 10.1177/1756283X15607414 (2016).
- 39. Smits, W. K., Lyras, D., Lacy, D. B., Wilcox, M. H., & Kuijper, E. J. *Clostridium difficile* infection. *Nat Rev Dis Primers* **2**, 16020, doi: 10.1038/nrdp.2016.20 (2017).
- 40. Czepiel, J., Dróżdż, M., Pituch, H., *et al. Clostridium difficile* infection: review. *Eur J Clin Microbiol Infect Dis* **38**, 1211-1221, doi: 10.1007/s10096-019-03539-6 (2019).
- 41. Gibson, G. R. & Roberfroid, M. B. Dietary modulation of the human colonic microbiota: introducing the concept of prebiotics. *J Nutr* **125**, 1401-1412 (1995).
- 42. Walter, J., Maldonado-Gomez, M. X., & Martinez, I. To engraft or not to engraft: an ecological framework for gut microbiome modulation with live microbes. *Curr Opin Biotechnol* **49**, 129-139, doi: 10.1016/j.copbio.2017.08.008 (2018).
- 43. Khoruts, A. Targeting the microbiome: from probiotics to fecal microbiota transplantation. *Genome Med* **10**, 80, doi: 10.1186/s13073-018-0592-8 (2018).
- 44. Tanoue, T., *et al.* A defined commensal consortium elicits CD8 T cells and anti-cancer immunity. *Nature.* **565**, 600–605, doi: 10.1038/s41586-019-0878-z (2019).
- 45. Aguilar-Toalá, J. E., *et al.* Postbiotics: an evolving term within the functional foods field. *Trends Food Sci.* **75**, 105-114, doi: 10.1016/j.tifs.2018.03.009 (2018).
- 46. Żółkiewicz, J., Marzec, A., Ruszczyński, M., & Feleszko, W. Postbiotics a step beyond pre- and probiotics. *Nutrients*. **12**, 2189, doi: 10.3390/nu12082189 (2020).
- 47. Gibson, G. R., *et al.* The international scientific association for probiotics and prebiotics (ISAPP) consensus statement on the definition and scope of prebiotics. *Nat Rev Gastroenterol Hepatol* **14**, 491-502, doi: 10.1038/nrgastro.2017.75 (2017).
- 48. Anand, S., *et al.* A review on Ayurvedic non-carbohydrate prebiotics. *J Electrochem* **107**, 13505-13514, doi: 10.1149/10701.13505ecst (2022).
- 49. Davani-Davari, D., *et al.* Prebiotics: Definition, Types, Sources, Mechanisms, and Clinical Applications. *Foods* **8**, 92, doi: 10.3390/foods8030092 (2019).
- 50. Quigley, E. M. M. Prebiotics and probiotics in digestive health. *Clin Gastroenterol Hepatol* **17**, 333-344, doi: 10.1016/j.cgh.2018.09.028 (2019).
- 51. Bedu-Ferrari, C., Biscarrat, P., Langella, P., & Cherbuy, C. Prebiotics and the human gut microbiota: from breakdown mechanisms to the impact on metabolic health. *Nutrients* **14**, 2096, doi: 10.3390/nu14102096 (2022).
- 52. Yan, Y. L., Hu, Y., & Ganzle, M. G. Prebiotics, FODMAPs and dietary fiber conflicting concepts in development of functional food products? *Curr Opin Food Sci* **20**, 30-37, doi: 10.1016/j.cofs.2018.02.009 (2018).
- 53. Bode, L. Human milk oligosaccharides: prebiotics and beyond. *Nutr Rev* **67**, S183-191, doi: 10.1111/j.1753-4887.2009.00239.x (2009).
- 54. Belzer, C. Nutritional strategies for mucosal health: the interplay between microbes and mucin glycans. *Trends Microbiol* **30**, 13-21, doi: 10.1016/j.tim.2021.06.003 (2022).
- 55. Briggs, J. A., Grondin, J. M., & Brumer, H. Communal living: glycan utilization by the human gut microbiota. *Environ Microbiol* **23**, 15-35, doi: 10.1111/1462-2920.15317 (2021).
- 56. Olveira, G. & Gonzalez-Molero, I. An update on probiotics, prebiotics and symbiotics in clinical nutrition. *Endocrinol Nutr* **63**, 482-494, doi: 10.1016/j.endoen.2016.10.011 (2016).

- 57. Sousa, V., Santos, E., & Sgarbieri, V. The importance of prebiotics in functional foods and clinical practice. *Food Sci Nutr* **2**, 133-144, doi: 10.4236/fns.2011.22019 (2011).
- 58. Brouns, F. & Vermeer, C. Functional food ingredients for reducing the risks of osteoporosis. *Trends Food Sci Technol* **11**, 22-33, doi: 10.1016/S0924-2244(99)00052-7 (2000).
- 59. Włodarczyk, M. & Śliżewska, K. Efficiency of Resistant Starch and Dextrins as Prebiotics: A Review of the Existing Evidence and Clinical Trials. *Nutrients* **13**, 3808, doi: 10.3390/nu13113808 (2021).
- 60. Zaman, S. A. & Sarbini, S. R. The potential of resistant starch as a prebiotic. *Crit Rev Biotechnol* **36**, 578-584, doi: 10.3109/07388551.2014.993590 (2016).
- 61. Lefranc-Millot, C., Guérin-Deremaux, L., Wils, D., Neut, C., Miller, L. E., & Saniez-Degrave, M. H. Impact of a resistant dextrin on intestinal ecology: how altering the digestive ecosystem with Nutriose, a soluble fibre with prebiotic properties, may be beneficial for health. *J Int Med Res* **40**, 211-224, doi: 10.1177/147323001204000122 (2012).
- 62. Lindstad, L. J., *et al*. Human gut *Faecalibacterium prausnitzii* deploys a highly efficient conserved system to cross-feed on β-mannan-derived oligosaccharides. *mBio* **12**, e03628-20, doi: 10.1128/mBio.03628-20 (2021).
- 63. Coyte, K. Z. & Rakoff-Nahoum, S. Understanding competition and cooperation within the mammalian gut microbiome. *Curr Biol* **29**, R538-544, doi: 10.1016/j.cub.2019.04.017 (2019).
- 64. Cockburn, D. W. & Koropatkin, N. M. Polysaccharide degradation by the intestinal microbiota and its influence on human health and disease. *J Mol Biol* **428**, 3230-52, doi: 10.1016/j.jmb.2016.06.021 (2016).
- 65. Salden, B. N., *et al.* Reinforcement of intestinal epithelial barrier by arabinoxylans in overweight and obese subjects: a randomized controlled trial: arabinoxylans in gut barrier. *Clin Nutr* **37**, 471-480, doi: 10.1016/j.clnu.2017.01.024 (2018).
- 66. Rogowski, A., *et al.* Glycan complexity dictates microbial resource allocation in the large intestine. *Nat Commun* **6**, 7481, doi: 10.1038/ncomms8481 (2015).
- 67. Zannini, E., Núñez B. Á., Sahin, A. W., & Arendt, E. K. Arabinoxylans as Functional Food Ingredients: A Review. *Foods* **11**, 1026, doi: 10.3390/foods11071026 (2022).
- 68. Desai, M. S., *et al.* A dietary fiber-deprived gut microbiota degrades the colonic mucus barrier and enhances pathogen susceptibility. *Cell* **167**, 1339-1353, doi: 10.1016/j.cell.2016.10.043 (2016).
- 69. Chen, H., *et al.* Arabinoxylan in wheat is more responsible than cellulose for promoting intestinal barrier function in weaned male piglets. *J Nutr* **145**, 51-58, doi: 10.3945/jn.114.201772 (2015).
- 70. Rezende, E., Lima, G., & Naves, M. Dietary fibers as beneficial microbiota modulators: a proposed classification by prebiotic categories. *Nutrition* **89**, 111-217, doi: 10.1016/j.nut.2021.111217 (2021).
- 71. Hamaker, B. R. & Tuncil, Y. E. A perspective on the complexity of dietary fiber structures and their potential effect on the gut microbiota. *J Mol Biol* **426**, 3838-3850, doi: 10.1016/j.jmb.2014.07.028 (2014).

- 72. Lancaster, S., *et al.* Global, distinctive, and personal changes in molecular and microbial profiles by specific fibers in humans. *Cell Host Microbe* **30**, 848-862, doi: 10.1016/j.chom.2022.03.036 (2022).
- 73. Soliman, G. A. Dietary fiber, atherosclerosis, and cardiovascular disease. *Nutrients* **11**, 1155, doi: 10.3390/nu11051155 (2019).
- 74. Brown, L., Bernard, R., Willet, W. W., & Sacks, F. M. Cholesterol-lowering effects of dietary fiber: a meta-analysis. *Am J Clin Nutr* **69**, 30-42, doi: 10.1093/ajcn/69.1.30 (1999).
- 75. Tong, L., *et al.* Effects of dietary wheat bran arabinoxylans on cholesterol metabolism of hypercholesterolemic hamsters. *Carbohydr Polym* **112**, 1-5, doi: 10.1016/j.carbpol.2014.05.061 (2014).
- 76. Story, J. A., Watterson, J. J., Matheson, H. B., Furumoto, E. J. Dietary fiber and bile acid metabolism. *Adv Exp Med Biol* **270**, doi: 10.1007/978-1-4684-5784-1_5 (1990).
- 77. Singh, J., Metrani, R., Shivanagoudra, S. R., Jayaprakasha, G. K., & Patil, B. S. Review on bile acids: effects of the gut microbiome, interactions with dietary fiber, and alterations in the bioaccessiblity of bioactive compounds. *J Agric Food Chem* **67**, 9124-9138, doi: 10.1021/acs.jafc.8b07306 (2019).
- 78. Kalaany, N. Y. & Mangelsdorf, D. J. LXRS and FXR: the yin and yang of cholesterol and fat metabolism. *Annu Rev Physiol* **68**, 1590191, doi: 10.1146/annurev.physiol.68.033104.152158 (2006).
- 79. Neyrinck, A. M., *et al.* Prebiotic effects of wheat arabinoxylan related to the increase in *Bifidobacteria*, *Roseburia* and *Bacteroides/Prevotella* in diet-induced obese mice. *PloS One* **6**, e20944, doi: 10.1371/journal.pone.0020944 (2011).
- 80. Abbeele, P., *et al.* Arabinoxylans and inulin differentially modulate the mucosal and luminal gut microbiota and mucin-degradation in humanized rats. *Environ Microbiol* **13**, 2667-2680, doi: 10.1111/j.1462-2920.2011.02533.x (2011).
- 81. Abbeele, P., Venema, K., Wiele, T., Verstraete, W., & Possemiers, S. Different human gut models reveal the distinct fermentation patterns of arabinoxylan versus inulin. *J Agric Food Chem* **61**, 9819-9827, doi: 10.1021/jf4021784 (2013).
- 82. Hughes, S. A., *et al.* In vitro fermentation by human fecal microbiota of wheat arabinoxylans. *J Agric Food Chem* **55**, 4589-4596 (2007).
- 83. Grootaert, C., *et al.* Comparison of prebiotic effects of arabinoxylan oligosaccharides and inulin in a simulator of the human intestinal microbial ecosystem. *FEMS Microbiol Ecol* **69**, 231-242, doi: 10.1111/j.1574-6941.2009.00712.x (2009).
- 84. Schupfer, E., *et al.* The effects and benefits of arabinoxylans on human gut microbiota a narrative review. *Food Biosci* **43**, 101267, doi: 10.1016/j.fbio.2021.101267 (2021).
- 85. Mathew, S., Karlsson E.V., & Adlercreutz P. Extraction of soluble arabinoxylan from enzymatically pretreated wheat bran and production of short xylo-oligosaccharides and arabinoxylo-oligosaccharides from arabinoxylan by glycoside hydrolase family 10 and 11 endoxylanases. *J Biotechnol* **260**, 53-61, doi: 10.1016/j.jbiotec.2017.09.006 (2017).
- 86. Faulds, C.B., *et al.* Synergy between xylanases from glycoside hydrolase family 10 and family 11 and a feruloyl esterase in the release of phenolic acids from cereal

- arabinoxylan. *Appl Microbiol Biotechnol* **71**, 622–629, doi: 10.1007/s00253-005-0184-6 (2006).
- 87. Vandermarliere, E., *et al.* Structural analysis of a glycoside hydrolase family 43 arabinoxylan arabinofuranohydrolase in complex with xylotetraose reveals a different binding mechanism compared to other members of the same family. *Biochem J* **418**, 39-47, doi: 10.1042/BJ20081256 (2009).
- 88. Saito, Y., *et al.* Multiple Transporters and Glycoside Hydrolases Are Involved in Arabinoxylan-Derived Oligosaccharide Utilization in Bifidobacterium pseudocatenulatum. *Appl Environ Microbiol* **86**, e01782-20, doi: 10.1128/AEM.01782-20 (2020).
- 89. Falck, P., Linares-Pastén, J. A., Karlsson, E. N., Adlercreutz, P. Arabinoxylanase from glycoside hydrolase family 5 is a selective enzyme for production of specific arabinoxylooligosaccharides. *Food Chem* **242**, 579-584, doi: 10.1016/j.foodchem.2017.09.048 (2018).
- 90. Dridi, L., *et al.* Identifying glycan consumers in human gut microbiota samples using metabolic labeling coupled with fluorescence-activated cell sorting. *Nat Commun* **14**, 662 doi: 10.1038/s41467-023-36365-8 (2023).
- 91. Lombard, V., Ramulu, H. G., Drula, E., Coutinho, P. M., Henrissat, B. The carbohydrate-active enzymes database (CAZy). *Nucleic Acids Res* **42**, D490-495, doi: 10.1093/nar/gkt1178 (2013).
- 92. Ordovas, J. M. & Mooser, V. Metagenomics: the role of the microbiome in cardiovascular diseases. *Curr Opin Lipidol* 17, 157-161, doi: 10.1097/01.mol.0000217897.75068.ba (2006).
- 93. Aguiar-Pulido, V., *et al.* Metagenomics, Metatranscriptomics, and Metabolomics Approaches for Microbiome Analysis. *Evol Bioinform* **12**, 5-16, doi: 10.4137/EBO.S36436 (2016).
- 94. Lagier, JC., *et al.* Culturing the human microbiota and culturomics. *Nat Rev Microbiol* **16**, 540–550, doi: 10.1038/s41579-018-0041-0 (2018).
- 95. Janda, J. M. & Abbott, S. L. 16S rRNA gene sequencing for bacterial identification in the diagnostic laboratory: pluses, perils, and pitfalls. *J Clin Microbiol* **45**, 2761-4, doi: 10.1128/JCM.01228-07 (2007).
- 96. Hatzenpichler, R., Krukenberg, V., Spietz, R. L., & Jay, Z. J. Next-generation physiology approaches to study microbiome function at single cell level. *Nat Rev Microbiol* **18**, 241-256, doi: 10.1038/s41579-020-0323-1 (2020).
- 97. Xu, W., *et al.* Characterization of shallow whole-metagenome shotgun sequencing as a high-accuracy and low-cost method by complicated mock micobiomes. *Front Microbiol.* **12**, 678319, doi: 10.3389/fmicb.2021.678319 (2021).
- 98. Moran, M. A. Metatranscriptomics: eavesdropping on complex microbial communities. *Microbe* **4**, 329-335 (2009).
- 99. Tringe, S. & Rubin, E. Metagenomics: DNA sequencing of environmental samples. *Nat Rev Genet* **6**, 805–814, doi: 10.1038/nrg1709 (2005).
- 100. Greub, G. Culturomics: a new approach to study the human microbiome. *Clin Microbiol Infect* **18**, 1157-59, doi: 10.1111/1469-0691.12032 (2012).

- 101. Lagier, J., *et al.* Microbial culturomics: paradigm shift in the human gut microbiome study. *Clin Microbiology Infect* **18**, 1185-93, doi: 10.1111/1469-0691.12023 (2012).
- 102. Bilen, M., *et al.* The contribution of culturomics to the repertoire of isolated human bacterial and archaeal species. *Microbiome* **6**, 94, doi: 10.1186/s40168-018-0485-5 (2018).
- 103. Martinez-Garcia, M., *et al.* Capturing single cell genomes of active polysaccharide degraders: an unexpected contribution of Verrucomicrobia. *PLoS ONE* **7**, e35314, doi: 10.1371/journal.pone.0035314 (2012).
- 104. Reintjes, G., Arnosti, C., Fuchs, B., & Amann, R. An alternative polysaccharide uptake mechanism of marine bacteria. *ISME J* 11, 1640–1650, doi: 10.1038/ismej.2017.26 (2017).
- 105. Hehemann, J. H., *et al.* Single cell fluorescence imaging of glycan uptake by intestinal bacteria. *ISME J* **13**, 1883–1889, doi: 10.1038/s41396-019-0406-z (2019).
- 106. Klassen, L., *et al.* Quantifying fluorescent glycan uptake to elucidate strain-level variability in foraging behaviors of rumen bacteria. *Microbiome* **9**, 23 doi: 10.1186/s40168-020-00975-x (2021).
- 107. Radajewski, S., Ineson, P., Parekh, N., Murrell, J. C. Stable-isotope probing as a tool in microbial ecology. *Nature* **403**, 646–649, doi: 10.1038/35001054 (2000).
- 108. Tao, J., *et al.* Use of a fluorescent analog of glucose (2-NBDG) to identify uncultured rumen bacteria that take up glucose. *App Environ Microbiol* **85**, e03018-18, doi: 10.1128/AEM.03018-18 (2019).
- 109. Schreiber, G. & Keating, A. E. Protein binding specificity versus promiscuity. *Curr Opin Struct Biol* **21**, 50-61, doi: 10.1016/j.sbi.2010.10.002 (2011).
- 110. Linhart, C. & Shamir, R. The degenerate primer design problem: theory and applications. *J Comput Biol* **12**, 431-456, doi: 10.1089/cmb.2005.12.431 (2005).
- 111. Depres, J., *et al.* Xylan degradation by the human gut *Bacteroides xylanisolvens* XB1A involves two distinct gene clusters that are linked at the transcriptional level. *BMC Genomics* **17**, 326, doi: 10.1186/s12864-016-2680-8 (2016).
- 112. Sonnenburg, J. L., *et al.* Glycan foraging in vivo by an intestine-adapted bacterial symbiont. *Science* **307**, 1955-1959, doi: 10.1126/science.1109051 (2005).
- 113. Stülke, J. & Hillen, W. Carbon catabolite repression in bacteria. *Curr Opin Microbiol* **2**, 195-201, doi: 10.1016/S1369-5274(99)80034-4 (1999).
- 114. Maier, R. M. & Pepper, I. L. Bacterial growth. *Environ Microb* 37-56, doi: 10.1016/B978-0-12-394626-3.00003-X (2015).
- 115. Sun, Y., *et al.* Gut firmicutes: Relationship with dietary fiber and role in host homeostasis. *Crit Rev Food Sci Nutr* 1-16, doi: 10.1080/10408398.2022.2098249 (2022).
- 116. Lau, J. T., *et al.* Capturing the diversity of the human gut microbiota through culture-enriched molecular profiling. *Genome Med* **8**, 72, doi: 10.1186/s13073-016-0327-7 (2016).
- 117. Bodner, S. J., Koenig, M. G., Treanor, L. L., & Goodman, J. S. Antibiotic Susceptibility Testing of *Bacteroides. Antimicrob Agents Chemother* **2**, 57-60, doi: 10.1128/AAC.2.2.57, (1972).

- 118. Kislak, J. W. The Susceptibility of *Bacteroides fragilis* to 24 Antibiotics. *J Infect Dis* **125**, 295-299, doi: 10.1093/infdis/125.3.295 (1972).
- 119. Sutter, V. L. & Finegold, S. M. Susceptibility of anaerobic bacteria to 23 antimicrobial agents. *Antimicrob Agents Chemother* **10**, 736-752, doi: 10.1128/AAC.10.4.736 (1976).
- 120. Matteuzzi, D., Crociani, F., & Brigidi, P. Antimicrobial susceptibility of *Bifidobacterium. Ann Microbiol* **134**, 339-49, doi: 10.1016/0769-2609(83)90009-1 (1983).
- 121. Delgado, S., Flórez, A. B., & Mayo, B. Antibiotic susceptibility of Lactobacillus and Bifidobacterium species from the human gastrointestinal tract. *Curr Microbiol* **50**, 202-207, doi: 10.1007/s00284-004-4431-3 (2005).
- 122. Kim, N. H., Kim, H. W., Moon, H., Rhee, M. S. Sodium chloride significantly enhances the bactericidal actions of carvacrol and thymol against the halotolerant species *Escherichia coli* O157:H7, *Listeria monocytogenes*, and *Staphylococcus aureus*. *Food Sci Technol* **122**, 109015, doi: 10.1016/j.lwt.2020.109015 (2020).
- 123. Tamblyn, K. C. & Conner, D. E. Bactericidal Activity of Organic Acids against *Salmonella typhimurium* Attached to Broiler Chicken Skint. *J Food Protect* **60**, 629-633, doi: 10.4315/0362-028X-60.6.629 (1997).
- 124. Liang, N., Neuzil-Bunesova, V., Tejnecky, V., & Ganzle, M. 3-Hydroxypropionic acid contributes to the antibacterial activity of glycerol metabolism by the food microbe *Limosilactobacillus reuteri*. *Food Microbiol* **98**, 103820, doi: 10.1016/j.fm.2020.103720 (2021).
- 125. Levison, M. E. & Levison, J. H. Pharmacokinetics and pharmacodynamics of antibacterial agents. *Infect Dis Clin North Am* **23**, 791-815, doi: 10.1016/j.idc.2009.06.008 (2009).
- 126. Shen, Y., Stojicic, S., & Haapasalo, M. Bacterial viability in starved and revitalized biofilms: comparison of viability staining and direct culture. *J Endod* **36**, 1820-1823, doi: 10.1016/j.joen.2010.08.029 (2010).
- 127. Fehlner-Peach, H., *et al.* Distinct polysaccharide utilization profiles of human intestinal *Prevotella copri* isolates. *Cell Host Microbe* **26**, 680–690 e685, doi: 10.1016/j.chom.2019.10.013 (2019).
- 128. Pacheco, A. R., *et al.* Fucose sensing regulates bacterial intestinal colonization. *Nature* **492**, 113–117, doi: 10.1038/nature11623 (2012).
- 129. Chao, Y. & Zhang, T. Optimization of fixation methods for observation of bacterial cell morphology and surface ultrastructures by atomic force microscopy. *Appl Microbiol Biotechnol* **92**, 381-392, doi: 10.1007/s00253-011-3551-5 (2011).
- 130. Lapébie, P., Lombard, V., Drula, E., Terrapon, N., & Henrissat, B. Bacteroidetes use thousands of enzyme combinations to break down glycans. *Nat Commun* **10**, 2043, doi: 10.1038/s41467-019-10068-5 (2019).
- 131. Cabral, D. J., *et al.* Microbial metabolism modulates antibiotic susceptibility within the murine gut microbiome. *Cell Metab* **30**, 800-823, doi: 10.1016/j.cmet.2019.08.020 (2019).

- 132. Jogia, W. & Maurice, C. F. Polysaccharide protection: how *Bacteroides thetaiotaomicron* survives an antibiotic attack. *Cell Metab* **30**, 619-621, doi: 10.1016/j.cmet.2019.09.011 (2019).
- 133. Karasawa, T., Ikoma, S., Yamakawa, K., & Nakamura, S. A defined growth medium for *Clostridium difficile. Microbiology* **141**, 371-375, doi: 10.1099/13500872-141-2-371 (1995).
- 134. Tang, Q., *et al.* Current sampling methods for gut microbiota: a call for more precise devices. *Front Cell Infect Microbiol* **10**, 151, doi: 10.3389/fcimb.2020.00151 (2020).
- 135. Reygner, J., *et al.* Freeze-dried fecal samples are biologically active after long-lasting storage and suited to fecal microbiota transplantation in a preclinical murine model of *Clostridioides difficile* infection. *Gut Microbes* **11**,1405-1422, doi: 10.1080/19490976.2020.1759489 (2020).
- 136. Routy, B., *et al.* Gut microbiome influences efficacy of PD-1–based immunotherapy against epithelial tumors. *Science* **359**, 91-97, doi: 10.1126/science.aan3706 (2018).
- 137. Messaoudene, M., *et al.* A natural polyphenol exerts antitumor activity and circumvents anti-PD-1 resistance through effects on the gut microbiota. *Cancer Discov* **12**, 1070-87 doi: 10.1158/2159-8290.CD-21-0808 (2022).

APPENDIX A: ABBREVIATIONS

Aβ: Amyloid beta

ABB: Anaerobe basal broth medium

ABBc: Custom anaerobe basal broth medium

ABB-AX: ABB supplemented with 0.1% AX

ABC: ATP-binding cassette transporters

AD: Alzheimer's disease

APP: Aβ precursor protein

Arabxylo-Fl: Arabinoxylotetraose fluorescein conjugate

AX: Arabinoxylan

AXOS: arabinoxylan oligosaccharide

BHI: Brain heart infusion

BAs: Bile acids

Bp: Base pairs

CAZymes: Carbohydrate-active enzymes

CD-F : β-cyclodextrin fluorescein conjugate

CDI: Clostridioides difficile infection

CEs: Carbohydrate esterases

CFU: Colony forming unit counts

CMB: Carbohydrate-binding modules

ESVs: Exact sequence variants

FACS: Fluorescence-activated cell sorting

FGCs: Fluorescent glycan conjugates

FITC: Fluorescein isothiocyanate

FLA-PS: Fluorescently-labeled polysaccharides

FMTs: Fecal microbiota transplantation/transplants

FOS: Fructooligosaccharides

FXR: Farnesoid X Receptor

GALT: Gut-associated lymphoid tissue GF: germ-free

GHs: Glycoside hydrolases

GMP: Galactosyl-mannopentaose

GMP-F: Galactosyl-mannopentaose fluorescein conjugate

GOS: Galactooligosaccharides

GRAS: generally regarded as safe

HMOs: Human milk oligosaccharides

HMP: Human Microbiome Project

HPLC: High-performance liquid chromatography

HTCS: Hybrid two component system

ICIs: Immune checkpoint inhibitors

LC-MS: Light chromatography-mass spectrometry

LXR: Liver X Receptor

MAR-FISH: Microautoradiography coupled with fluorescent in situ hybridization

MBC: Minimal bactericidal concentration

Meta-HIT: Metagenomics of the Human Intestinal Tract Consortium

MFS: Major facilitator superfamily

MIC: Minimal inhibitory concentration

MM: Minimum medium

MM-AX: MM supplemented with 0.1% AX

MMe: Enriched minimum medium

MMe-AX: Enriched minimum medium supplemented with 0.1% AX

mMSA: Modified Mannitol Salt Agar

NCBI: National Center for Biotechnology Information

NYST-F: Nystose fluorescein conjugate

OD: Optical density

ONT: Oxford Nanopore Technologies

PBS: Phosphate buffered saline

PCR: Polymerase chain reaction

PE: Phycoerythrin

PFA: Paraformaldehyde

PLs: Polysaccharide lyases

PRRs: Pattern recognition receptors

PUL: Polysaccharide utilization loci

PULDB: PUL database

RGII: Rhamnogalacturonan-II

rrnDB: Ribosomal RNA operons database

RT: Retention time

sBHI: Supplemented BHI

SBPs: Solute binding proteins

sCMB: Supplemented Cooked Meat Broth

SCFAs: Short-chain fatty acids

SGBP: Surface glycan-binding protein

SHIME: Simulator of the Human Intestinal Microbial Ecosystem

SIP: Stable isotope probing

Sus: Starch utilization system

TBDT: TonB-dependent transporter

WMS: Whole-metagenome shotgun sequencing

XylL: Large xylan

XylS: Small xylan

YM: Yeast α-mannan

Anaerobe Basal Broth (ABB)

Peptone (16 mg/mL), yeast extract (7 mg/mL), NaCl (5 mg/mL), potato starch (1 mg/mL), glucose (1 mg/mL), sodium pyruvate (0.5 mg/mL), sodium succinate (0.5 mg/mL), sodium thioglycolate (0.5 mg/mL), L-arginine (1 mg/mL), L-cysteine (0.5 mg/mL), NaHCO₃ (0.4 mg/mL), FeSO₄ · 7H₂O (0.5 mg/mL), haemin (5 μ g/mL), vitamin K1 (0.5 μ g/mL), dithiothreitol (1 mg/mL), MilliQ water (up to desired volume)

* The typical recipe for ABB (Oxoid website) uses iron pyrophosphate instead of FeSO₄ · 7H₂O, however iron pyrophosphate was replaced as it was precipitating from the medium. In this thesis, ABB refers to this adapted recipe and is not called a modified/custom medium because **custom ABB** (**ABBc**) refers a carbohydrate-free ABB (exclude starch and glucose)

Arabinoxylan (AX)

10 g/L arabinoxylan (Megazyme P-WAXYL), 95% ethanol (8% v/v), MilliQ water (adjust to desired total AX solution volume)

To prepare 25 mL of arabinoxylan solution (1%), measure out 250 mg of arabinoxylan (Megazyme P-WAXYL). Wet the powder with 2 mL of 95% ethanol and then adjust the volume to 25 mL with MilliQ water. Add a magnetic stirring rod to the glass beaker and heat while stirring the solution. Cover the beaker with aluminum foil to prevent heat loss. Slowly increase the heat until the solution comes to a boil or you see that the powder has all dissolved. Move the beaker to a magnetic stirrer at room temperature and keep stirring to cool solution to room temperature (~20 min). Finally, adjust the dissolved solution to a volume of 25 mL with MilliQ water.

DNA Gel-loading dye

Glycerol (3.9% v/v), EDTA (10 μ M), Tris-HCl (10 mM), bromophenol blue (2.5 mg/mL), and MilliQ water (up to desired volume)

Minimum Medium (MM)

KH₂PO₄ (6.6 mM), NaCl (15 mM), MgCl₂ · 6H₂O (1 mM), CaCl₂ · 2H₂O (175 μM), MnSO₄ · H₂O (50 μM), (NH₄)₂SO₄ (5 mM), NaHCO₃ (24 μM), L-cysteine (1 mg/mL), FeSO₄ · 7H₂O (15 μM), vitamin B12 (200 ng/mL), haemin (6 μM), hematin (1.9 μM), and MilliQ water (up to desired volume)

- * Enriched minimum medium (**MMe**): add yeast extract (0.14 mg/mL) and beef extract (0.14 mg/mL) to MM
- * Enriched minimum medium supplemented with AX (0.1%) (**MMe-AX**): add yeast extract (0.14 mg/mL), beef extract (0.14 mg/mL) and AX (0.1% v/v) to MM

Modified Mannitol Salt Agar (mMSA)¹¹³

Peptone (10 mg/mL), beef extract (1 mg/mL), NaCl (5 and 7.5% v/v), mannitol (10 mg/mL)

Supplemented BHI (sBHI)¹¹³

BHI (37 mg/mL), L-cysteine (4.1 mM), haemin (15.3 μ M), vitamin K (2.2 μ M), propionic acid (0.5 and 1% v/v)

Supplemented Cooked Meat Broth (sCMB)¹¹³

Beef extract (30 mg/mL), peptone (20 mg/mL), glucose (2 mg/mL), NaCl (5 mg/mL), L-cysteine (4.1 mM), haemin (15.3 μ M), vitamin K (2.2 μ M)